UNIVERSITÉ DE MONTRÉAL

ELECTROSPINNING OF CONDUCTING POLYMER FIBERS FOR STRETCHABLE ELECTRONICS

FANNY BOUBÉE DE GRAMONT

INSTITUT DE GÉNIE BIOMÉDICAL

ÉCOLE POLYTECHNIQUE DE MONTRÉAL

MÉMOIRE PRÉSENTÉ EN VUE DE L'OBTENTION

DU DIPLÔME DE MAÎTRISE ÈS SCIENCES APPLIQUÉES

(GÉNIE BIOMÉDICAL)

MARS 2017

UNIVERSITÉ DE MONTRÉAL

ÉCOLE POLYTECHNIQUE DE MONTRÉAL

Ce mémoire intitulé :

ELECTROSPINNING OF CONDUCTING POLYMER FIBERS FOR STRETCHABLE ELECTRONICS

présenté par : BOUBÉE DE GRAMONT Fanny

en vue de l'obtention du diplôme de : Maîtrise ès sciences appliquées

a été dûment accepté par le jury d'examen constitué de :

M. AJJI Abdellah, Ph. D., président

M. CICOIRA Fabio, Ph. D., membre et directeur de recherche

M. DE CRESCENZO Gregory, Ph. D., membre et codirecteur de recherche

M. PELLERIN Christian, Ph. D., membre

DEDICATION

To my family, for their continuous and extensive support.

ACKNOWLEDGEMENTS

I would like to start by thanking my supervisor and my co-supervisor, Professors Fabio Cicoira and Gregory de Crescenzo, for their help, advice and for giving me the opportunity to attend many interesting training sessions throughout the whole course of this project. I would also like to thank Marie-Hélène Bernier for giving me the opportunity to train students, as a lab assistant for the Microfabrication class.

I would like to thank the Professor Peter Grütter from McGill university and his group, and more particularly Maddy, for the help and advice they provided in the course of a collaborative project related to the one presented in these pages.

I am grateful to all the funding agencies and governmental groups without which this project would not have been possible: the Groupe de Recherche en Sciences et Technologies Biomédicales (GRSTB) and CMC Microsystems.I am also thankful to École Centrale-Supélec for giving me the opportunity to come to École Polytechnique Montréal for my studies. This experience abroad certainly was an instructive and enjoyable one.

I would like to thank Christophe Clément for his help and training on microfabrication, Daniel Pilon for his technical help on electrospinning and good advice, and Marie Richard-Lacroix for spending some of her time just before her thesis defense to discuss electrospinning with me. Your help and support were always valued.

I am also deeply grateful to all my colleagues and friends who helped me through this project, and more specifically to Zhihui and Eduardo for training me on general lab related work, Prajwal for training me on electrospinning, Shiming for his awesome knowledge about stretchable electronics and for his contagious motivation, and Gaia and Irina for their help and their totally not chocolate-free moral support. I'm thankful to all my other colleagues and former colleagues, Guido, Tania, Xu, Alexander, William, Francis, Jonathan, Côme, Yang, Xiang, Tian, Martin, Dominic, Zhaojing, Manuel, Michael, for all the time we spent together, both in lab and outside. To Bogdan, Shalin and Tom, that I had the pleasure to train in lab, I was happy that you all patiently listened to my explanations and asked way too many questions. Also, I would like to thank my other friends here, and especially Julien and Adrien for being like a family for the time they spent here, and Edwige, Sylvain, Alona, the Jacks (including the mad one) for always being a blast at parties, but also Alfredo, Olivier, Benji, and all the others for all the nice and crazy moments we spent together,

playing board games or spending the night cooking and talking. I was very fortunate to have you all around. I also was very lucky to have Alice, Anaïs, Gwen, Alex', Baudouin, Charlie and Thibaut who all supported me even though we had an ocean and 6 hours of time difference between us. Thank you for giving me the motivation to come back home as soon as possible.

Finally, these last few lines are for my family. To my parents, who somehow managed to decide that it was ok to encourage me to fly across the Atlantic just so I could do what I wanted, to Peyot and Nanon, who went back to using Skype while pretending this did not bother them, and to Oscar and Candice, who always reminded me that half a world still was not *quite* enough to stop siblings from jokingly bickering: thank you, and I love you.

RÉSUMÉ

L'électronique étirable est un domaine prometteur en ce qui concerne les applications au biomédical. En effet, les dispositifs étirables peuvent être utilisés pour remplir diverses fonctions, qui incluent l'électronique portable (ou les vêtements intelligents), la peau artificielle, et de façon plus générale l'ensemble des fonctions qui exigent d'avoir de l'électronique placée directement sur la peau apte à se conformer au style de vie du patient, par exemple pour de la surveillance quotidienne des constantes biologiques d'un patient. De nombreuses stratégies ont été mises en place jusqu'à présent pour produire de l'électronique étirable, cependant celles-ci peuvent être grossièrement séparées en deux catégories principales. Dans la première se retrouvent toutes les stratégies où les matériaux sont étirés grâce à l'utilisation d'une géométrie spécifique, tandis que la seconde catégorie comprend l'ensemble des matériaux qui sont intrinsèquement étirables. Ainsi, des formes spécifiques comme des fibres peuvent être utilisées pour améliorer la capacité à s'étirer d'un matériau autrement peu étirable, ce qui inclut des matériaux conducteurs comme les métaux ou certains polymères conducteurs et semi-conducteurs utilisés en électronique organique. Cependant, la mise en pratique de ces fibres requière l'utilisation d'une technique apte à aisément générer des fibres conductrices. Pour les applications en biomédical, les matériaux électroniques organiques présentent l'avantage sur l'électronique classique de posséder une bonne compatibilité avec les systèmes biologiques du fait de leur capacité à aisément faire l'interface avec le milieu biologique. Ils présentent aussi l'avantage pour ces applications de disposer d'une capacité à conduire à la fois les ions et les électrons.

Le but de ce projet de recherche est de démontrer la faisabilité de la fabrication de tels films, faits de nanofibres en polymère conducteur, qui maintiennent leur capacité à conduire le courant même lorsque ceux-ci sont étirés.

Bien que de nombreuses méthodes existent pour produire de telles fibres, l'électrofilage apparaît comme étant l'une des méthodes les plus simples pour réaliser des couches poreuses et non tissées de nanofibres, couches qui peuvent aisément se conformer à la surface de leur substrat. En combinant l'électrofilage avec une technique appelée la polymérisation en phase vapeur, nous avons fabriqué des nanofibres conductrices de poly(3,4-éthylènedioxythiophène) dopé avec de l'acide paratoluènesulfonique (tosylate, PEDOT:Tos) directement sur du polydiméthylsiloxane (PDMS), un élastomère organique siliconé. Cette méthode simple à deux étapes nous a permis de

produire des nanofibres de poly(3,4-éthylènedioxythiophène) dopé avec du tosylate (PEDOT:Tos) sur du PDMS. Des couches fibreuses non tissées composées de nanofibres conductrices possédant un diamètre moyen d'un peu moins de 700 nm ont ainsi été obtenues directement sur le PDMS. Nous avons caractérisé ces fibres pour étudier leur comportement électrique lorsqu'une tension était appliquée à leurs extrémités. Ces tapis de fibres ont alors pu être étirés tandis qu'un voltage fixé appliqué directement dessus forçait l'écoulement d'un courant à l'intérieur des films, courant qui a été mesuré. Cela nous a permis de démontrer que ces films possédaient la capacité de s'étirer jusqu'à 140% de leur longueur initiale sans variation majeure de la quantité de courant s'écoulant dans les films.

ABSTRACT

Stretchable electronics is a promising field for biomedical applications. Stretchable devices can be used for various purposes, including wearable electronics (or smart clothes), artificial skin, and more generally for any purpose requiring to have on-skin electronics that conform to the lifestyle of the patient, for example day-by-day biomonitoring. Many strategies have been used so far to produce stretchable electronics, however these can be split between two main categories. In the first one are the materials that stretch due to a specific geometry, while in the second category are the materials that are intrinsically stretchable. Specific shapes such as fibers can thus be used to improve the stretchability of an otherwise poorly-stretchable material, including conductive materials such as metals or conducting and semi-conducting polymers used in organic electronics. However, the practical application of fibers in stretchable electronics requires the use of a technique that can easily yield conductive fibers. For biological applications, organic electronic materials present the advantage over conventional electronic materials to possess a good compatibility with biological systems due to their ability to easily interface with the biological milieu and their mixed ionic / electronic conduction.

The objective of this research project is to demonstrate the fabrication of such films, made with conductive polymer nanofibers that can still conduct the current even when stretched.

Although many methods exist to produce such fibers, electrospinning is one of the easiest ways to directly make non-woven porous nanofiber mats that can conform to the surface of their substrate. By combining electrospinning with vapor phase polymerization, we fabricated conductive nanofibers of poly-(3,4-ethylenedioxythiophene) doped with paratolenesulfonate (tosylate, PEDOT:Tos) directly on polydimethylsiloxane (PDMS), an organosilicon elastomer. Non-woven fiber mats composed of conductive nanofibers with an average diameter of around 700 nm were obtained directly on PDMS. We characterized these fibers to study their electrical behavior when a strain was applied to them. These mats were then stretched while the current flowing inside them was measured, at fixed voltage. This allowed us to demonstrate a stretchability up to 140% of the initial length without major variation of the current flowing in the mats.

TABLE OF CONTENTS

DEDICATION III

ACKNOWLEDGEMENTS IV

RÉSUMÉ VI

ABSTRACT VIII

TABLE OF CONTENTS IX

LIST OF TABLES XII

LIST OF FIGURES XIII

LIST OF SYMBOLS AND ABBREVIATIONS XIX

CHAPTER 1 INTRODUCTION 1

1.1 General context 1

1.1.1 Stretchable electronics 1

1.1.2 Organic electronics 2

1.1.3 Principles of electrospinning 2

1.1.4 Principles of vapor phase polymerization 3

1.2 Problematics 3

1.3 Research objectives 3

1.4 Organization of the memoir 3

CHAPTER 2 CRITICAL REVIEW OF LITERATURE 5

2.1 Stretchable electronics 5

2.1.1 Stretching non-stretchable materials 5

2.1.2 Organic materials for stretchable purposes 10

2.2 Fibers 12

2.2.1 Interest of fibers 12

2.2.2 Fabrication methods 13
2.2.3 Electrospinning 17
2.3 Vapor phase polymerization 38
2.3.1 Working principle of vapor phase polymerization 39
2.3.2 Production of PEDOT fibers using vapor phase polymerization 41
CHAPTER 3 MATERIALS AND METHODS 43
3.1 Substrate preparation 43
3.2 Electrospinning 44
3.2.1 Preparation of the mixture 44
3.2.2 Cleaning of the syringe 44
3.2.3 Electrospinning parameters 44
3.3 Vapor phase polymerization 45
3.4 Sample rinsing 46
3.5 Characterization 47
3.5.1 Diameter of the fibers 47
3.5.2 Electrical characterization during stretching 47
CHAPTER 4 ARTICLE 1: HIGHLY STRETCHABLE ELECTROSPUN CONDUCTING POLYMER NANOFIBERS 49
4.1 Article presentation 49
4.2 Authors 49
4.3 Abstract 50
4.4 Article 50
4.5 Acknowledgements 59
4.6 References 60
CHAPTER 5 COMPLEMENTARY RESULTS 62

5.1 Patterning of the fibers 62
5.2 Complementary electrical measurements 63
5.2.1 Unrinsed fibers 63
5.2.2 PEDOT:Tos fibers with a strain-sensing behavior 64
5.3 Cell cultures 65
CHAPTER 6 GENERAL DISCUSSION 66
6.1 Main results 66
6.1.1 Appearance of the fiber mats before/after stretching 66
6.1.2 Current measurement while stretching 67
6.2 Future challenges 68
6.2.1 Preparation of the solution 68
6.2.2 Relative humidity during electrospinning 69
6.2.3 Limitations of using PDMS as the support for the fibers 69
6.2.4 Improving the stretchability 70
6.2.5 Testing the removal of the PVP core 71
CHAPTER 7 CONCLUSION AND RECOMMENDATIONS 72
BIBLIOGRAPHY 75

LIST OF TABLES

Table 2.1: Effect of different parameters on the diameter and the morphology of electrospun fibers. 26

LIST OF FIGURES

Figure 2.1: Three-dimensional profile of a Au surface wave after release from 15% pre-stretch [34-35]. © 2004 IEEE 7

Figure 2.2: SEM image of an array of stretchable, 3-stage CMOS ring oscillators in a twisted configuration. [36] © 2008 National Academy of Sciences 7

Figure 2.3: Finite element analysis (FEA) was used to estimate the internal stresses in several copper track patterns in the idealized case considering linear behavior (Young modulus E = 117 GPa) of the materials and neglecting the influence of any substrate material. By taking a horseshoe shape instead of an elliptical shape with the same wavelength/amplitude ratio, the maximum internal stress was reduced from 3610 to 1942 MPa. Splitting up the track into four parallel narrow tracks leads to a further reduction from 1942 to 230 MPa. (a) Elliptic. (b) Horseshoe. (c) Multitrack horseshoe. [39] © 2007 IEEE 8

Figure 2.4: Optical image of a folded circuit (left) consisting of an array of CMOS inverters and scanning electron microscopy image (center). The images on the right provide views at the folded edge (right top) and side (right bottom). [40] © 2009 John Wiley and Sons 9

Figure 2.5: Scheme of a compliant zinc carbon dry gel cell. The cell is based on pastes as electrodes, chemically active cells, and an electrolyte gel to close the circuit. Intermixing and short-circuiting of the electrochemical power supply are prohibited by laterally separating the electrodes with an elastomer separator [50]. © 2010 John Wiley and Sons 10

Figure 2.6: Schematic illustration of nanofibers fabrication by direct drawing process from molten poly(trimethylene terephthalate) (PTT). I, An iron or silica rod is approaching the molten PTT. II, The rod end is immersed into the molten PTT. III, The rod conglutinated PTT is being drawn out. IV, A PTT nanofiber is formed. [83] © 2008 Optical Society of America 14

Figure 2.7: Schematic diagram of a wet-spinning apparatus [88]. © 2007 Elsevier 15

Figure 2.8: Number of publications in the database Web of Science(TM) containing the words "electrospinning", "electrospun" or "electrical spinning" since 1997. The histogram on the left shows the detail between 1997 and 2002, while the one on the right shows all the results for the years 1997 to 2016. The results were obtained on the 01/10/2017. 20

Figure 2.9: Schematic drawing of an electrospinning setup. The syringe is usually connected to a syringe pump to ensure a constant flow rate in the nozzle. The mandrel (or "collector") can be made in different shapes and composed of different materials. It is usually grounded or put at a slightly negative voltage (around -3 kV), while the syringe is put at a high voltage (tens of kV). 21

Figure 2.10: First 1.4cm of a glycerin jet 4.66cm long, showing the structure known as Taylor cone on the right, at the tip of the nozzle [137]. © 1969, The Royal Society 22

Figure 2.11: Evolution of the shape of a fluid drop. The time 0 was chosen as the time when the jet first appeared. The electrical potential was applied for a little more than 28 ms earlier. The first picture (-28 ms) thus shows the elongation of the drop into a cone-shape due to the electrical potential. The second (-8 ms) and third (-2 ms) pictures show the further elongation of the drop into a cone, followed by the apparition of the jet (0 ms). Finally, the shape rapidly changed into a rounder one, in the form of the Taylor cone (+32 ms). This last shape was stable as long as enough fluid was brought to the nozzle to compensate for the fluid lost in the jet [141]. © 2008 Elsevier 22

Figure 2.12: Jet images of a 2 wt% solution of PEO (MW = 2 000 000) in water during electrospinning. (a) Stable jet (scalebar = 5mm); (b) unstable jet (scalebar = 5 mm, 1 ms exposure); (c) close-up of the onset of instability (scalebar = 1 mm, 18 ns exposure) [142]. © 2001 AIP Publishing LLC.....23

Figure 2.13: Schematic diagram of an electrospinning jet, showing three different levels of bending instability [141]. © 2008 Elsevier 24

Figure 2.14: A scanning electron microscopy (SEM) picture of beaded fibers [144]. © 1999 Elsevier.....25

Figure 2.15: Scheme of various kinds of collecting systems used in electrospinning, showing (a) a metal plate collector, (b) a rotating drum, (c) a triangular frame placed near a single plate and (d) a parallel dual plate. [151] © 2004 Elsevier.....27

Figure 2.16: (A) Schematic illustration of the setup for electrospinning used to generate uniaxially aligned nanofibers. The collector contained two pieces of conductive silicon stripes separated by a gap. (B) Calculated electric field strength vectors in the region between the needle and

the collector. The arrows denote the direction of the electrostatic field lines. (C) Electrostatic force analysis of a charged nanofiber spanning across the gap. The electrostatic force (F1) resulted from the electric field and the Coulomb interactions (F2) between the positive charges on the nanofiber and the negative image charges on the two grounded electrodes. Reprinted with permission from [161]. Copyright 2003 American Chemical Society. 28

Figure 2.17: Continuous as-spun nanofibers deposited on a rotating multi- frame structure [106]. © 2003 Elsevier.....29

Figure 2.18: Schematic drawing of the electrospinning process with a rotating disk collector, showing the jet path and the region where the bending instability rapidly grew into a conical envelope. This later changed into an inverted conical envelope with its apex on the rotating disk's edge. The disk is made of aluminium and has an overall diameter of 200 mm and thickness of 5 mm [164]. DOI: https://doi.org/10.1088/0957-4484/12/3/329 © IOP Publishing. Reproduced with permission. All rights reserved. 30

Figure 2.19: On the left: scheme of a dual grounded ring configuration for the collection system. On the right: once the fibers are formed, the ground on the right is rotated while the ground on the left stays stationary. This allows for the formation of a yarn. [151] © 2004 Elsevier 30

Figure 2.20: Aligning electrospun fibers with an auxiliary electric field [106]. © 2003 Elsevier.31

Figure 2.21: A multiple-field technique to obtain aligned fibers [167]. © 2001 Elsevier 32

Figure 2.22: (a) Schematic illustration of fabrication of fibrous tubes by electrospinning technique using 3D columnar collectors. 1: 3D columnar collectors. 2: relevant fibrous tubes. (w, working collector; pa, plane assistant collector; sa, stick assistant collector) (b) Fibrous tube with diameter of 500 μm (inset is the cross-section image). (c) SEM image of fiber assemblies of tube shown in panel b. Reprinted with permission from [169]. Copyright 2008 American Chemical Society.....33

Figure 2.23: Schematic of electrolyte-assisted electrospinning (ELES) to self-assemble electrospun fibers. a) Experimental setup of ELES to self-assemble electrospun fibers on a collector made of an electrolyte solution (potassium chloride). b) Self-assembled nanofiber membranes on a curved surface. Scale bar: 10 μm [172]. © 2015 John Wiley and Sons.....34

Figure 2.24: Schematic drawing of the setup used in [194] and chemical structures of MEH-PPV and P3HT (written here as PHT). © 2004 John Wiley and Sons 36

Figure 2.25: PEDOT:PSS/PEO fibers as "stranding fibers" trying to reach the spinning nozzle [203]. © 2015 Elsevier 38

Figure 2.26: A typical procedure for deposition of conjugated polymer films by VPP. Alternative methods, such as sublimation, have been used to achieve oxidant preapplication (Step I). [207] © 2012 John Wiley and Sons 39

Figure 2.27: Chemical reaction between EDOT and Tosylate leading to PEDOT:Tos [222-223]. 42

Figure 3.1: Glass slide (dark blue) with a home-made support (orange) attached on it. A PDMS substrate (transparent lighter blue) is attached on top on the support. This configuration allows for an easier removal of the PDMS substrate after electrospinning by limiting the contact and thus the adherence between the PDMS and its support. The PDMS can also be removed by cutting if necessary. 43

Figure 3.2: Schematic drawing of the fibers structure before and after vapor phase polymerization (VPP). The yellow coating also contains imidazole (not specified on the schematic), while the PVP core (in grey) also contains Fe^{3+}, Tos and Imidazole. 46

Figure 3.3: Setup used to measure the current while stretching the samples. EGaIn is used as a liquid metallic electrode to ease the connection between the fibers (in blue) on the PDMS substrate and the copper wires. 48

Figure 4.1: Process used to obtain fibers of PEDOT:Tos. A mixture containing PVP, Fe(III)Tos and Imidazole is electrospun directly on a PDMS substrate attached to a rotating cylindrical collector. The applied voltage is 20 kV, and the distance is 15 cm (Step 1). The PDMS covered with fibers is placed inside a chamber at atmospheric pressure. A crucible containing EDOT is warmed at 50°C to evaporate the monomer, thus allowing the polymerization of PEDOT:Tos on the fibers (Step 2). The fibers are rinsed with ethanol to remove the unreacted chemicals (monomer and oxidant) and to dissolve the PVP core of the fibers. Removing the PVP core allows for better long-term stability of the fiber mat, by preventing the PVP from melting by absorbing ambient water later. 54

Figure 4.2: PEDOT:Tos fibers on PDMS obtained after 3 min of electrospinning at 20 kV and 15 cm nozzle-collector distance, 30 min of VPP and rinsing in ethanol. a) SEM micrograph of a network of fibers. The fibers appear to be fused together at the intersections, which suggests an easier conduction of the current at the junctions. A few fibers show beaded structures. The "flatness" of the fibers is due to the removal of the PVP core following rinsing with ethanol (the scale bar is 20 µm). b) Close-up of one PEDOT:Tos fiber (scale bar is 1 µm) with a diameter of about 600 nm. c and d) optical microscopy of a network of fibers c) before and d) after a 100% stretch. The white arrow shows the stretching direction, and the oval highlights a small tear in the network, as well as a few broken fibers (the scale bars in c) and d) are 20 µm). 55

Figure 4.3: a) Current vs time plots for PEDOT:Tos fibers on PDMS. A logarithmic scale is used for the current. The sample was stretched in cycles, from 20% to 140% strain percentages at 0.1 cm/s. Five consecutive cycles of stretching and release were performed at each of the different strains percentage between 20% and 140%. The PDMS substrate broke at 160% strain. The samples were kept in each state (stretched or released) for a resting time of 1min. Inset: scheme of the setup used for this measurement. EGaIn was used for the connection between the fiber mat and the copper wires. The arrows show the stretching direction of the sample. b) Current vs time plots for a similar sample stretched at 100% strain percentage for 50 cycles, with a stretching speed of 0.1 cm/s. One stretching cycle consisted of stretching at 100% strain during 15 s followed by release to the initial length during 15 s. The 50 cycles were performed without pause. Inset: Close-up of the behavior of the current during three cycles, with indication of the time during which the strains were applied and released. The samples were 1.5 cm long and 1 cm wide. The fibers were obtained after 3 min of electrospinning at 20 kV and 15 cm nozzle-collector distance, 30 min of VPP, and rinsing with ethanol. The measurements were made at 200 mV.....57

Figure 5.1: Patterned PEDOT:Tos nanofibers on PDMS. These were produced using a parylene mask. The patterns shown are 800 µm wide and 2 mm long. The top patterns appear to be slightly deformed, due to small wrinkles on the PDMS or on the parylene during the patterning. Bubbles under the PDMS are also visible on the top left and right corners, as well as in the bottom right and on the pattern. 62

Figure 5.2: Current vs time for fibers obtained after 3min of electrospinning and VPP on PDMS, without ethanol bath, with a voltage of 200mV applied. The initial 120% stretching leads to a drop in the current. After this first drop, the sample was brought back to its initial position, but no recovery of the current was observed.....63

Figure 5.3: Current vs time for fibers obtained after 3min of electrospinning and VPP on PDMS, with a voltage of 200mV applied, when the PDMS underwent a UV-ozone treatment before the electrospinning, stretched at 50% 2 times, followed by a third stretch at 100%. The PDMS film broke during this third stretch.....64

LIST OF SYMBOLS AND ABBREVIATIONS

Ag	silver
Al	aluminium
Ar	argon
Au	gold
BEC	block copolymer elastic conductors
$CHCl_3$	chloroform
CNT	carbon nanotube
CTAB	cetyl trimethylammonium bromide
CVD	Chemical Vapor Deposition
DBSA	dodecylbenzene sulfonic acid
DEHS	di(2-ethylhexyl) sebacate
DMF	N,N-Dimethylformamide
DMSO	dimethylsulfoxide
ECM	extracellular matrix
EDOT	3,4-ethylenedioxythiophene
EGaIn	eutectic gallium indium
F8BT	poly[(9,9-dioctylfluorenyl-2,7-diyl)-alt-*co*-(1,4-benzo-{2,1′,3}-thiadiazole)]
Fe(III)Tos	iron(III) p-toluenesulfonate, or ferric *p*-toluenesulfonate
$FeCl_3$	iron(III) chloride, or ferric chloride
$FeCl_3 \cdot 6H_2O$	ferric chloride hexahydrate
FTIR	Fourier transform infrared spectroscopy
GO	graphene oxide
HCSA	amphorsulfonic acid

ICP	Intrinsically Conducting Polymer
LED	light emitting diode
MEH-PPV	poly[2-methoxy-5-(2-ethylhexyloxy)-1,4-phenylenevinylene]
Mw	Molecular weight
N_2	nitrogen
NaDEHS	di(2-ethylhexyl) sulfosuccinate sodium salt
NW	nanowire
oCVD	oxidative chemical vapor deposition
OECT	organic electrochemical transistor
P3DDT	poly(3-dodecylthiophene)
P3HT	poly(3-hexylthiophene)
PAN	polyacrylonitrile
PANI	polyaniline
PANI:HCSA	polyaniline doped with aphorsulfonic acid
PCBM	(6,6)-phenyl-C_{61}-butyric acid methyl ester
PCL	poly(ε-caprolactone)
PDMS	polydimethylsiloxane
PEDOT	poly-(3,4-ethylenedioxythiophene)
PEDOT-PIL	poly-(3,4-ethylenedioxythiophene) mixed with poly(ionic liquid)
PEDOT:PSS	poly-(3,4-ethylenedioxythiophene) doped with poly(styrenesulfonic acid)
PEDOT:Tos	poly-(3,4-ethylenedioxythiophene) doped with tosylate
PEEA	poly(ether-b-ester)
PEO	poly(ethylene oxide)
PET	poly(ethylene terephthalate)

PI	polyimide
PIL	poly(ionic liquid)
PLGA	poly(lactide-co-glycolide)
PMMA	poly(methyl methacrylate)
PPV	poly(phenylene vinylene)
PPy	polypyrrole
PPy-Tos	polypyrrole with p-toluenesulfonate
PS	polystyrene
PSS	poly(styrenesulfonic acid)
PTT	poly(trimethylene terephthalate)
PU	polyurethane
PVA	poly(vinyl alcohol)
PVF2-TrFE	poly(vinylidene fluoride-trifluoroethylene)
PVP	poly(vinylpyrrolidone)
SEBS	poly(styrene-co-ethylenebutylene-co-styrene)
SEM	Scanning Electron Microscopy
SIBS	poly (styrene-block-isobutylene-block-styrene)
SWCNT	single-walled carbon nanotubes
Tos	tosylate, or p-toluenesulfonate
UV	ultraviolet
VDP	Vapor Deposition Polymerization
VPP	Vapor Phase Polymerization
Zonyl	fluorosurfactant Zonyl-FS300

CHAPTER 1 INTRODUCTION

1.1 General context

Healthcare in our societies is currently seeking for innovative solutions, mostly because of the aging of the population and the rise in medical costs. One of the main objectives is personalized healthcare [1-2], which would give patients access to a more personalized medicine. A primary role in the creation of personalized healthcare systems will be played by materials and technologies that could allow the creation of more affordable and more specific healthcare systems. Systems and devices for personalized healthcare need to be both inexpensive and easy to use for non-professionals, so that patients can safely and properly monitor their conditions from home whenever required. Moreover, a more personalized access to healthcare should limit the use of invasive devices while promoting systems that are as non-obtrusive as possible [3]. For instance, diagnostic devices, such as biosensors, need to become less bulky, more flexible and stretchable, so that they can be put in direct contact with the human skin or integrated in wearables [4]. This would allow them to even be used as ambulatory systems, thus leading to easier ways to monitor the patients over long periods of time [5].

1.1.1 Stretchable electronics

Wearable and on-skin electronics require devices that maintain their electrical properties when a tensile strength is applied. These are known as “stretchable electronic devices”. The human skin can be stretched to a about 30% without breaking [6], although some authors report variations from 35% to 115% in the human population [7]. These differences in the literature can be explained by the changes in elasticity underwent by the human skin during life, since babies’ skins are a lot more elastic than seniors’ skins. With these values in mind, it appears important to ensure that a device in direct contact with a patient’s skin would be able to stretch at least as much, without rupturing or undergoing important changes that would render it unable to function. Stretchability of electronic materials can be achieved using two different and complementary approaches, i.e. by shaping the electronic components in a specific geometry, or by exploiting the intrinsic mechanical properties of the materials used.

1.1.2 Organic electronics

Biomedical applications such as biosensing require stretchable devices possibly made of materials that can be either functionalized or fine-tuned during their synthesis or the processing and that can be interfaced with a biological milieu. These specifications are achieved with organic conductors and semiconductors.

Electrical conductivity in organic materials was discovered in the beginning of the 1970's by H. Shirakawa, A.J. Heeger and A.G. MacDiarmid [8]. This discovery, that opened up the field of organic electronics, was awarded the Nobel Prize in 2000 [9]. Since then, organic electronic materials have been widely investigated due to their exciting properties for lighting, electronics and energy applications. There are a wide range of conducting or semi-conducting organic materials available, with virtually as many choices for one specific application. What is more, they are easily processed from solutions, and they allow ionic and electronic conduction, which allows them to be used as an interface with the biological milieu [10-11]. All these properties are intriguing for biological applications and thus lead to a wide investigation of these materials for biomedical applications.

1.1.3 Principles of electrospinning

During this work, a technique called electrospinning was used to obtain fibers of organic conducting polymers. This method consists of using an electric field between two metallic parts (one charged and one grounded) in order to cause a liquid to go from a nozzle (usually the charged part) to a mandrel (usually the grounded part) in the form of a jet, if the mixture presents satisfactory mechanical properties. The mixture can either contain a polymer in solution or a molten polymer. In the latter case, the technique is sometimes called "melt electrospinning".

The jet formed between the nozzle and the mandrel solidifies. This is done either by evaporation of the solvent used or by solidification of the molten polymer (case of the melt electrospinning). This allows to collect fibers made of the mixture materials. Electrospinning will be discussed more in detail in Chapter 2.

1.1.4 Principles of vapor phase polymerization

Another important technique called Vapor Phase Polymerization (VPP) was used during this work. In VPP, a monomer is evaporated in a closed chamber in the presence of a film containing an oxidant (or polymerization initiator). The evaporated monomer reacts with the oxidant and polymerizes directly on the film. This technique, when combined with electrospinning, allows to obtain fibers of conducting polymers. This will be discussed more in Chapter 2.

1.2 Problematics

This memoir focuses on the following problematics:

- How to produce stretchable conducting polymer fibers able to follow the natural human movements of the skin?
- Is it possible to pattern such materials to obtain a functioning device usable for complex applications?

1.3 Research objectives

This work was based around several objectives:

- The production of conducting organic fibers, first on a flexible substrate then on a stretchable one;
- The characterization of the stretchable fibers;
- The patterning of the obtained fibers to fabricate a functioning device usable for complex applications.

1.4 Organization of the memoir

This introductory chapter presented the context, the problematics and the research objectives that this memoir is meant to tackle. This introduction is followed by six other chapters. Chapter 2 consists of a literature review about the main topics of this work, i.e. stretchable electronics, electrospinning and vapor phase polymerization. Chapter 3 explains the different materials and methods used during this memoir. This chapter is divided into several sections, explaining substrate preparation, formation of the fibers with a method using a combination of electrospinning and

vapor phase polymerization, and their characterization. Chapter 4 is comprised of the article related to this work as it was submitted, and thus also includes the main results of this project. Supplementary results are presented in Chapter 5. Chapter 6 consists of a discussion, leading to conclusion and perspectives in Chapter 7.

CHAPTER 2 CRITICAL REVIEW OF LITERATURE

2.1 Stretchable electronics

Stretchability is a crucial property for several non-invasive biomedical applications, including artificial muscles [12], artificial skin [13-14], and on-skin devices [15], a category of systems placed directly on the user's skin in a conformable way, while being mechanically undetectable for the patient. Stretchable electronics can be used to achieve different functions, e.g. strain sensing, bio sensing, radio frequency induction, electrical sensing for the heart or the brain, motion detection [16]. By using stretchable electronic devices, a higher conformability to living tissues can be achieved [17], allowing for a better monitoring of biological parameters (e.g. cardiac rate, temperature, strain due to the contraction of the muscles, biomolecules concentrations) without putting any unnecessary strain on the patient's daily life [18]. Examples are stretchable sweat biosensors [19], heart rate monitoring devices [20] or techniques like surface electromyography [21]. As mentioned in the introduction, two different strategies can be used to achieve this intriguing property. The first one is to use specific shapes with particular geometrical properties that allow to get usually non-stretchable materials to stretch, using the fact that any material in thin form will be able to bend [22]. This method is mostly used for traditional electronic materials, since most of them are non-stretchable and it will be discussed in more detail later in this section. The second strategy is to use intrinsically stretchable materials to achieve the stretchability of the whole device. These two strategies can also be combined, particularly in organic electronics. Below I will discuss the methods used to stretch both non-stretchable materials for conventional electronics (e.g. metals) and organic electronic materials.

2.1.1 Stretching non-stretchable materials

Several methods have been developed to achieve stretchability with materials that are intrinsically non-stretchable. Most of these methods are based on the conversion of stretching motions into microscopic bending strains, thus linking stretchability to a more easily achievable flexibility. The peak strain experienced by a film during bending is linked to the substrate thickness, the film thickness and the radius of curvature according to the following equation (Equation 2.1) [23]:

$$\varepsilon = \left(\frac{d_f + d_s}{2r}\right) \times 100\%$$

Equation 2.1: Relation between ε the peak strain, d_f the thickness of the film, d_s the thickness of the substrate used, and r the curvature radius

The bending strain can be converted into tensile strain by using coiling and buckling [24], thus using flexibility to achieve stretchability. This means that by locally improving the flexibility of the materials with shape-engineering, stretchability of the whole structure can be achieved.

As for the methods used, they are diverse and require different levels of shape-engineering. Some groups focused on directly using the surface shape of the film deposited on top of a stretchable substrate, with the "buckling" method using vapor deposition or lamination directly on pre-strained elastomers used as substrates [25-26]. Once released, the film compresses and forms buckles, leading to the conversion of the stretching motions into unbuckling of the structure [27]. This leads to structures such as conductive "surface waves" that can be stretched flat [28] (Figure 2.1) and "wavy" silicon electronics [29-30]. These structures were even used in fully integrated circuits using single crystalline silicon in a wavy structure on stretchable elastomers [31]. In these different cases, the top structure is designed in such a way that it changes its form in order to accommodate the strain exerted on the whole device, while being mechanically supported by the underlying polydimethylsiloxane (PDMS) substrate, a clear semi-transparent silicon-based organic polymer widely used in stretchable devices. Once the force stops, the elastomer ensures that the original shape is restored. However, this is not the only available solution to obtain stretchable devices from non-stretchable materials. The controlled formation of micro-cracks during stretching on a film formed directly on a stretchable substrate can also ensure the uninterrupted stretchability and the conduction using percolated pathways [32]. Unfortunately, these quite simple methods yield materials with a limited ability to stretch: the films cannot be stretched more than a few tens of percent of their initial length without using a few tricks to boost the performance. Such "tricks" lead to a stretchability that can be improved up to 100%. This is done by increasing the roughness of the substrate, by pre-stretching it, and by raising the thickness of the metallic layer deposited [33].

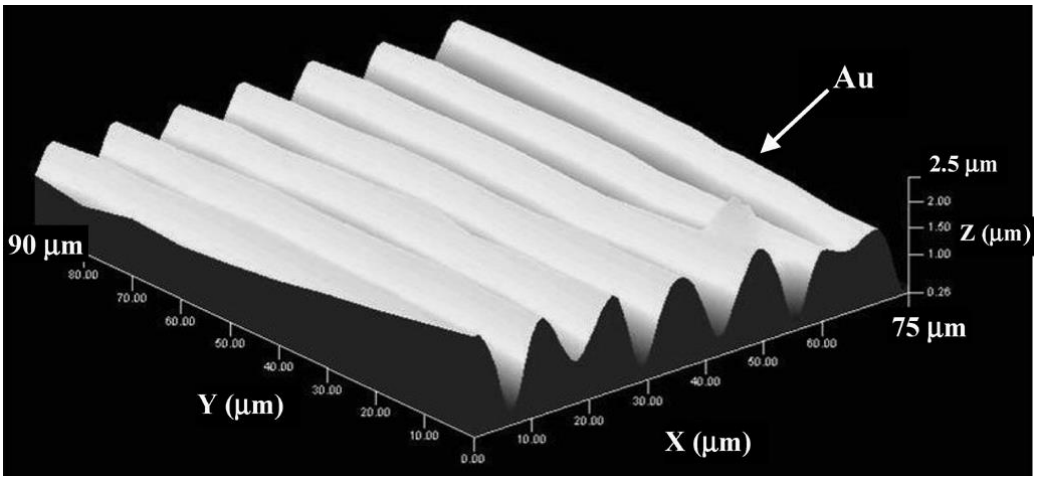

Figure 2.1: Three-dimensional profile of a Au surface wave after release from 15% pre-stretch [34-35]. © 2004 IEEE

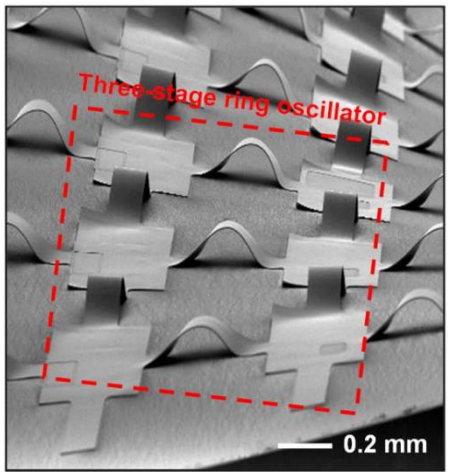

Figure 2.2: SEM image of an array of stretchable, 3-stage CMOS ring oscillators in a twisted configuration. [36] © 2008 National Academy of Sciences

Other groups rely on engineering the shape of the conducting materials in order to improve their stretchability. The shapes used to achieve this goal range from simple structures, such as highly stretchable (up to 370%) long metallic nanowires (NWs) [37] or hexagonal and triangular metallic nanosheets [38], to more complex structures, such as 3D pop-up structures that flatten when stretched [36] (Figure 2.2), or 2D ellipses and variations of horseshoe-like shapes [39] (Figure 2.3),

or 2D serpentine meshes [40] (Figure 2.4). These more complex shapes can yield stretchability to up to 300% [41].

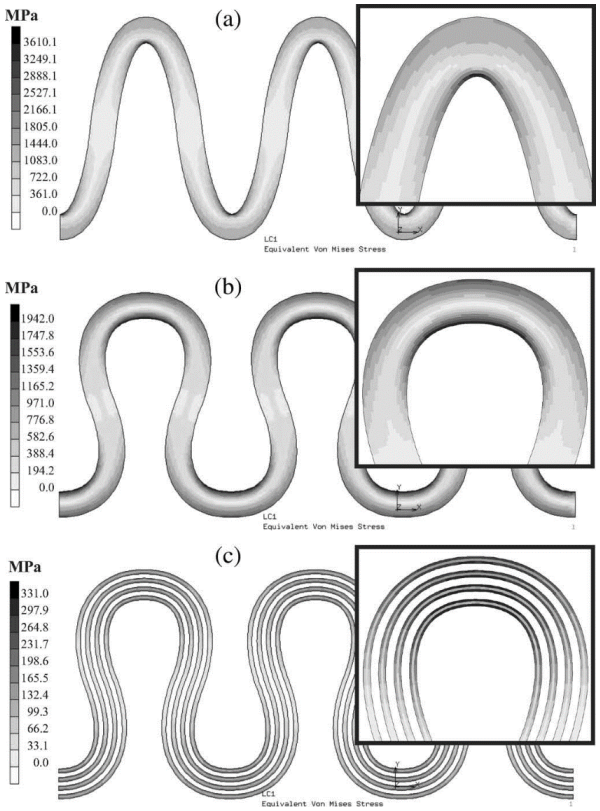

Figure 2.3: Finite element analysis (FEA) was used to estimate the internal stresses in several copper track patterns in the idealized case considering linear behavior (Young modulus E = 117 GPa) of the materials and neglecting the influence of any substrate material. By taking a horseshoe shape instead of an elliptical shape with the same wavelength/amplitude ratio, the maximum internal stress was reduced from 3610 to 1942 MPa. Splitting up the track into four parallel narrow tracks leads to a further reduction from 1942 to 230 MPa. (a) Elliptic. (b) Horseshoe. (c) Multitrack horseshoe. [39]

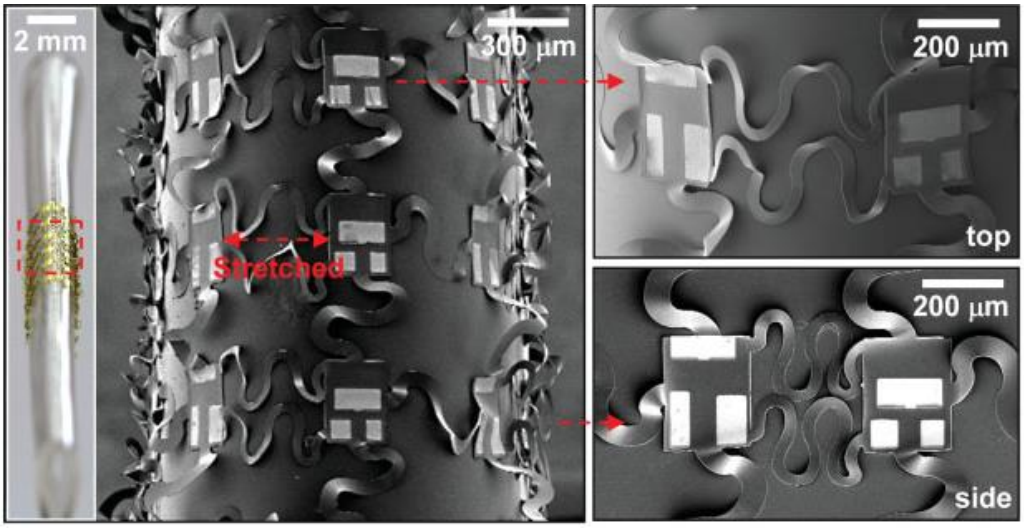

Figure 2.4: Optical image of a folded circuit (left) consisting of an array of CMOS inverters and scanning electron microscopy image (center). The images on the right provide views at the folded edge (right top) and side (right bottom). [40] © 2009 John Wiley and Sons

Silver (Ag) has been widely used to improve the conductivity of stretchable materials, either in the form of nanowires (NWs) or as flakes. Ag NWs embedded inside a PDMS elastomer were reported [42], while Ag NWs were also used with a carbon nanotubes (CNTs) percolation network to achieve conductive films that could be stretched to up to 460% before losing their conductive properties [43]. The use of CNTs or single-walled carbon nanotubes (SWCNT) was also widely studied and yields good results when trying to obtain stretchable electronics [44-46], allowing some groups to obtain conductivities as high as 100S/cm for films that could be stretched at more than 100% [47] while others managed to maintain a conductive behavior with strains superior to 700%, although they noticed the appearance of an increasing number of non-conductive areas the more they stretched their films [48]. Conductivities ranging from 5710 S/cm (at 0% stretch) to 20 S/cm (at 140% stretch) were also achieved by adding materials such as silver flakes in the CNTs structures [49]. The use of carbon paste supporting metallic pastes has also been reported for printable stretchable electronics. This method also required the use of an electrolyte gel to ensure the electrical contact between the two metals. The devices were completed by enclosing the pastes and the gel inside an elastomer structure (Figure 2.5), thus ensuring that the metallic pastes do not physically contact with each other during the stretching [50]. Graphene oxide (GO) was also used several times. In particular, it was used in combination with Ag NWs for a fully-stretchable LED

[51]. Carbon-based inks were also used to print fully stretchable devices embedded inside highly stretchable elastomers, by using a method called embedded 3D printing [52]. Finally, transfer methods allow for the production and patterning of the films on a solid substrate before transferring them on stretchable substrates such as PDMS [53]. All these solutions allow for the use of non-intrinsically stretchable organic and inorganic materials in complex systems.

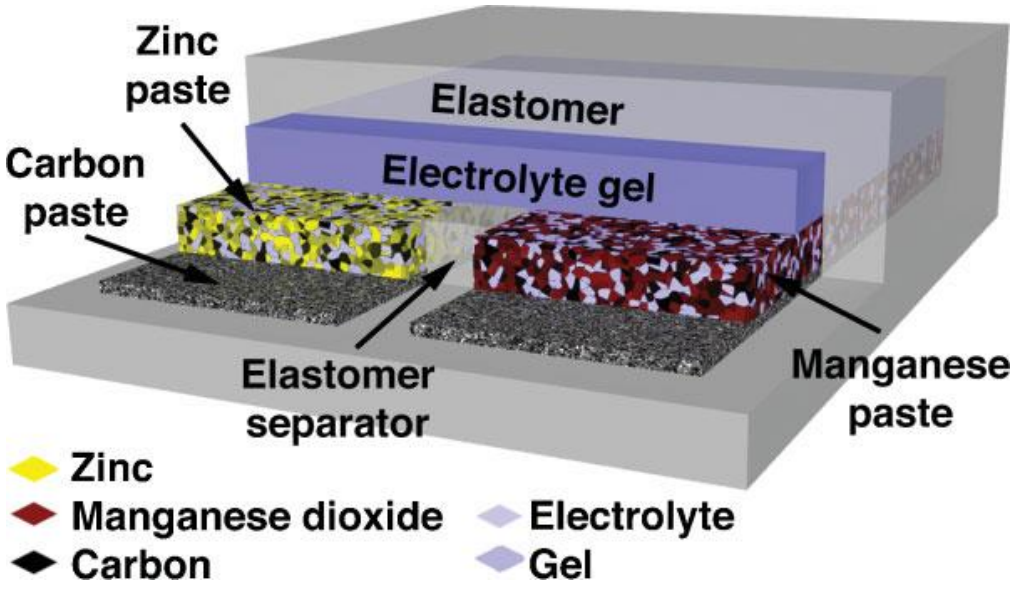

Figure 2.5: Scheme of a compliant zinc carbon dry gel cell. The cell is based on pastes as electrodes, chemically active cells, and an electrolyte gel to close the circuit. Intermixing and short-circuiting of the electrochemical power supply are prohibited by laterally separating the electrodes with an elastomer separator [50]. © 2010 John Wiley and Sons

2.1.2 Organic materials for stretchable purposes

The strategy based on shape-engineering of the materials is not solely limited to purely inorganic materials. Some authors developed devices using non-stretchable platforms called “islands” connected by stretchable organic electronics; by using the geometry of the elastomer substrates, the strain can be limited to the connections, thus protecting the more brittle electronics [54]. Other authors used matrix shapes [55] or honeycomb meshes [56] to obtain fully stretchable organic devices.

Another strategy using both organic and inorganic is to include organic materials such as polyacrylate composites [57] in the conducting materials to obtain stretchable metallic-organic devices. The opposite strategy of adding inorganic materials, in particular conductive nanoparticles or CNTs, into organic elastomers can also yield good results, with a stretchability as high as 600% obtained by including silver flakes into a polyurethane (PU) elastomer [58].

However, due to the large spectrum of mechanical properties shown by organic materials, intrinsically stretchable organic materials are also widely studied for stretchable devices, to be used either alone or in combination with a shape designed to improve the stretchability of the system. Simple films made of poly-(3,4-ethylenedioxythiophene) doped with poly(styrenesulfonic acid) (PEDOT:PSS), a widely used conducting polymer, mixed with a fluorosurfactant, for example Zonyl-FS300 (Zonyl), and with dimethylsulfoxide (DMSO) as a secondary dopant already yield good stretchability results [59]. It was also reported that using the slightly brittle surface created on PDMS by the UV-ozone treatment allowed the formation of wavy structures in films composed of PEDOT:PSS mixed with Zonyl and DMSO. These structures allowed the films to be reversibly stretchable with conductivities as high as 550S/cm for a 0-188% stretchability [60]. PEDOT:PSS can also be used with other compounds, such as a blend of regioregular poly(3-hexylthiophene) (P3HT) and (6,6)-phenyl-C_{61}-butyric acid methyl ester (PCBM) (P3HT:PCBM) and processed as a film on a PDMS substrate for applications in stretchable organic solar cells in a sandwich structure. This resulted in a 0-25% stretchability, with a surface resistivity of around 750 Ω/sq [61]. In another work, PEDOT mixed with a poly(ionic liquid) (PIL) or PEDOT-PIL was used to increase the miscibility of PEDOT with a non-conducting elastomeric polymer called poly(ether-b-ester) (PEEA) so that an homogeneous blend of the two polymers could be obtained. A stretchability as high as 350% was obtained, although the resultant surfacic resistivity was quite high, with a value of 8.10^8 Ω/sq [62]. More recently, a blend of PEDOT:PSS and PU was reported for a pressure sensor using PDMS shaped as a micro-pyramids array. The blend was used to form electrodes on top of the pyramids, and thus was required to keep a high conductivity (around 168 S/cm for a blend with 60 wt% PU, and around 120 S/cm for the 73 wt% PU blend) [63]. Work was also done to improve the geometry of the PEDOT:PSS used, for example by making nano-arches out of a nanowire of PEDOT:PSS that led to a stretchability as high as 240% without having to compromise on the electrical conduction, keeping a 200S/cm conductivity during the whole stretching [64].

Some of these organic materials achieve a conductivity high enough to be used as electrodes, as reflected in the use of stretchable polypyrrole (PPy) with p-toluenesulfonate (Tos), or PPy-Tos electrodes for battery applications. The PPy-Tos electrodes are placed on top of an Au/poly (styrene-block-isobutylene-block-styrene) (SIBS) substrate and can stretch up to 30%, with a surfacic resistivity going up from 171 Ω/cm^2 (0% stretch) to 240 Ω/cm^2 (30% stretch) after 2000 cycles [65]. High conductivity in stretchable electronics is also achieved with more complex structures, such as "block copolymer elastic conductors" (BEC) based on conductive polyaniline (PANI) and the block copolymer poly(styrene-co-ethylenebutylene-co-styrene) (SEBS) [66], or by using SWCNT-polymer composite electrodes [67]. Metallic conductivities were also achieved by directly injecting the liquid metal eutectic Gallium Indium (EGaIn) in hollow fibers made of SEBS. This resulted in a very high conductivity, coupled with an ultra-high stretchability of 700% [68].

2.2 Fibers

2.2.1 Interest of fibers

One-dimensional nanostructures such as nanofibers, nanotubes or nanowires have been largely studied in the recent years. This is due to their intriguing properties related to their small size. Fibers present a real interest in stretchable and wearable devices. They exhibit a good flexibility and tensile strength, and can thus be stretched, twisted, bent or sheared [69]. Due to their mechanical properties and their usually light weight [70], they can be used for textiles and thus are the more obvious candidates for wearable electronics or intelligent clothing [44] [71] and more specific applications such as artificial muscles [12]. They also exhibit a high surface area and a good flexibility regarding their surface functionalization [72]. These properties make them excellent candidates to achieve both the stretchability and the high functionality required for applications in the biomedical field, in particular for wearable biosensors. Conducting fibers thus present the double advantage of being usable for wearable applications and for electronic applications, rendering it possible for the development of smart textiles [73] for smart or intelligent clothing [74] that could then be functionalized for specific applications. Due to the fibers flexibility and stretchability, it would allow for intelligent wearable systems that are non-obtrusive, by avoiding bulky options for biomedical applications [5]. Sensors based on fibers have already been

demonstrated by several groups [75-76], rendering it possible to use them more widely for biomonitoring in the future. The path of wearable sensors has already been opened by several groups [77-80] but more work on the materials is necessary to improve the already encouraging results obtained.

2.2.2 Fabrication methods

Several methods exist to produce fibers from polymers. This section will focus on explaining some of the main methods used in literature by different groups. As for the electrospinning process, it will be discussed in the next section.

2.2.2.1 Drawing

Drawing is a method consisting of pulling a mixture over a relatively long distance to obtain a thin liquid fiber. Two drawing techniques are typically employed: dry spinning and melt spinning, which differ by the way the fibers are obtained from the original mixture. Once the mixture is drawn, the evaporation of the solvent (dry spinning) or the solidification of the whole mixture due to cooling (melt spinning) yields solid one-by-one fibers. In the case of melt spinning, heating of the mixture before drawing is necessary [81]. The melt spinning technique is explained in Figure 2.6. This method requires the use of a highly viscoelastic material that can undergo strong deformations and still stay cohesive enough to avoid ruptures during the drawing process due to stress [82]. If the material used satisfies this constraint, drawing is a fast, easy and cheap method to obtain one-by-one single fibers. Diameters as low as 60 nm have been reported with poly(trimethylene terephthalate) (PTT) [83]. However, some materials do not fulfill these requirements and cannot be drawn. Drawing has been demonstrated for the polymers polyethylene (PE), polypropylene (PP), polyoxymethylene (POM), nylon-6 (Ny-6), polyvinylalcohol (PVA) [84], PTT [83], mixtures of SWNT and poly(methyl methacrylate) (PMMA) [85] as well as mixtures of SWNT and PVA [86].

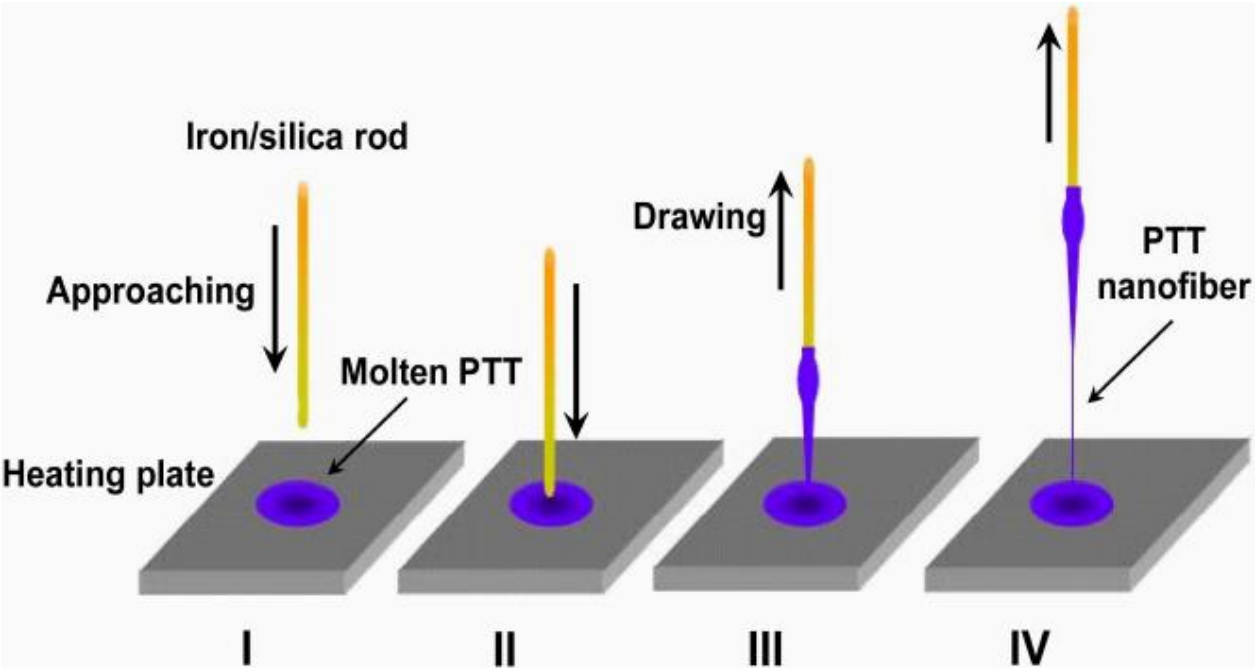

Figure 2.6: Schematic illustration of nanofibers fabrication by direct drawing process from molten poly(trimethylene terephthalate) (PTT). I, An iron or silica rod is approaching the molten PTT. II, The rod end is immersed into the molten PTT. III, The rod conglutinated PTT is being drawn out. IV, A PTT nanofiber is formed. [83] © 2008 Optical Society of America

2.2.2.2 Wet-spinning

Wet-spinning is a method in which the desired polymer or other material is in solution inside a spinneret, a device used to form fibers. The liquid is slowly pushed out of the nozzle immersed into a solvent bath, in which it coagulates in the form of fibers [87]. Once the fibers are formed, they can be collected using a take-up system, so that the total time spent in the solvent is carefully controlled, or stay in the solvent until the end of the spinning process for less-controlled processes. A coagulation solvent adapted to the specific solution is necessary for this process to yield fibers, as shown on Figure 2.7.

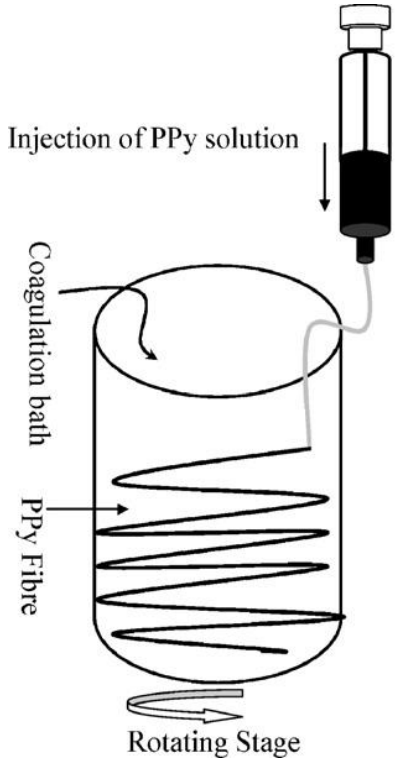

Figure 2.7: Schematic diagram of a wet-spinning apparatus [88]. © 2007 Elsevier

This method has been used to produce conductive fibers. In particular, PEDOT:PSS conductive microfibers by using acetone as the coagulation bath [89-90], polyaniline (PANi) in a coagulation bath of either acetone, butyl acetate or 4-methyl-2-pentanone [87], poly(pyrrole) (PPy) in a coagulation bath of 40wt% dimethyl formamide (DMF) in water [88], continuous macroscopic graphene fibers in a coagulation bath of hexadecyltrimethyl ammonium bromide (CTAB) solution [91] and graphene oxide fibers in liquid nitrogen [92]. Wet-spinning was also used for several non-conductive materials, including poly(lactic acid) [93] and natural cellulose [94],

The wet-spinning process requires the use of a solvent where the fibers will be formed. As such, this process can be more expensive and less eco-friendly than other processes mentioned in this section, such as drawing [93].

2.2.2.3 Template synthesis

Template synthesis is a method based on the utilisation of a template (usually a nanoporous membrane) to form nanofibers. The templates used can also be of various kinds. They can be small features like step-edges or V-shaped grooves on solid substrates; channels inside of porous materials; self-assembled structures such as cylindrical micelles made of surfactant molecules; or they can be made of a pre-existing nanofibers or nanowires [95] on which the material of interest is grown, for example using vapor phase polymerization. In this last case, another fabrication method yielding nanofibers is obviously required to produce the pre-existing structure that will serve as the template.

Due to the high diversity of techniques that can be labelled as "template synthesis", this method presents the main advantage of being usable for the fabrication of several kinds of materials, including electronically conducting polymers, metals, semiconductors, metal oxides, carbon, and composite materials [96]. To form the nanofibers, several methods are possible, depending on the material, e.g. sol-gel processing, electrochemical synthesis, in-situ polymerization, chemical vapor deposition. The membrane or template used is generally destroyed in the process to recover the nanofibers formed within, e.g. by etching. This low-cost and rapid method yields well-ordered bundles of nanofibers either with a solid shape, called "fibrils" or with a hollow shape, called "tubules" [97]. However, it cannot easily be used by itself to produce long continuous one-by-one fibers, and it is limited by the necessity to find inexpensive templates adapted to the required dimensions. A variety of materials have been used to produce fibers by template synthesis, including metals such as lithium [98], gold, palladium, nickel, and tantalum [99] or germanium [100]; semiconductors such as silicon [101] or cadmium sulfide [102]; polymers such as PPy [103] or PANI [104]; and even polymer-metal hybrid nanotubes [105].

2.2.2.4 Phase separation

Phase separation is a relatively complex and long five-step process allowing the transformation of a solid polymer into a nano-porous foam [106]. The first step consists of the dissolution of a polymer into a suitable solvent, followed by phase separation and gelation, solvent extraction from the gel with water, freezing and finally by a freeze-drying under vacuum step [107]. This method yields membranes without going through the full textile processing, with several control parameters

to change the morphology of the final product, such as gelation time and temperature (which can also be changed during the process). However, phase separation is relatively complex and requires a long processing time to obtain the final product.

This method is well-adapted for structures requiring scaffolds made from polymers, such as polyester [107], poly(α-hydroxyl acids)/hydroxyapatite porous composites [108], poly (L-lactic acid)/apatite composites [109], but also simple poly (L-lactic acid), poly (D,L-lactic acid) and poly (D,L-lactic-co-glycolic acid) [110] and nano-hydroxyapatite/poly (L-lactic acid) [111].

2.2.2.5 Self-assembly

Self-assembly is a process in which pre-existing components assemble in a way that can be controlled by designing the "disordered" components properly so that they assemble in the intended way. Different kinds of interactions can be used to achieve the self-assembly, such as van der Waals, electrostatic, hydrophobic interactions or hydrogen bonds, to the macroscopic level with gravitational or electromagnetic interactions among others. Regardless of the interactions that take place in one specific self-assembly process, it is always necessary that the different components are easily able to move and thus do not irreversibly aggregate together after colliding. This necessity to achieve movement between the different components makes it more common to obtain self-assembly processes in fluids or on smooth surfaces [112].

Self-assembly processes that do not correspond to any of the other categories mentioned in this memoir have been reported in the literature to yield nanofibers. In particular, a group reported the formation of nanofibers by a selective photo-cross-linking of the cylindrical domains of a bulk block copolymer [113-114]. Others reported the pH-induced self-assembly of a peptide-amphiphile into a scaffold made of fibers. This rendered a structure similar to the extracellular matrix (ECM) [115].

2.2.3 Electrospinning

Electrospinning is a process in which an electrical field is used to form a jet from a polymer solution. The jet travels from a nozzle to a metallic collector as the solvent evaporates, thus forming a solid fiber that is collected directly on the metal [116]. One of the many possible setups is shown

in Figure 2.9. This process is similar to the dry, melt and wet spinning processes described above, with the notable difference that the force used to draw the fiber is electrical [75]. It is all at once a versatile, simple, inexpensive and scalable method to produce fibers [117].

In this section, a brief history, the working principle and the applications of electrospinning will be presented.

2.2.3.1 A brief history of electrospinning

Although its history has roots in the early days of science in the 17th century [118], the electrospinning method was first invented in the beginning of the 20th century, when John Francis Cooley obtained the first patents about it in 1900 in Great Britain [119] and in 1902 in the US [120]. The same year, another US patent related to electrospinning was published by William James Morton [121], followed by several other international patents by different inventors more than 20 years later [122-123]. Anton Formhals patented in 1931 (in France) [124] and in 1934 (in the US) an electrospinning process and apparatus, and then kept on depositing more than 20 patents related to electrospinning between 1931 and 1944 [125-128] in the US, France, Germany and UK. The further development of this method was however hindered by technical limitations. This explains why it only became a popular technique twenty years ago, around the year 1997, when the term "electrospinning" was coined [106].

The apparatus designed by Formhals in 1934 allowed to produce and collect cellulose acetate fibers on a mobile belt. However, the spinneret and the collector were too close, preventing the complete evaporation of the solvent before the fibers hit the belt. This led to fibers that tended to stick to each other as well as to the collector. In his second design in 1939, Formhals solved this problem by increasing the distance between the spinneret and the collector. Formhals also introduced the first electrospinning process with several spinnerets, worked on different nozzle designs, made shorter fibers by interrupting the liquid current flow, worked on a way to control the fibers formation by controlling the electric field, proposed a design to electrospin composite fibers, and made serious attempts at collecting the fibers in a directly usable form by designing different winding devices to do so.

In the mean time during the 1930's, Nikolai Albertowich Fuchs was also working on electrospinning in the Aerosol Laboratory in the L. Ya Karpov Institute in the USSR. He and co-workers managed to use electrospinning to produce commercial filters, named after one of their

inventor, the "Petryanov filters" [129]. These filters were later used in gas masks and as a protection from nuclear-active aerosol releases, radioactive particles released in the air through ventilation stacks in nuclear power plants. As such, this technique was not disclosed to the western world for decades, being considered a military secret in the Soviet Union.

The theory of electrospinning takes root in the theory of another technique called electrospraying, a method used to spray a liquid into small charged droplets directly on a surface. This other method has been used for applications in mass spectrometry as the ionization source [130] and in drug delivery to allow for a smaller dosage of the drug [131]. The theoretical study of both electrospinning and electrospraying started in 1907, when Zeleny began a series of papers in which he studied the electrical discharge of a liquid or a solid surface and the effects of various parameters on the discharge [118]. In particular, between 1914 and 1917, he worked solely on the discharge from a liquid surface [132-133], laying the foundation of the theoretical studies of electrospinning and its sister method electrospraying. In 1953, Bernard Vonnegut and Raymond L. Neubauer developed an apparatus for electrical atomization able to produce streams of highly electrified droplets with uniform diameters around 0.1mm [134], leading to the further development of electrospraying. Further work was performed by Vadim G. Drozin in 1955 who managed to obtain highly dispersed aerosols composed of relatively uniform droplets [135].

In 1966, a patent by Harold L. Simons disclosed a method to produce patterned non-woven fabrics [136] with an electrospinning method. The most viscous solutions yielded relatively continuous fibers whereas the less viscous solutions yielded fibers that tended to be both shorter and finer.

In 1969, Sir Geoffrey Ingram Taylor published a significant work on the theory behind electrospinning, including a mathematical model of the shape of the cone formed by the fluid at the tip of the nozzle when put in the presence of an electric field [137]. This characteristic shape has since been renamed Taylor cone. This study led to a better understanding of the necessary conditions for electrospinning to work.

In 1971, Peter Karl Baumgarten designed an electrospinning apparatus able to electrospin acrylic fibers with diameters ranging from 50 nm to 1.1 μm and devised a way to take photographs of in-flight electrospun fibers [138]. This allowed him to investigate the effects on fiber diameter and jet length of several parameters, among which the solution viscosity, the voltage and the jet radius.

This also allowed him to confirm that the electrospinning process yields one single fiber, although the spun filament loops a lot when electrospun.

The electrospinning process as described by Baumgarten is the one that has been used since the 1980's, with slight variations depending on the authors and the applications. In recent years, the electrospinning process regained the scientific community's attention and has been largely studied, as can be seen in Figure 2.8, showing the number of publications related to electrospinning by year since 1997 (source: database Web of Science™). The increase in the number of publications related to electrospinning in the recent years has been almost constant, with a considerable growth between 1997 and 2014.

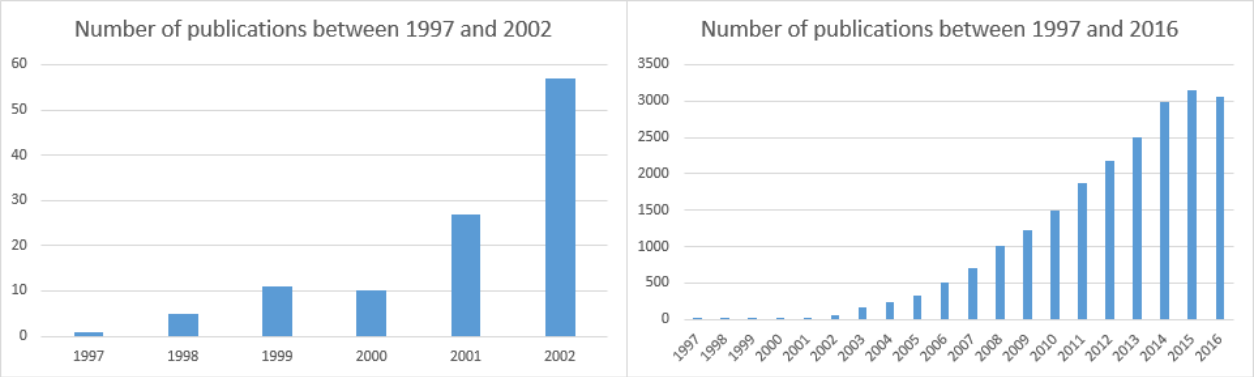

Figure 2.8: Number of publications in the database Web of Science(TM) containing the words "electrospinning", "electrospun" or "electrical spinning" since 1997. The histogram on the left shows the detail between 1997 and 2002, while the one on the right shows all the results for the years 1997 to 2016. The results were obtained on the 01/10/2017.

2.2.3.2 Working principle of electrospinning

The general setup used in electrospinning is displayed on Figure 2.9. This setup is similar to the one used in electrospraying. Due to this similarity, electrospinning greatly benefits from the knowledge obtained by studying the theory behind the electrospraying method, as was mentioned in the history part.

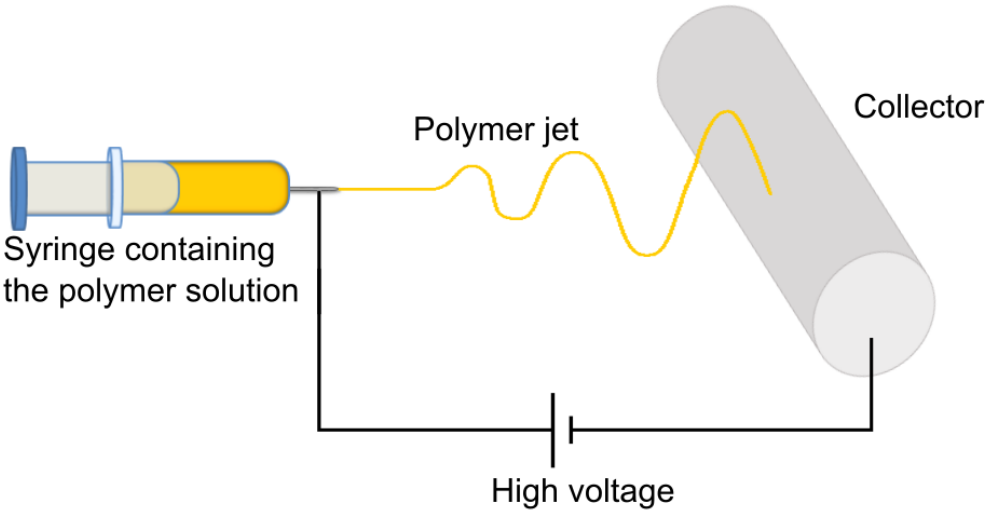

Figure 2.9: Schematic drawing of an electrospinning setup. The syringe is usually connected to a syringe pump to ensure a constant flow rate in the nozzle. The mandrel (or "collector") can be made in different shapes and composed of different materials. It is usually grounded or put at a slightly negative voltage (around -3 kV), while the syringe is put at a high voltage (tens of kV).

In electrospinning, the surface tension holds the polymer in a continuous form, despite the mutual repulsion between the charges induced inside the liquid by the electric field. The charge injection is therefore a critical step of the process. It can be done directly by induction in the case of a fluid with a conductivity in the order of 10^{-2} S/m [139]. In the case of polymer melts and other non-conductive fluids, the charge injection can be realised directly into the fluid by using two electrodes, with one in direct contact with the fluid [140].

Once the charges are injected, the process requires the surface tension to be overcome for a jet to be formed. Sufficient increase of the electric field intensity leads to the elongation of the hemispherical liquid surface at the nozzle into a conic shape, known as the Taylor cone [137]. By increasing the electric field intensity even further, the equilibrium is broken and the repulsion between the charges overcomes the surface tension. This results in the ejection of a charged jet from the Taylor cone, following the electric field (Figure 2.10). The fact that the jet is ejected from the top of the cone explains why electrospinning can yield fibers with a diameter noticeably smaller than the nozzle diameter.

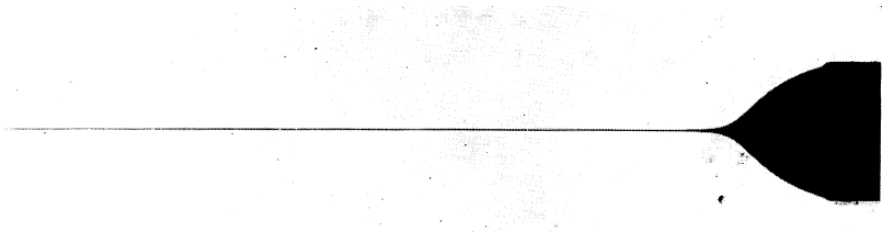

Figure 2.10: First 1.4cm of a glycerin jet 4.66 cm long, showing the structure known as Taylor cone on the right, at the tip of the nozzle [137]. © 1969, The Royal Society

The formation of the jet and the cone was studied more recently by Darrell H. Reneker and Alexander L. Yarin [141]. They recorded a frame every 2 ms to highlight the important parts of the process. The main steps of the formation of the Taylor cone and the jet are shown in Figure 2.11. The round drop becomes sharper in presence of an electric field, until the jet breaks from the tip. After that, the elongated drop went back to a rounder shape, the one known as "Taylor cone". This final shape, shown on the last picture of the Figure 2.11, was stable according to the authors. They reported the ability to maintain the shape whilst sufficient solution was still provided to the tip.

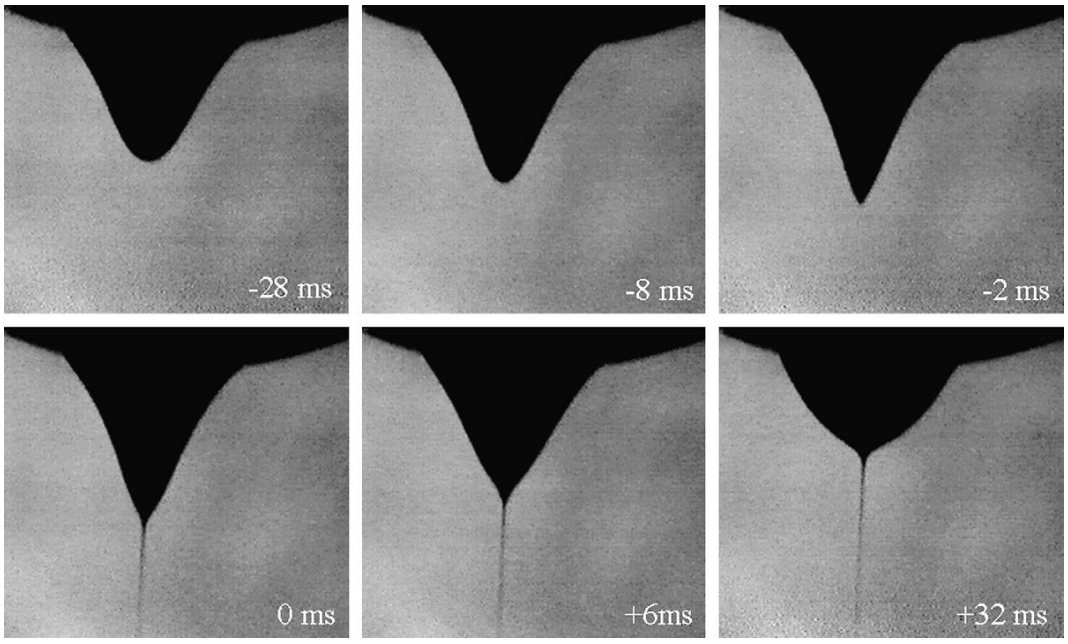

Figure 2.11: Evolution of the shape of a fluid drop. The time 0 was chosen as the time when the jet first appeared. The electrical potential was applied for a little more than 28 ms earlier. The first picture (-28 ms) thus shows the elongation of the drop into a cone-shape due to the electrical potential. The second (-8 ms) and third (-2 ms) pictures show the further elongation of the drop

into a cone, followed by the apparition of the jet (0 ms). Finally, the shape rapidly changed into a rounder one, in the form of the Taylor cone (+32 ms). This last shape was stable as long as enough fluid was brought to the nozzle to compensate for the fluid lost in the jet [141]. © 2008 Elsevier

The "cone-jet" regime is specific to electrospinning, and represents the first step of the fibers formation. The liquid jet is attracted towards the collector (usually grounded) in the form of a very thin and continuous filament as it follows the electric field formed by the nozzle at high potential and the grounded collector. This electric field has a complex behavior since the charges inside the liquid jet itself tend to affect it. During the fluid travel between the spinneret and the collector, jet instabilities commonly appear. Among these, the "whipping" instability is the most common. In this regime, the jet shifts laterally from the nozzle-collector direction. Examples of this instability can be seen on the Figure 2.12. Another important instability in electrospinning is the one called "droplet break-up". In a similar way to the process behind electrospraying, part of the fluid manages to leave the nozzle as droplets. Instabilities in electrospinning are currently still an object of study, with authors developing models to understand it better.

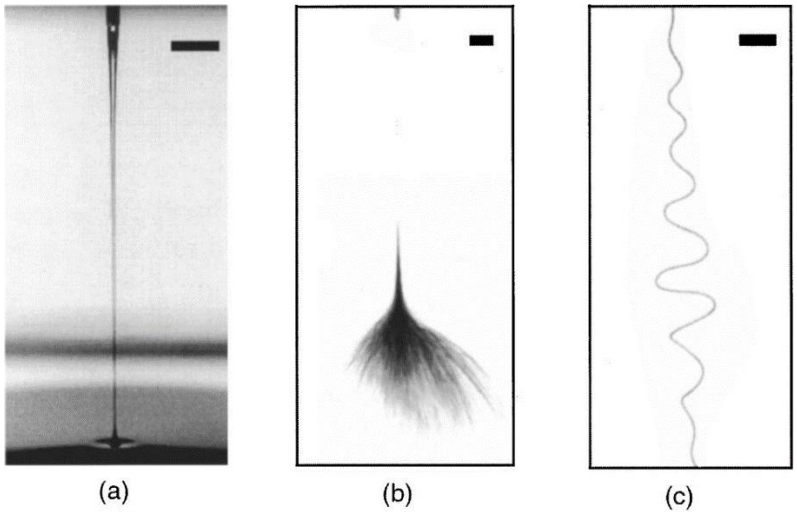

Figure 2.12: Jet images of a 2 wt% solution of PEO (Mw = 2 000 000) in water during electrospinning. (a) Stable jet (scalebar = 5 mm); (b) unstable jet (scalebar = 5 mm, 1 ms exposure); (c) close-up of the onset of instability (scalebar = 1 mm, 18 ns exposure) [142]. © 2001 AIP Publishing LLC

An important work for the study of the instability in the electrospinning jet was performed by Darrell H. Reneker, Alexander L. Yarin, Hao Fong and Sureeporn Koombhongse in 1999. The authors calculated the three-dimensional paths of the continuous jets both in the nearly straight region (when the instability is still low) and in the further region, where the instability dominates the path of the jet [143]. They highlighted that the usual path of the jet was composed of a straight segment that is followed by a coil of increasing diameter. This first bending instability is then followed by a second bending instability, as a smaller second coil starts from the first coil, as shown on Figure 2.13. A third and even a fourth bending instability can also occur if the jet is long enough.

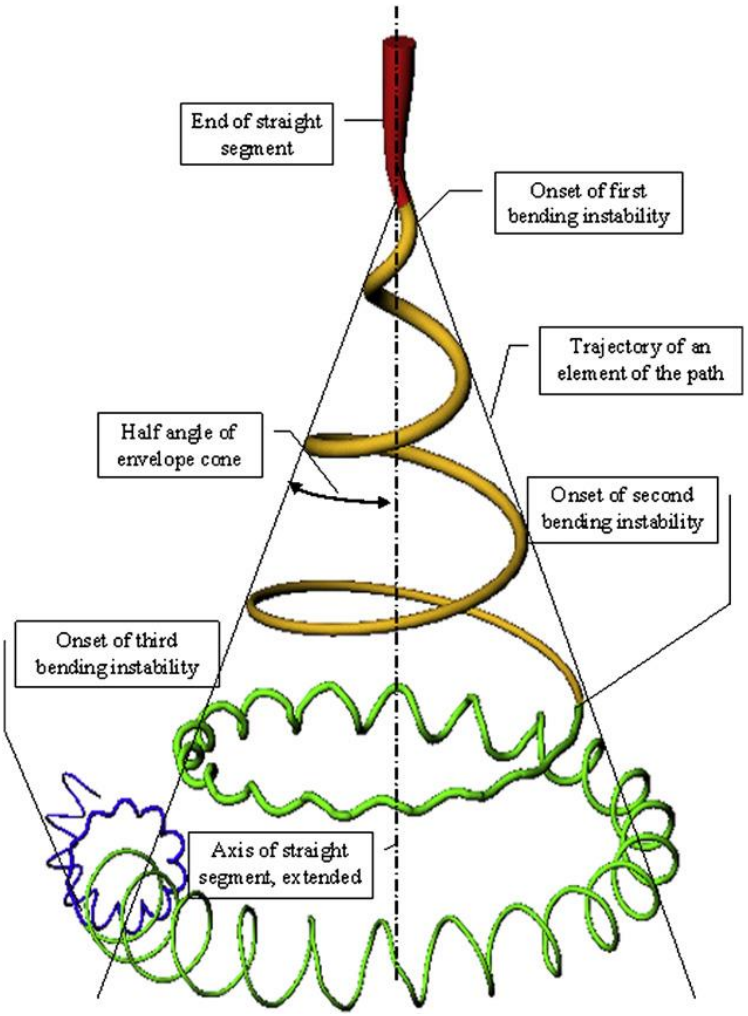

Figure 2.13: Schematic diagram of an electrospinning jet, showing three different levels of bending instability [141]. © 2008 Elsevier

2.2.3.3 Parameters of interest in electrospinning

Several parameters were identified to affect the electrospinning process in a work realized by Jayesh Doshi and Darrell H. Reneker as early as 1993 [116]. These parameters can have an effect on the diameter of the fibers or on the morphology of the film, with for example the appearance of "beaded structures" (Figure 2.14) on the fibers.

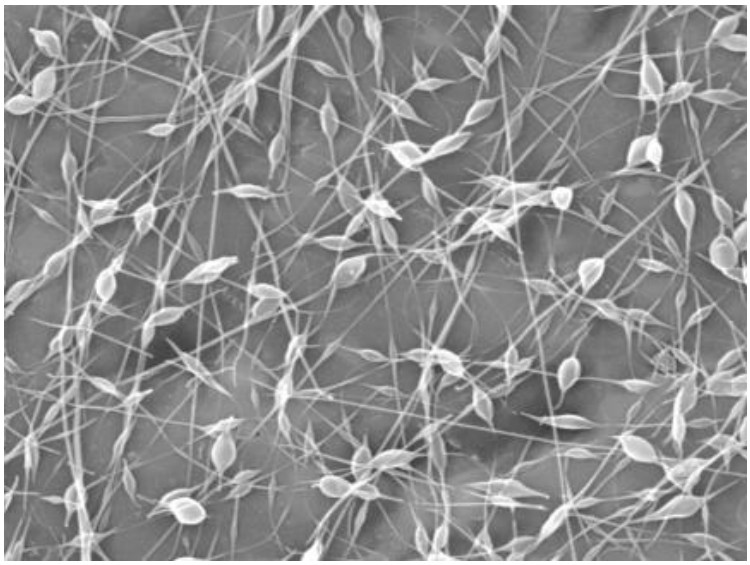

Figure 2.14: A scanning electron microscopy (SEM) picture of beaded fibers [144]. © 1999 Elsevier

These parameters can be divided into three main categories: the solution properties, the variables set by the experimenter, and the ambient parameters. The solution properties relevant for electrospinning include viscosity, elasticity, surface tension, and conductivity. Some parameters can be easily set by the experimenter to change drastically the final results, including the distance between the spinneret and the collector, the flow rate at the tip of the nozzle (adjusted by controlling the pressure inside the spinneret), and the electric potential at the tip (or voltage between the nozzle and the collector). Ambient parameters can be controlled to a certain extent, and include the solution temperature, relative humidity, and even the air velocity inside the chamber used for the electrospinning process. A few more parameters can be identified in particular setups, most of them due to the use of a specific collector, and in particular of a rotating or moving collector.

A review by Travis J. Still and Horst A. von Recum [145] highlighted the impact of several of these parameters on the diameter of the fibers, on their morphology and on the appearance of beaded structures (Figure 2.14). These results are summarized in Table 2.1, together with results from more recent works [146].

Table 2.1: Effect of different parameters on the diameter and the morphology of electrospun fibers.

Parameter	Fiber diameter	Effect on the morphology of the fibers
Applied voltage ↑	Initially ↓ then ↑	Beads appear on the structure with very high voltages [147]
Flow rate ↑	↑	Beads if the flow rate is too high
Nozzle diameter ↑	↑ [148]	-
Nozzle to collector distance ↑	↓	Beads if the distance is too short
Polymer concentration (viscosity) ↑	↑	-
Relative humidity ↑	↓ [149]	-
Solution conductivity ↑	↓	-
Solution viscosity ↑	↑	Beaded structure then droplets form instead of fibers when the viscosity becomes too low [150]
Solvent volatility ↑	-	↑ in the number of pores (↑ in the surface area)

2.2.3.4 Collectors used in electrospinning

The choice of the collector has a huge impact on the appearance of the fibers. Depending on the collector used, very different results can be obtained. The first electrospinning design by Anton

Formhals used a mobile belt as the collector [123]. More recent experiments at the end of the 1990's were performed using a simple metal plate as the collector (Figure 2.15 (a)). Due to its simplicity, this kind of collector is still widely used, although new types of collection systems were also developed. Rotating drum-like collectors (Figure 2.15 (b)) are commonly used to collect fibers in a more uniform way, either on large (fully-metallic collectors) or small surfaces (insulated collectors with only a metallic ring). These collectors can also be used to slightly reduce the diameter of the fibers or to improve their alignment to a certain extent by increasing the rotation speed of the drum.

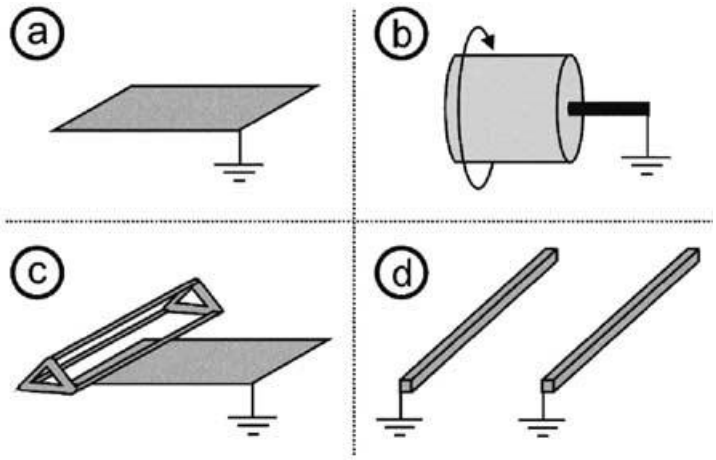

Figure 2.15: Scheme of various kinds of collecting systems used in electrospinning, showing (a) a metal plate collector, (b) a rotating drum, (c) a triangular frame placed near a single plate and (d) a parallel dual plate. [151] © 2004 Elsevier

Although non-woven fibers can be used for filtration [152-153], sensing [154], drug delivery [155], tissue scaffolds [156] and wound dressing [157], uniaxially aligned fibers have also attracted a lot of attention. The alignment can be used in biology, for example to facilitate the synthesis of collagen when mimicking the extracellular matrix [158] or in a more general way to give the cells a preferred growth direction [159]. Aligned fibers can also be used in other fields, for example as a reinforcement of a pre-existing structure [159] or to produce aligned carbon nanofibers from PANI nanofibers precursor [160] among others. Thus, some authors tried to design collectors to achieve this goal. One such design was proposed in 2003 [161]. This design uses the electrostatic

interactions to force the charged fibers to stretch in order to span across the gap between the two rods (Figure 2.16). The gap can either be a “void gap” (nothing between the two conducting rods) or an “insulating gap” (an insulating substrate patterned with conducting electrodes used as the rods). The authors demonstrated that when a void gap was used, the fibers could be transferred onto other substrates for direct application, while in the case of an insulating gap, it was possible to selectively modify the pattern of the aligned fibers by designing the pattern of the electrodes. In both cases, the obtained fibers were stackable and thus could be used as multi-layered structures [162].

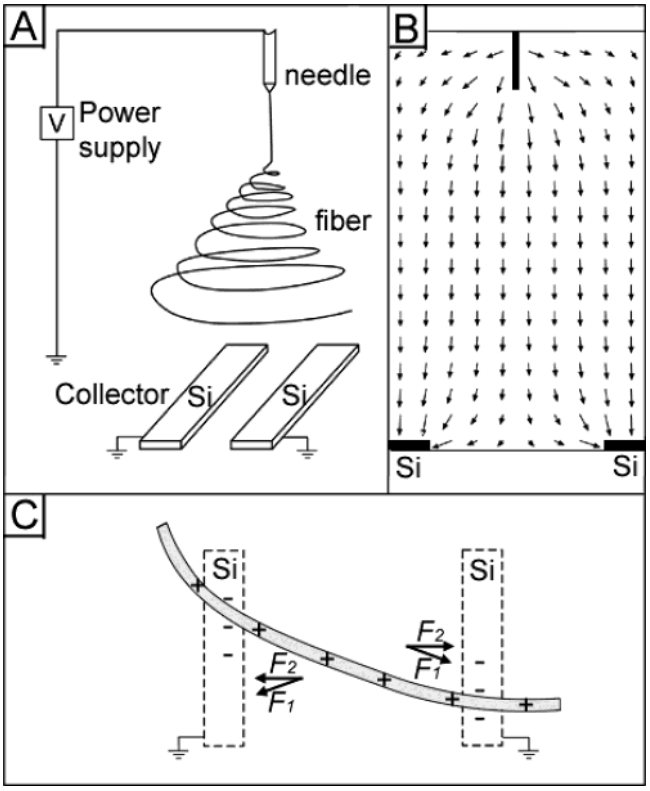

Figure 2.16: (A) Schematic illustration of the setup for electrospinning used to generate uniaxially aligned nanofibers. The collector contained two pieces of conductive silicon stripes separated by a gap. (B) Calculated electric field strength vectors in the region between the needle and the collector. The arrows denote the direction of the electrostatic field lines. (C) Electrostatic force analysis of a charged nanofiber spanning across the gap. The electrostatic force (F_1) resulted from the electric field and the Coulomb interactions (F_2) between the positive charges on the nanofiber and the

negative image charges on the two grounded electrodes. Reprinted with permission from [161]. Copyright 2003 American Chemical Society.

More collectors were specifically designed to obtain aligned fibers. These can be made with simple systems using either two plates or two rods, both at the same voltage (Figure 2.15 (d) and Figure 2.16) [163], or a triangular shape (Figure 2.15 (c)) sometimes close to a metallic plate, or with more (complex systems using a rotating multi-frame structure (Figure 2.17). Alignment can also be achieved with a rotating disk collector with a sharp edge that acts as a charged tip for the electric field (Figure 2.18). For the cases where the fibers are meant to be collected as yarns, specific collectors such as dual collection rings have also been reported (Figure 2.19) [164].

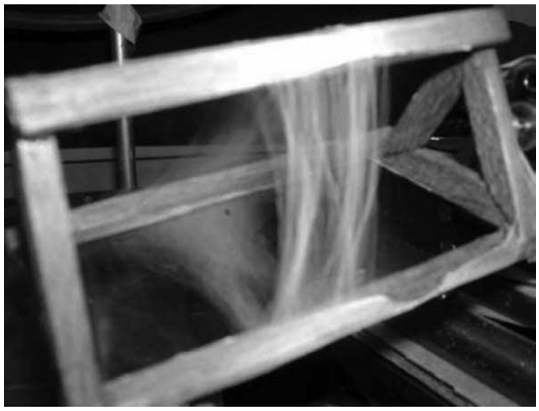

Figure 2.17: Continuous as-spun nanofibers deposited on a rotating multi- frame structure [106]. © 2003 Elsevier

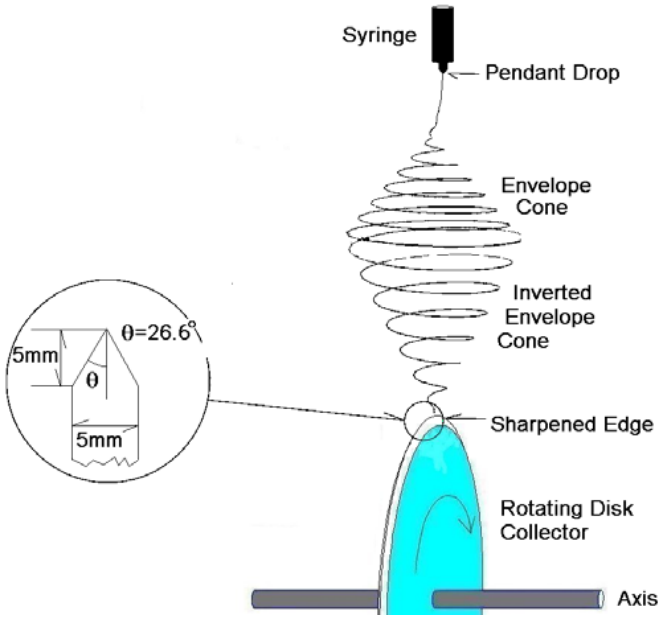

Figure 2.18: Schematic drawing of the electrospinning process with a rotating disk collector, showing the jet path and the region where the bending instability rapidly grew into a conical envelope. This later changed into an inverted conical envelope with its apex on the rotating disk's edge. The disk is made of aluminium and has an overall diameter of 200 mm and thickness of 5 mm [164]. DOI: https://doi.org/10.1088/0957-4484/12/3/329 © IOP Publishing. Reproduced with permission. All rights reserved.

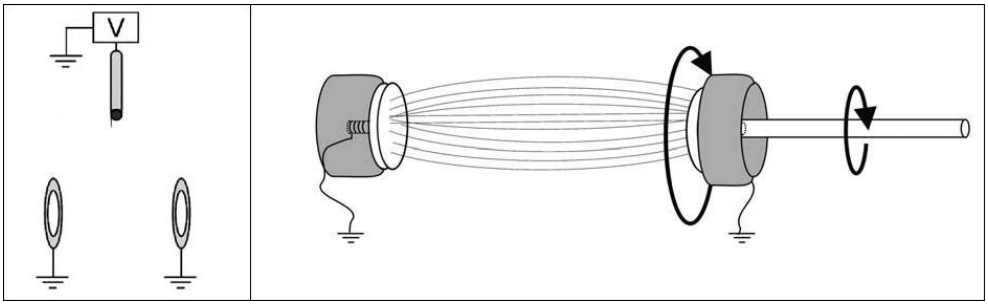

Figure 2.19: On the left: scheme of a dual grounded ring configuration for the collection system. On the right: once the fibers are formed, the ground on the right is rotated while the ground on the left stays stationary. This allows for the formation of a yarn. [151] © 2004 Elsevier

To obtain aligned fibers, the collection system can also use an auxiliary electric field in addition to the usual mandrel. A US patent was filed in 1985 demonstrating the use of a metallic grid placed behind the actual collector to improve the alignment of the fibers (as shown on Figure 2.20 (a)) [165]. A US patent filed in 1989 showed an improved alignment of the fibers by placing the collecting mandrel between two charged plates, as shown on Figure 2.20 (b) [166].

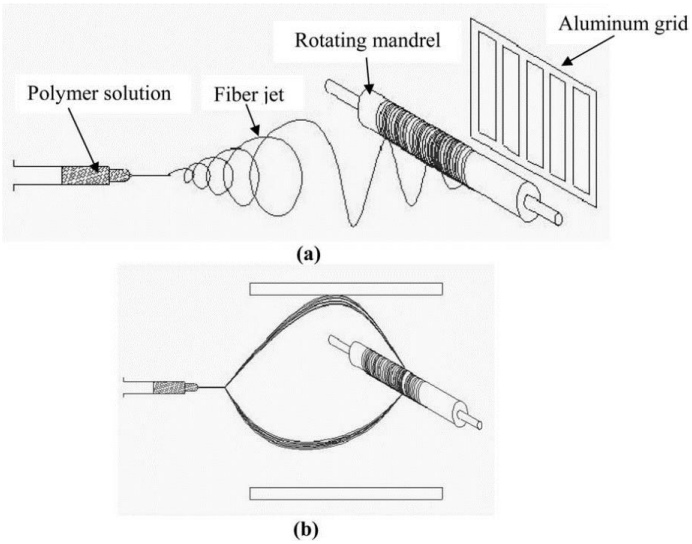

Figure 2.20: Aligning electrospun fibers with an auxiliary electric field [106]. © 2003 Elsevier

Deitzel et al. reported that by using several electric fields as a guide for the liquid, the instabilities that usually appear in the jet can be avoided to some extent, thus facilitating the formation of aligned fibers [167]. Their design is shown on Figure 2.21.

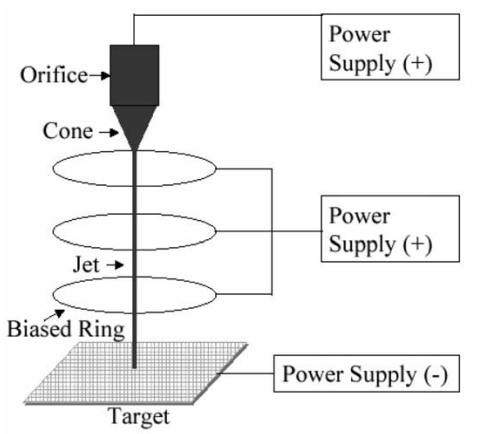

Figure 2.21: A multiple-field technique to obtain aligned fibers [167]. © 2001 Elsevier

Besides the geometry of the collector and the necessity of an auxiliary electric field, the materials used to build the collector could significantly change the results of electrospinning [168]. The final morphology of the fibers depends on how well the charges in the liquid are dissipated, *if* they are, and on the effect of the collecting material on the solvent that remain inside the fibers. For example, fibers made on paper show only a few defects and possess a smooth surface, with relatively uniform diameters. Fibers collected on water however have a diameter distribution in a broader range, and are more densely packed together. With electrically conductive collectors, the charges are more easily dissipated. This reduces the charge repulsion between the filaments, and leads to a more compact distribution of the fibers and a thicker membrane structure. Conversely, a non-conductive collector leads to a more loosely packed network.

2.2.3.5 Patterning the electrospun fibers

A lot of work has been done in the past years to go from aligned to patterned electrospinning. 3D structures were demonstrated in 2008. The authors built these structures directly by electrospinning, by using the 3D shape of tubular collectors as a template, as shown on Figure 2.22 [169].

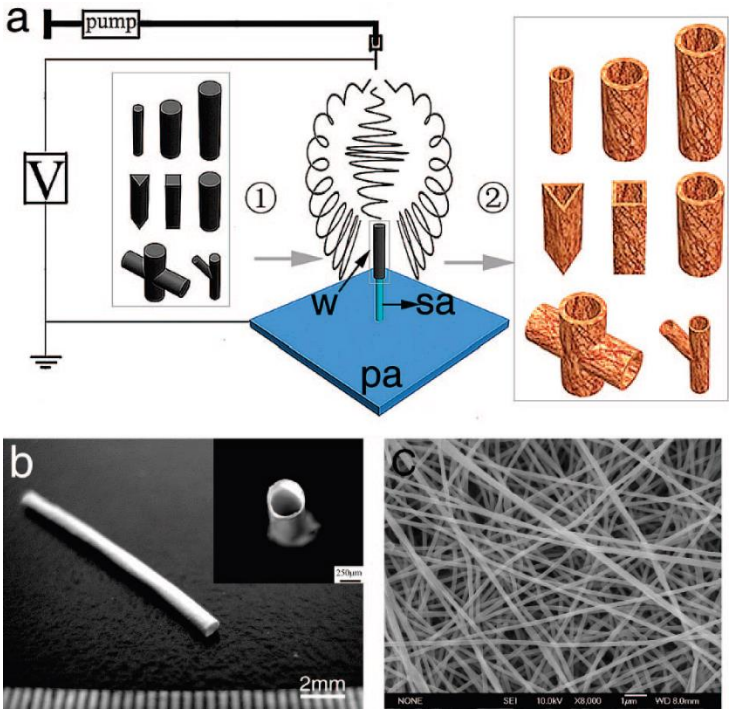

Figure 2.22: (a) Schematic illustration of fabrication of fibrous tubes by electrospinning technique using 3D columnar collectors. 1: 3D columnar collectors. 2: relevant fibrous tubes. (w, working collector; pa, plane assistant collector; sa, stick assistant collector) (b) Fibrous tube with diameter of 500 μm (inset is the cross-section image). (c) SEM image of fiber assemblies of tube shown in panel b. Reprinted with permission from [169]. Copyright 2008 American Chemical Society.

Other methods such as photopatterning [170] and direct writing by way of melt electrospinning [171] have also been demonstrated as possible patterning methods, but they are limited in use. Photopatterning is a derivative of photolithography, in which crosslinking of the previously electrospun polymer occurs in a control way by adding a photoinitiator into the mixture and selectively exposing it to a 365nm light. It is only usable for a specific application, i.e. pore formation. Direct writing requires to decrease the distance between the spinneret and the collector in order to avoid the bending instability and uses the stable jet directly, by moving either the spinneret or the target to create the pattern. Due to the required proximity, this method is limited to melt electrospinning since a solvent would not have enough time to evaporate during the short trajectory.

Another method called Electrolyte-Assisted Electrospinning (ELES) was recently demonstrated in 2015 by Sang Min Park and Dong Sung Kim as a possible way to directly pattern fibers on curved surfaces [172]. This method uses an electrolyte as the collector (Figure 2.23).

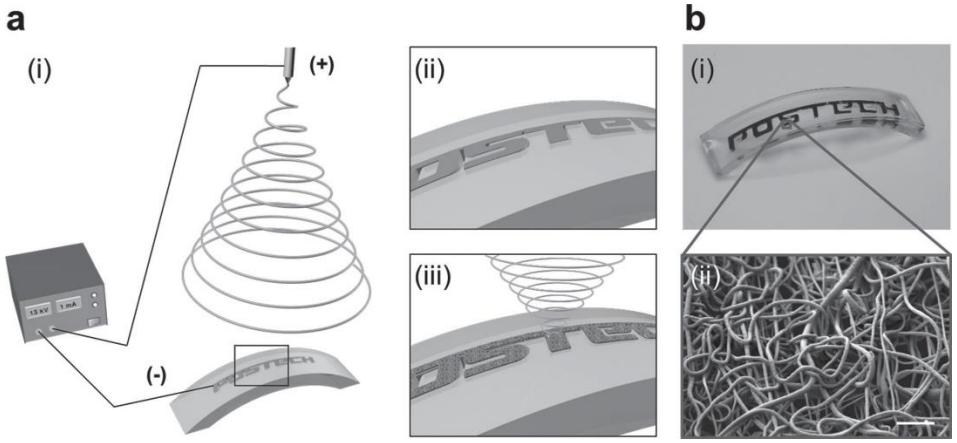

Figure 2.23: Schematic of electrolyte-assisted electrospinning (ELES) to self-assemble electrospun fibers. a) Experimental setup of ELES to self-assemble electrospun fibers on a collector made of an electrolyte solution (potassium chloride). b) Self-assembled nanofiber membranes on a curved surface. Scale bar: 10 µm [172]. © 2015 John Wiley and Sons

2.2.3.6 Electrospinning of conductive polymers

In the past two decades, several polymers have been successfully electrospun by different groups. This part of the literature review will mention some of the most noteworthy works in the field of the electrospinning of ICPs.

2.2.3.6.1 Direct electrospinning of conductive polymers

Conducting polymers cannot be easily electrospun. This is due to low molecular weights, poor mechanical properties and the presence of the rigid backbone [173]. Moreover, although it has been suggested that a high solubility is not always improving the electrospinning results [174], the limited solubility of conductive polymers renders it difficult to prepare solutions having the

minimum viscosity required for fibers formation. The rigid backbone does not allow them to reach the level of chain entanglement required for the formation of fibers [175].

Poly-p-phenylenes (PPVs) are a note-worthy exception to the rule of low molecular weight and low solubility of conducting polymers [176]. For example, transistors made with a single light-emitting nanofiber of pure poly(2-methoxy-5-(2-ethylhexoxy)-1,4-phenylenevinylene) were electrospun without defects [177].

Others conjugated polymers were also successfully electrospun without the necessity to add another polymer to the mixture. P3HT was reported to be successfully electrospun, with González and Pinto demonstrating the electrospinning of regio-regular P3HT dissolved in chloroform ($CHCl_3$) [178]. PPy was synthetized, doped with dodecylbenzene sulfonic acid (DBSA), a surfactant, and successfully electrospun [179]. Another group reported the successful electrospinning of pure PPy, by electrospinning a $[(PPy3)^+ (DEHS)^-]_x$ solution, prepared using the functional doping agent di(2-ethylhexyl) sulfosuccinate sodium salt (NaDEHS) [180]. PANI was also electrospun directly, by using an acetone bath on the collector to help the fibers formation by allowing the remaining solvent to diffuse in the acetone [181]. More recently, poly(phenylenevinylene) (PPV) was electrospun directly from a solution in ethanol/water. The fibers had a smooth surface, and displayed fluorescence peaks similar as the ones in PPV films [182].

2.2.3.6.2 Electrospinning of conductive polymers in blends

In most cases however, the conjugated polymers cannot be electrospun directly and need to be mixed in solution with another more electrospinnable polymer. Several blends have been reported in the literature, using easily electrospun non-conductive polymers as a carrier to allow the electrospinning of ICPs.

PANI doped with amphorsulfonic acid (HCSA) or PANI:HCSA was mixed with poly(ethylene oxide) (PEO). This blend, called PANI:HCSA/PEO, was successfully electrospun by Norris and coworkers [183]. Others successfully electrospun PANI:HCSA by blending it with PEO [184-185] or with polystyrene (PS) [186]. The electrical conductivity of the PANI:HCSA/PEO fibers can also

be improved by adding functionalized graphene inside the mixture and electrospinning it to form the fibers [187].

PEO was also used in a blend to electrospin regio-random P3HT (P3HT/PEO) [188]. This work was followed by more studies on the electrospinning of P3HT in blends. For example, P3HT was also electrospun with poly(ε-caprolactone) (PCL), as P3HT/PCL [189], or with poly(methyl methacrylate) (PMMA) as P3HT/PMMA. In this last case, the PMMA was successfully extracted once the fibers were formed [190]. For solar energy harvesting applications, P3HT (a hole conducting polymer) is typically mixed with PCBM (an electron conducting material). However, the blend cannot be directly electrospun. A P3HT/PCBM/PVP blend was thus prepared by mixing a P3HT/PCBM blend in chloroform/toluene with a PVP solution in chloroform/ethanol. This P3HT/PCBM/PVP blend was successfully electrospun [191]. Finally, another polymer from the polythiophene family called poly-3-dodecylthiophene (P3DDT) was also successfully electrospun in a blend with PEO, as reported in 2007 [192].

A blend of PPV was mixed with poly(vinylalcohol) (PVA), or PPV/PVA blend, was reported to have been successfully electrospun from an aqueous solution [193]. Previously, poly[2-methoxy-5-(2-ethylhexyloxy)-1,4-phenylenevinylene] (MEH-PPV) had been electrospun using a two-capillary spinneret, as shown on Figure 2.24. A similar setup was used to electrospin a blend of MEH-PPV/P3HT with PVP [194].

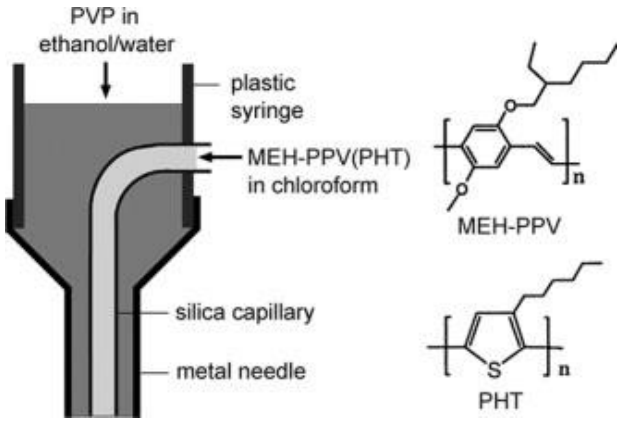

Figure 2.24: Schematic drawing of the setup used in [194] and chemical structures of MEH-PPV and P3HT (written here as PHT). © 2004 John Wiley and Sons

PPy blended with PEO was also electrospun, in a paper also reporting direct electrospinning of PPy [180].

To electrospin poly[(9,9-dioctylfluorenyl-2,7-diyl)-alt-*co*-(1,4-benzo-{2,1′,3}-thiadiazole)] (F8BT), two different blends were used, namely F8BT/PEO and F8BT/PS. Polystyrene (PS) appeared to be more compatible with F8BT than PEO and thus to yield better fibers. These nanofibers showed electroluminescence [195].

Finally, the highly conductive PEDOT doped with PSS (or PEDOT:PSS) was successfully electrospun from a *N*,*N*-Dimethylformamide (DMF) solution, by using polyacrylonitrile (PAN) as the carrier polymer. However, the reported procedure yielded PEDOT:PSS/PAN self-assembled yarn instead of a non-woven mat. Moreover, a "standing fiber" problem was reported: part of the fibers would stand vertically during the electrospinning process (see Figure 2.25) [196]. In 2009, a method to electrospin PEDOT:PSS using poly(vinylidene fluoride-trifluoroethylene) (PVF2-TrFE) as a PVF2-TrFE/PEDOT:PSS blend from a solution in DMF was reported. The PEDOT:PSS concentration needed to be kept low in order to avoid phase separation. This had for consequence that the individual fiber conductivity was too low to be measured [197]. PEDOT:PSS was also successfully electrospun when blended with PEO [198-199] or with PVA [200]. PEDOT:PSS blended with PVA, in which DMSO was added was recently electrospun on a kapton substrate and encapsulated into PDMS to avoid contamination and damages, making it a stretchable device [201]. Electrospun plasma-modified chitosan/PEDOT:PSS fibers using PVA as a carrier were also recently reported [202]. A very recent work published in 2015 reported a method to correct the "standing fibers" issue previously reported (Figure 2.25). This work was performed in the case of PEDOT:PSS/PEO blends. The "standing fibers" problem was solved by simply blowing air vertically downward to counter the Coulomb forces between the PEDOT:PSS/PEO fibers and the spinneret during the electrospinning process. After that, conductivities as high as 35.5 S/cm were reported [203].

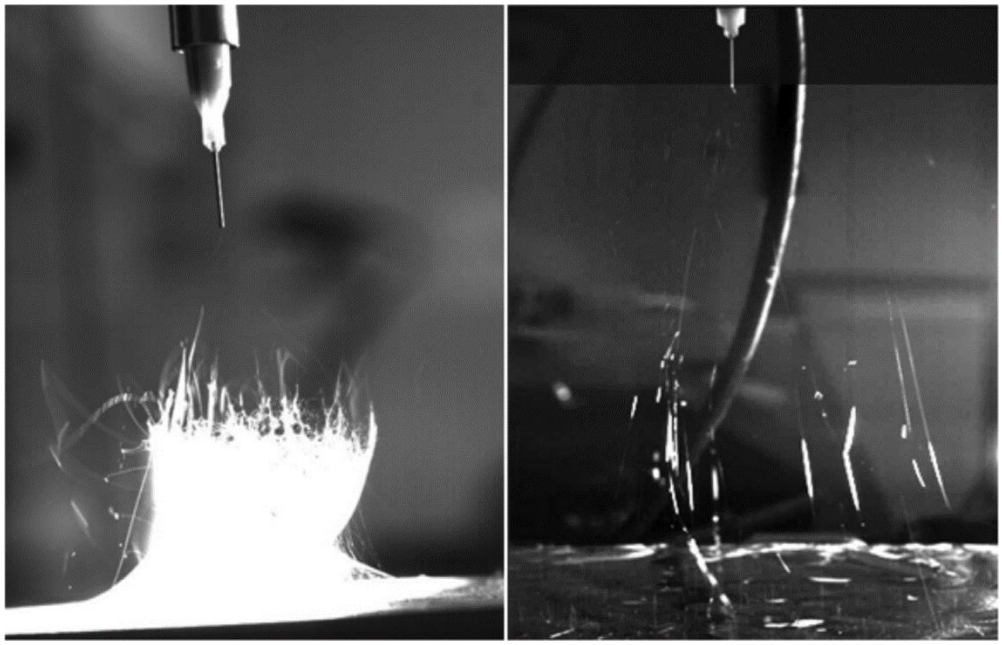

Figure 2.25: PEDOT:PSS/PEO fibers as “stranding fibers” trying to reach the spinning nozzle [203]. © 2015 Elsevier

In 2016, a roll-to-roll hybrid process using both electrospinning and solution casting was reported to yield flexible and even stretchable devices with PEDOT:PSS fibers. This was done by mixing PEDOT:PSS with PVP at high molecular weight (Mw ≈ 4,000,000). This allowed the authors to reduce the concentration of PVP in the electrospun mixture and to increase the conductivity of the fibers. They completed their devices by casting solutions containing either PMMA, polyimide (PI), or polyurethane (PU) on top of the fibers to obtain an elastomer substrate [204].

2.3 Vapor phase polymerization

Vapor Phase Polymerization (VPP), is a technique used for in-situ polymerization of conducting polymers. This method can be used to polymerize complex structures by using a template. The next section will focus on the working principle of the vapor phase polymerization while mentioning a few main historical landmarks. Succcessively, I will focus on the use of VPP to obtain conductive fibers.

2.3.1 Working principle of vapor phase polymerization

Vapor phase polymerization (VPP) is a two-step process, as shown on Figure 2.26. First, a mixture containing an oxidant is applied, by spin-coating or other deposition methods (Figure 2.26 Step I) onto a substrate. Then, in-situ polymerization takes place inside a polymerization reactor where the oxidant covered surface is exposed to a monomer (Figure 2.26 Step II). The polymerization can be performed either under vacuum or at atmospheric pressure, in air conditions or in a chamber filled with a gas (usually nitrogen or an inert gas such as argon). Finally, the obtained polymer is usually rinsed with an alcohol (methanol or ethanol in most cases) to remove the unreacted oxidant and/or monomer, as well as other by-products such as short oligomers [205-206].

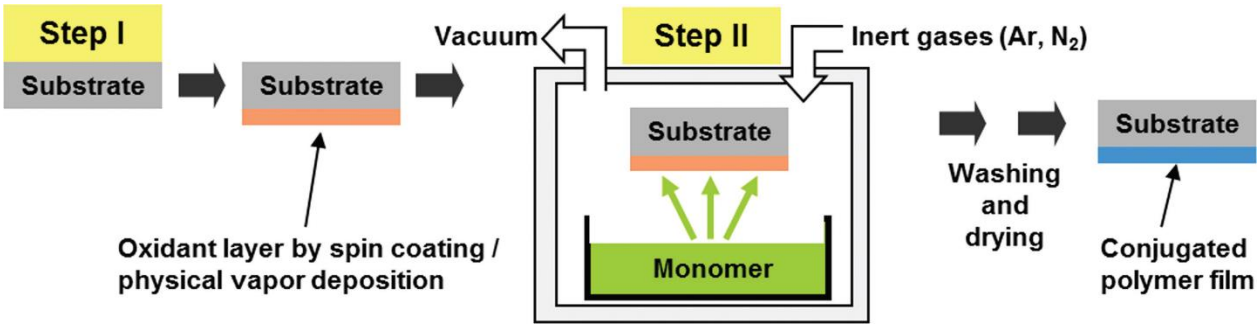

Figure 2.26: A typical procedure for deposition of conjugated polymer films by VPP. Alternative methods, such as sublimation, have been used to achieve oxidant preapplication (Step I). [207] © 2012 John Wiley and Sons

One of the main advantages of VPP is the conformability to the surface on which the polymerization takes place. The polymerization is also easy to control, since the thickness of the obtained film will mostly depend on the time of polymerization and the thickness of the oxidant film deposited in the first step.

The term of "Vapor phase polymerization" was first mentioned in the literature in 1986 by Ojio and al. when they reported the deposition of conductive PPy by exposing pyrrole monomer in vapor phase to a film of PVA containing iron(III) chloride ($FeCl_3$) [208]. They also reported that the conductivity of the obtained films depended on several parameters, namely the polymerization time, the temperature of polymerization, and the concentration of the $FeCl_3$ [207]. Another group

reported the successful polymerization of PPy using a similar method, named “Chemical vapour deposition” or CVD, in which the oxidant and the monomer are both delivered in vapor phase in a one-step process [209]. The term “oxidative chemical vapor phase deposition”, or oCVD, has also been used.

In 2003, a group reported the successful polymerization of PEDOT doped with Cl^-, using $FeCl_3$ hexahydrate ($FeCl_3 \cdot 6H_2O$) as the oxidant [210]. In 2004, another group reported the polymerization of PEDOT doped with tosylate (Tos), PEDOT:Tos, using iron(III) p-toluenesulfonate (Fe(III)Tos) as the oxidant. This reaction as-is led to the formation of a non-conjugated polymer along with the formation of PEDOT:Tos. The side reaction was more likely to happen in a more acidic milieu. It was deemed undesirable as it reduced the conductivity of the film. The authors thus used pyridine as a base to avoid this side reaction. This yielded films with high conductivities, exceeding 1000 S/cm [205] with highly mobile charge carriers [211]. However, as the polymerization went on, acidity increased again, leading to the formation of non-conductive PEDOT on the top of the film if the polymerization was not stopped on time [212]. This base-inhibited oxidative polymerization of PEDOT:Tos made the object of another publication by Winther-Jensen and coworkers in 2005, in which they compared several base inhibitors: imidazole, pyridine, pyrazine, and quinolone. They noticed that pyridine was the best candidate for the inhibition to take place. Imidazole posed homogeneity problems in the film as it could form crystals with Fe^{3+}, pyrazine was not effective enough as an inhibitor to prevent the side reaction from happening, and quinolone low vapor pressure required either long waiting time or heat for the compound to evaporate [213]. It was suggested that the iron salt used in the VPP could have an ordering effect that tended to increase the conductivities obtained in the PEDOT:Tos films [214].

Several other groups reported the successful polymerization of PEDOT by VPP in presence of a base inhibitor, using mixtures containing Fe(III)Tos and pyridine for the production of PEDOT:Tos [212] [215]. Another group also reported polymerization of PEDOT by VPP without the base inhibitor, by simply using Fe(III)Tos for the production of PEDOT:Tos [216]. In 2010, Jang and coworkers reported the synchronous copolymerization of PEDOT and P3HT with VPP for optoelectronic devices, using $Fe(III)Cl_3 \cdot 6H_2O$ as the oxidant [217].

2.3.2 Production of PEDOT fibers using vapor phase polymerization

One of the main advantages of VPP is that it allows for a good conformability to the surfaces on which the in-situ polymerization takes place, and as such can be used even on irregular surfaces or even already shaped surfaces produced during the first step on Figure 2.26. In particular, VPP can be used for the production of conductive fibers, e.g. PEDOT fibers, when combined with electrospinning. First, fibers containing oxidant are produced by electrospinning, and in a second step VPP is used to polymerize the conductive polymer on them.

A first paper regarding the polymerization of PEDOT fibers using VPP was published in 2008. The electrospinning was done using PVP as the carrier polymer, and the polymerization used Fe(III)Tos as the oxidant and a heating step at 100-120°C [218]. The chemical reaction leading to the polymerization is shown on Figure 2.27. A. Laforgue et al. produced a great amount of work on the combination of electrospinning and VPP for the production of conducting fibers. The carrier polymer used was PVP, and their polymerization step used Fe(III)Tos as the oxidant and pyridine as the base to inhibit the acidic side reaction. Cyclic voltammetry demonstrated that the PEDOT:Tos fibers obtained by this method showed completely reversible doping/dedoping characteristics, which are suitable for organic electronic and energy storage devices such as Organic Electrochemical Transistors (OECTs) [219]. The same procedure was then used to produce colour-changing textiles by coating thermochromic inks on the obtained PEDOT mats [220]. Successively the same group published one more paper combining electrospinning and VPP that demonstrated an all-textile flexible supercapacitor using PEDOT:Tos nanofibers [221]. In these papers, it was also highlighted that humidity uptake could cause the PVP fibers to dissolve, and thus special care must be taken when handling the produced fibers between the different steps to avoid the effects of ambient humidity.

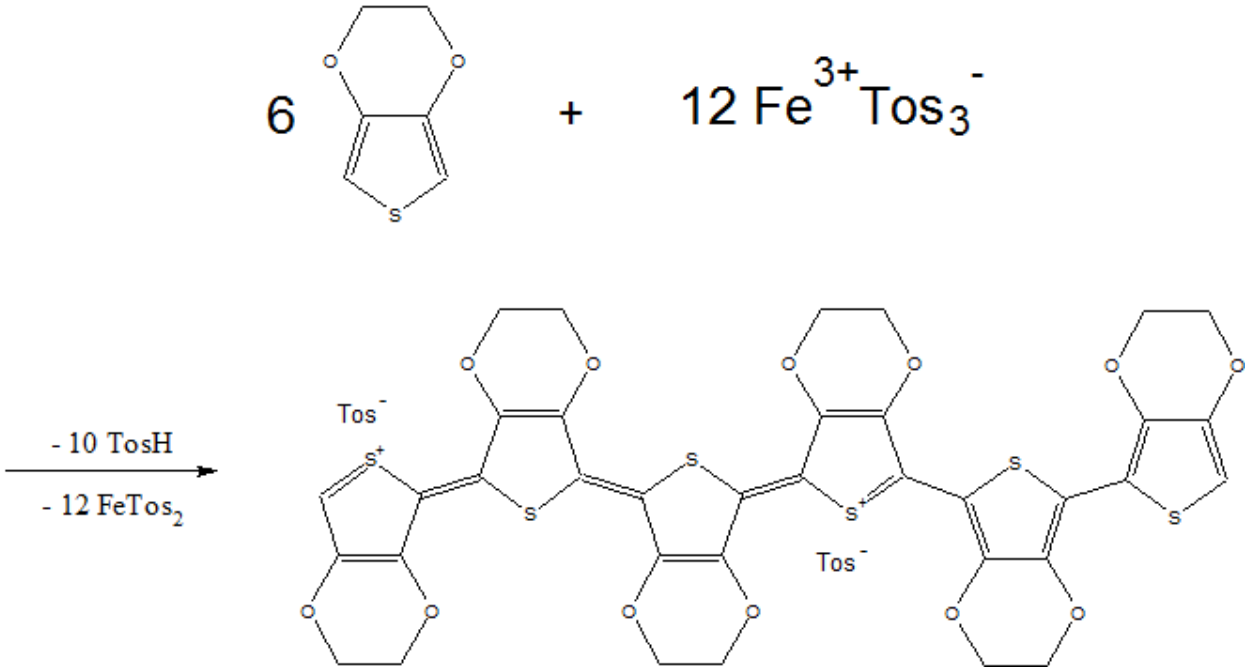

Figure 2.27: Chemical reaction between EDOT and Tosylate leading to PEDOT:Tos [222-223].

More recently, a group reported the electrospinning with a secondary electric field to obtain highly-aligned nanofibers, followed by VPP to obtain PEDOT nanotubes. This work used hydroxylated EDOT as a co-monomer to functionalize the final fibers to detect organophosphates for applications as a chemical nerve agent sensor, that is sensors that can detect the presence of chemicals able to disrupt the transmission of signals between the nerves and the organs, and in particular odorless ones such as sarin gas. The whole work was performed using thick poly(ethylene terephthalate) (PET) as the substrate [224]. VPP was also used for the production of conducting nanofibers by simply coating commercially available viscose yarns with oxidant and polymerizing PEDOT on top of these fibers [225].

In 2013, a group reported the fabrication of PEDOT fibers and tubes using a method similar to the VPP process. This was done by electrospinning of poly(lactide-co-glycolide) (PLGA) loaded with EDOT monomer to produce the fibers and by dripping the oxidant $FeCl_3$ solution directly onto the mandrel to produce the PEDOT fibers themselves [226]. A similar process was used by Park and coworkers to obtain PMMA/PEDOT fibers by electrospinning PMMA fibers containing EDOT onto an oxidant solution [227].

CHAPTER 3 MATERIALS AND METHODS

3.1 Substrate preparation

Hexadecyltrimethylammonium bromide (CTAB) (purity ≈ 99%) from Sigma-Aldrich was dissolved in MilliQ quality water obtained from a Millipore Reference purification system to produce a CTAB solution with a concentration of 10^{-3} M. This solution was then spin-coated at 500 rpm for 30 s on top of a glass slide. Right after that, a 10:1 mixture of polydimethylsiloxane (PDMS) and its curing agent from a Sylgard® 184 Silicone Elastomer kit was spin-coated at 500 rpm for 30 s on the glass slide. After waiting for 30 s, the slide was removed from the spin-coater and put onto a hot plate at 90°C for baking of the PDMS for 30 min. The PDMS mixture had been previously obtained by mixing it with its curing agent for 5 min at 2000 rpm using a planetary mixer (Thinky Mixer).

Once the PDMS was solidified, the edges were cut using a razor blade and a glass slide as a ruler. They were then peeled off to avoid any edge effect. The remaining PDMS was then carefully peeled off and attached to a home-made support using tape. This step allows for an easier removal of the PDMS with fibers in future steps, by reducing the contact surface between the PDMS and the glass slide. A schematic drawing of the support used with PDMS on top of it is shown in Figure 3.1.

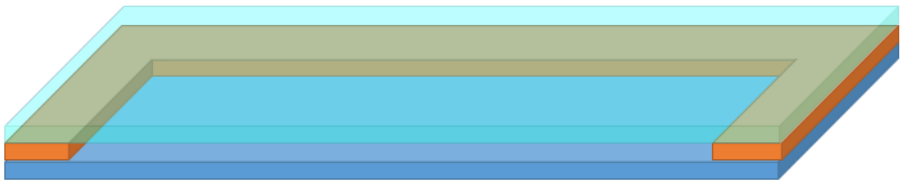

Figure 3.1: Glass slide (dark blue) with a home-made support (orange) attached on it. A PDMS substrate (transparent lighter blue) is attached on top on the support. This configuration allows for an easier removal of the PDMS substrate after electrospinning by limiting the contact and thus the adherence between the PDMS and its support. The PDMS can also be removed by cutting if necessary.

3.2 Electrospinning

3.2.1 Preparation of the mixture

A solution containing 22.6 g of CLEVIOS C-B 54 V3 (Iron Tosylate, or Fe(III)Tos in butanol to bring into the solution the oxidant Fe^{3+} and the dopant tosylate) from Heraeus Electronic Materials GmbH, 0.23 g of the carrier polymer polyvinylpyrrolidone (PVP) at Mw ≈ 1,300,000 from Sigma-Aldrich, and 0.73 g of the weak base Imidazole (purity ≥ 99%) from Sigma-Aldrich was prepared and thoroughly mixed using a planetary mixer (Thinky Mixer) for 30 minutes at 2000 rpm. 4 mL of this mixture were then collected and mixed with 1 mL of 2-propanol (IPA) (purity ≥ 99.9%) from Sigma-Aldrich, using once again the planetary mixer (Thinky Mixer) for 30 minutes at 2000 rpm.

3.2.2 Cleaning of the syringe

The syringe used in the electrospinning experiments was systematically thoroughly washed with IPA before the experiments were performed. After each experiment, the syringe was emptied from the solution and washed with methanol. A metal wire was used to ensure that the nozzle was perfectly clean at the end of each experiment. The syringe was then washed again with IPA and dried using a nitrogen blowgun.

3.2.3 Electrospinning parameters

Electrospinning was performed with an RT-collector system equipped with a cylindrical collector (Linari Engineering). The substrate previously prepared on its support was taped directly on the collector. The syringe with a 0.8 mm diameter nozzle was installed on a syringe pump from Razel Scientific Instruments, with a distance “tip of the nozzle-collector” of about 15 cm. This distance was chosen based on a previously reported procedure that we modified for our needs [219]. Once the distance was fixed, we only modified the other parameters depending on the results we could directly observe. The collector was grounded while the nozzle was maintained at 20 kV during the whole process. This choice was made to ensure that the voltage would be high enough to electrospin without droplets, while still being low enough to limit the number of beads that would appear on the structure. The electrospinning was carried out inside a hood where the temperature

was controlled and the relative humidity was monitored. A heater provided by Linari Engineering was used to raise the temperature to 35°C to reduce the humidity, thus reducing the humidity uptake by the PVP fibers freshly electrospun. The relative humidity was kept lower than 20% to mitigate its effect on the freshly electrospun PVP fibers.

Electrospinning was carried out for 3 min, while the drum-like collector was rotating at 500 rpm. The duration of the electrospinning was chosen this way because it was sufficient to obtain conductive fiber mats by the end of the process, and was not long enough to yield thick mats that might delaminate from the substrate. Rotation was used to ensure that the whole sample was covered as homogeneously as possible. The arm holding the collector was also moving at 20 mm/s in order to ensure that the whole sample got covered by the electrospun fibers. Right after electrospinning, the remaining charges were removed from the collector and the nozzle using a grounded metallic bar, and the sample covered in oxidant fibers was detached from the collector.

During electrospinning, the mixture containing PVP, Fe(III)Tos and Imidazole in butanol and IPA was inside the syringe on the syringe pump. The PVP, as a carrier polymer, formed the jet due to the electrospinning process. The smaller molecules (Fe^{3+}, Tos and Imidazole) were embedded inside the fibers. When the solvents evaporated during the flight between the spinneret and the collector, the smaller molecules tended to migrate with the solvents while the PVP fibers were forming, yielding fibers that were made of a PVP core still containing some of the small molecules, coated with a layer of oxidant (Fe^{3+}), dopant (tosylate) and base inhibitor (imidazole), as shown on Figure 3.2 (the core is simplified as solely PVP but other molecules are expected to still be embedded inside it).

3.3 Vapor phase polymerization

The freshly electrospun fibers were quickly removed from the collector and attached to a beaker cover with tape. This cover was used to close a beaker inside which a few drops of 3,4-ethylenedioxythiphene (EDOT) (purity $\geq$ 97%) from Sigma-Aldrich. This beaker was placed inside an oven with typical temperatures around 50°C for 30 min. The polymerization takes place during that time and can easily be followed by witnessing the color change of the fibers, from yellow to blue. Shorter polymerization usually was not completed, as yellow fibers could still be visible. On

the other hand, longer polymerization sometimes yielded non-conductive fiber mats. A 30 min polymerization was thus deemed sufficient.

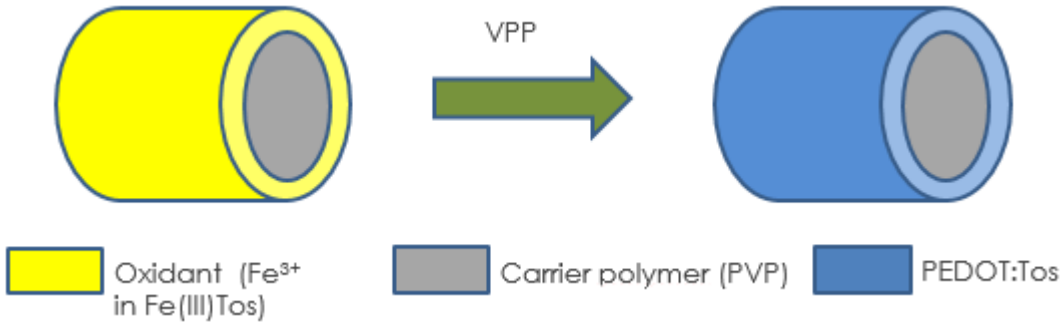

Figure 3.2: Schematic drawing of the fibers structure before and after vapor phase polymerization (VPP). The yellow coating also contains imidazole (not specified on the schematic), while the PVP core (in grey) also contains Fe^{3+}, Tos and Imidazole.

This second step yielded fibers made of a PVP core coated with PEDOT:Tos, as shown on Figure 3.2. Imidazole, EDOT, Fe^{3+} and tosylate were also expected to still be present on the fibers after this step. Moreover, the PEDOT:Tos coating is expected to contain defects in the form of small holes everywhere on the structure, which can be exploited for the following rinsing step.

3.4 Sample rinsing

Right after polymerization, the samples were removed from the beaker and put on the spin-coater with vacuum. Denatured ethanol from Sigma-Aldrich was poured over the samples and kept there for 30 s, after which the spin-coater was ran at 500 rpm for 30 s to remove the ethanol. This procedure was performed two times per sample, to remove most of the remaining PVP and other unwanted chemicals from the samples. By doing so, we ensured that the PVP core would not uptake ambient humidity on the long-term, which could have an impact on the structure of the fibers and is expected to reduce conductivity due to the simple presence of a non-conductive material inside the fiber mats.

3.5 Characterization

3.5.1 Diameter of the fibers

A thin layer of gold (a few nm) was deposited on freshly prepared samples to ensure a good image quality on the whole samples. Scanning Electron Microscopy (SEM) was than performed. The ImageJ software was then used to analyze the different pictures taken and to measure the diameters of 150 different fibers in total. The average diameter was then computed from these different measurements.

3.5.2 Electrical characterization during stretching

The samples were attached on a home-made computer-controlled tensile tester. Eutectic Gallium-Indium (EGaIn) was used to form two liquid electrodes to ensure a good connection between the PEDOT:Tos fibers and the copper electrodes used for the connection between the samples and an Agilent measuring system (setup shown on Figure 3.3). Not using EGaIn could result in a loss of contact during the following stretching, as it would mean directly contacting a wire with fibers that can be affected by the stretching.

Once the films were in place, a voltage of 200 mV was applied during the measurement. The samples were stretched while the current was measured using an Agilent system. A home-made program was used to control the tensile tester and induce different cycling patterns. The results were obtained in the form of an Excel worksheet including for each point the time, the voltage and the current measured. The stretching percentage was deduced from the cycling patterns programmed into the stretcher and had to be added later. The data was then processed into graphs using the software Igor Pro.

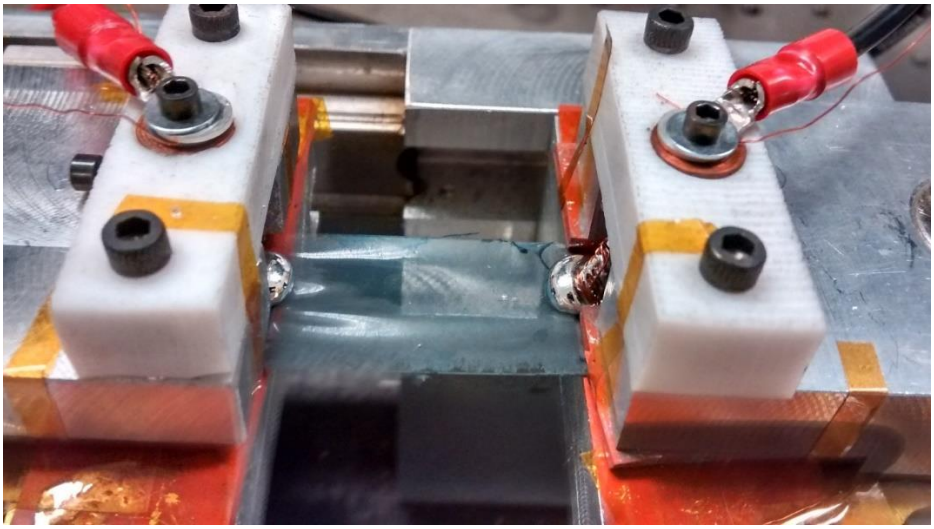

Figure 3.3: Setup used to measure the current while stretching the samples. EGaIn is used as a liquid metallic electrode to ease the connection between the fibers (in blue) on the PDMS substrate and the copper wires.

CHAPTER 4 ARTICLE 1: HIGHLY STRETCHABLE ELECTROSPUN CONDUCTING POLYMER NANOFIBERS

4.1 Article presentation

This letter, entitled "Highly stretchable electrospun conducting polymer nanofibers" was submitted to Applied Physics Letters. The aim of this letter is to present the main results obtained with the conducting PEDOT:Tos fibers produced during this master project. These fibers were produced using a two-step method. First, a mixture containing an oxidant (iron tosylate), a carrier polymer (PVP) and a weak base (imidazole) in alcohol was electrospun to form nanofibers on PDMS. These nanofibers were then placed into a chamber for the vapor phase polymerization performed in the second step, before finally being rinsed with ethanol. The aspect and the electrical properties under stretching of these fibers once rinsed were then studied. The fiber mats were arranged into a non-woven structure, and the fibers had an average diameter of 686 nm. The mats on PDMS were stretched to 100% of their initial length. The current after a first stretch was performed appeared to be relatively stable and did not change much when the mats were released or stretched back, although dynamic rearrangements of the conductive pathways led to small spikes in the observed current. The study concluded that despite these spikes, the stability of the current in the fibers mats even under stretching was promising for a future functionalization of the fibers, and could possibly be exploited for use in sensing.

4.2 Authors

Highly stretchable electrospun conducting polymer nanofibers

Fanny Boubée de Gramont,[1] Shiming Zhang,[1] Gaia Tomasello,[1] Prajwal Kumar,[1] Andranik Sarkissian,[2] and Fabio Cicoira [1,a)]

[1]Department of Chemical Engineering, Polytechnique Montreal, Montreal, Quebec, Canada, H3C 3A7.

[2]PLASMIONIQUE Inc., 171-1650 boul. Lionel Boulet, Varennes, Quebec, Canada, J3X 1S2.

[a)] Author to whom correspondence should be addressed. Electronic mail: Fabio.cicoira@polymtl.ca

4.3 Abstract

Biomedical electronics research targets both wearable and biocompatible electronic devices easily adaptable to specific functions. To achieve such goals, stretchable organic electronic materials are some of the most intriguing candidates. Herein, we develop a highly stretchable poly-(3,4-ethylenedioxythiphene) (PEDOT) doped with tosylate (PEDOT:Tos) nanofibers. A two-step process involving electrospinning of carrier polymer (with oxidant) and vapor phase polymerization was used to produce fibers on polydimethylsiloxane (PDMS) substrate. The fibers can be stretched up to 140% of the initial length maintaining high conductivity and show excellent cyclic stability.

4.4 Article

Organic electronic materials are widely investigated for biomedical applications, such as sensing [1], stimulation or recording of the brain activity [2]. These materials present intriguing properties that are specifically interesting for biological application: they can interface with aqueous solutions without leading to the formation of an oxide layer, thus favoring direct contact with the biological milieu, and can support a mixed ionic/electronic conduction [3]. These properties, together with ease of process and possibility of tuning properties via chemical synthesis, make organic electronic devices good candidates for applications in the biomedical field. Other properties desirable for application in bioelectronics are flexibility and stretchability, which permit to accommodate devices on objects with irregular shapes [4]. Two main strategies are used to achieve stretchable electronics [5], i.e. using intrinsically stretchable materials or impart stretchability using substrates with buckled geometry [6-7]. Alternatively, structures such as fibers can be used to improve the stretchability of poorly-stretchable materials such organic conducting polymers, to obtain highly stretchable organic conductors [8]. To date, several techniques have been used to obtain conductive fibers, such as drawing [9], template synthesis [10], phase separation [11], wet-spinning [12-13] and electrospinning [14]. These methods, however, present limitations. Drawing consists of

mechanically pulling a liquid to stretch it into thin filaments and let it solidify. As such, it can only be used for fluids with a high viscoelasticity that are resistant enough to be drawn without breaking under the stress caused by the process. Template synthesis consists of depositing a material by following a pre-existing template. To produce fibers, it thus requires an adapted template, usually a membrane with an adequate diameter, inside which the material is deposited. Phase separation is a complex process that yields nanoporous polymer membranes that can be used directly as a fibrous scaffold. It necessitates polymer dissolution, phase separation and gelation, solvent extraction, freezing and freeze-drying under vacuum, making it both a long and complex process. Wet-spinning consists of pushing a liquid through a nozzle and into a coagulation bath to obtain solidification of the filaments. This process yields fibers with a large diameter (typically more than 10 µm), which limits their potential applications [15]. Electrospinning is a technique that yields fibers of various kinds of polymers with average diameters ranging from a few tens of nm to a few tens µm [16], depending on the parameters chosen for the process. Electrospinning uses an electrostatic force to spin polymer fibers from the tip of a syringe needle (or spinneret) containing a polymer solution. The spinneret is maintained at a high voltage (typically tens of kV) with respect to a grounded target substrate (collector). When the electrostatic force overcomes the surface tension of the polymer solution, the liquid spills out of the spinneret and forms thin filaments, which are collected on the substrate [14]. Electrospinning permits tuning of the diameters of the fibers and their morphology, simply by changing parameters, such as voltage applied between the needle and the collector, distance between the needle and the collector, injection speed, duration of the spinning, type of collector used and viscosity of the polymer solution [14]. Despite the advantages of electrospinning, conjugated polymers are difficult to process with this technique because their rigid backbone does not allow them to reach the level of chain entanglement required for the formation of fibers [17]. In this letter, we obtained poly(3,4-ethylenedioxythiophene) PEDOT doped with Tosylate (PEDOT:Tos) fibers on polydimethylsiloxane (PDMS), by first electrospinning fibers containing an oxidant with a carrier polymer, followed by vapor phase polymerization [18]. The fibers show ultrahigh stretchablity while maintain their high conductivity up to ca. 140% strain. This work paves the way for developing highly stretchable organic electronics for applications in conformable biomedical devices and stretchable interconnects for wearable electronics.

PDMS substrates (thickness of about 300 μm) were prepared by spin coating a 10:1 mixture of the elastomer and its curing agent (Sylgard® 184 Silicone Elastomer kit, Dow Corning) at 500 revolutions per minute (rpm) for 30 seconds on a glass substrate treated with a 10^{-3} M solution (500 rpm for 30 seconds) of hexadecyltrimethylammonium bromide (CTAB, Sigma-Aldrich). The CTAB treatment is necessary to facilitate successive peel-off of PDMS from glass. The PDMS was then baked at 90°C for 30 min before being gently peeled off from the slide. It was then attached to the cylindrical metallic collector of an RT-collector electrospinning setup (Linari Engineering) equipped with a cylindrical collector. Electrospinning of fibers of the carrier polymer polyvinylpyrrolidone (PVP, Step 1 in Figure 1) was carried out with a mixture containing 0.23 g of PVP at Mw ≈ 1,300,000 (Sigma-Aldrich), 22.6 g of a solution of the oxidant Fe(III)Tos in butanol (CLEVIOS C-B 54 V3, Heraeus Electronic Materials GmbH), which acts as a polymerization initiator, and 0.73 g of the weak base Imidazole (Sigma-Aldrich), thoroughly mixed before use with a planetary mixer. This composition of the mixture is based on a previously reported procedure that we optimized for electrospinning on PDMS [18]. Imidazole was included to act as a proton acceptor during the polymerization step, to prevent the reaction milieu from becoming acidic, which would lead to a side reaction producing non-conductive species [19]. The mixture was diluted 4:1 into isopropyl alcohol, thoroughly mixed and transferred into a 5 mL glass syringe with a 0.8 mm diameter needle. The syringe was placed on a syringe pump (Razel Scientific) to ensure a constant flow of the mixture during electrospinning. We performed electrospinning for 3 min, with the collector rotating at 500 rpm, keeping a distance of 15 cm between the tip of the needle and the metallic collector and applying a 20 kV voltage between the needle and the grounded collector. These parameters allowed for a satisfactory thickness of the final fiber mat without risking a partial delamination. The process resulted in a non-woven mat of nanofibers made of PVP imidazole and Fe(III)Tos [18]. According to the literature, the oxidant and the proton acceptor are found in higher concentrations in the external layer of the fibers. After electrospinning, the fibers were transferred to a Vapor Phase Polymerization (VPP) reactor, where they were exposed to vapors of the monomer 3,4-ethylenedioxythiphene (EDOT, Sigma Aldrich, Step 2 in Figure 1). When in contact with the fibers containing the oxidant, EDOT polymerized to yield PEDOT doped with the counter ion tosylate, i.e. PEDOT:Tos. We set the exposure time of the fibers to EDOT to 30 minutes. Based on electrical conductivity measurements and visual inspection, we estimate this time to be long enough for the polymerization to occur while avoiding

the full consumption of imidazole, which would lead to formation of insulating species with deleterious effects on electrical conductivity. Once polymerized, the samples were rinsed with ethanol (Sigma-Aldrich) using a “double-puddle” method: they were fixed on the chuck of a spin-coater, covered with ethanol for 30 s, then spin-coated at 500 rpm for 30 s to remove the ethanol. This procedure was performed twice for each sample. This method was chosen to prevent any delamination of the fiber film from PDMS from occurring upon a complete immersion in ethanol. The main purpose of this last step is to remove unreacted species (monomer and imidazole), oxidant residues and nonconductive species generated by side reactions. Moreover, as PVP is soluble in ethanol, this step also dissolves the core of the fibers, leading to a material which is more stable in ambient air. Indeed, PVP can easily react with the ambient humidity and melt by absorbing water, which could compromise the properties of the fiber mat over the long term. A relatively high current (of the order of tens of mA) could be recorded by placing electrodes at the two extremities of our samples, although the electrical conductivity could not be extracted due to the difficulty to measure the thickness of the fiber mat.

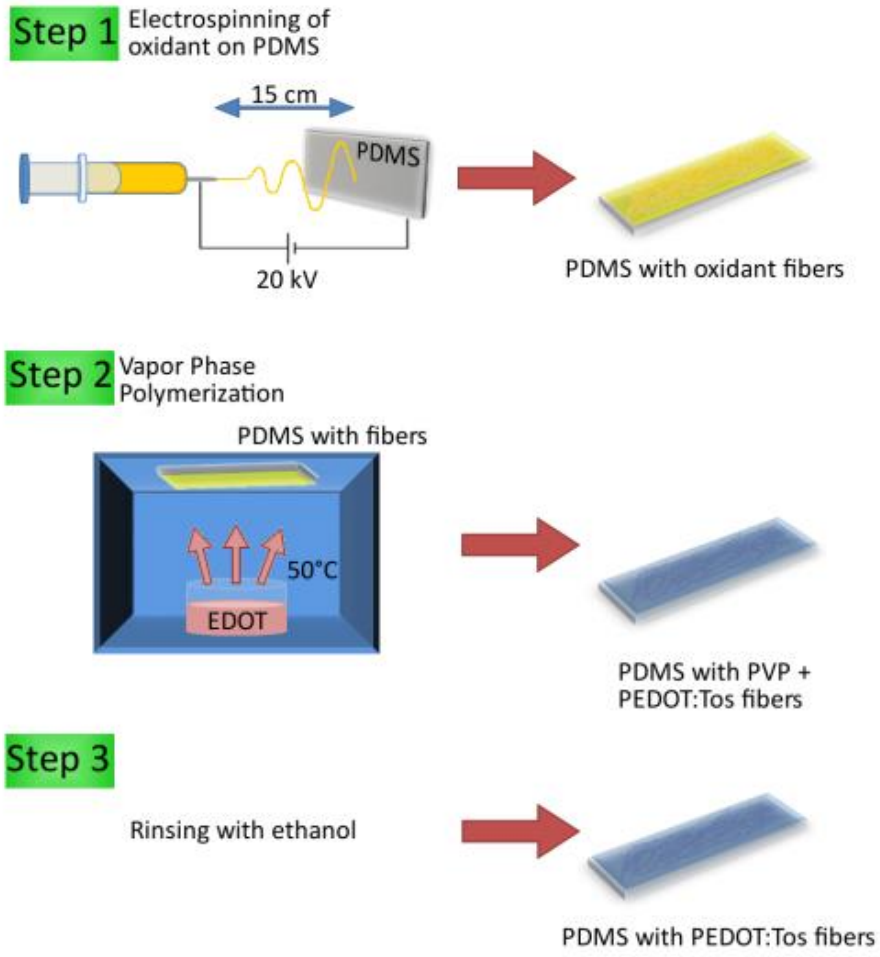

Figure 4.1: Process used to obtain fibers of PEDOT:Tos. A mixture containing PVP, Fe(III)Tos and Imidazole is electrospun directly on a PDMS substrate attached to a rotating cylindrical collector. The applied voltage is 20 kV, and the distance is 15 cm (Step 1). The PDMS covered with fibers is placed inside a chamber at atmospheric pressure. A crucible containing EDOT is warmed at 50°C to evaporate the monomer, thus allowing the polymerization of PEDOT:Tos on the fibers (Step 2). The fibers are rinsed with ethanol to remove the unreacted chemicals (monomer and oxidant) and to dissolve the PVP core of the fibers. Removing the PVP core allows for better long-term stability of the fiber mat, by preventing the PVP from melting by absorbing ambient water later.

Images of the fibers were taken by with a FEI Quanta 450 environmental scanning electron microscope (FE-ESEM) and by optical microscopy using a Zeiss Imager M1 microscope equipped

with an AxioCam MRm camera by Carl Zeiss. The combination of electrospinning, VPP and ethanol rinsing resulted in non-woven mats. SEM images show that most of the fibers appeared flat (Figure 2 a) and b)). This confirms the removal of the PVP core during the ethanol rinsing, which leads to the collapse of the PEDOT:Tos fibers. Some of the fibers also presented small beaded structures (Figure 2 a), which could be explained by a partial melting of the PVP fibers before the start of the VPP step, due to the ambient humidity. The SEM images were used to estimate the average diameter of the fibers (using the ImageJ software from the National Institute of Health), which was of about 700 nm over an area of 480×360 μm^2.

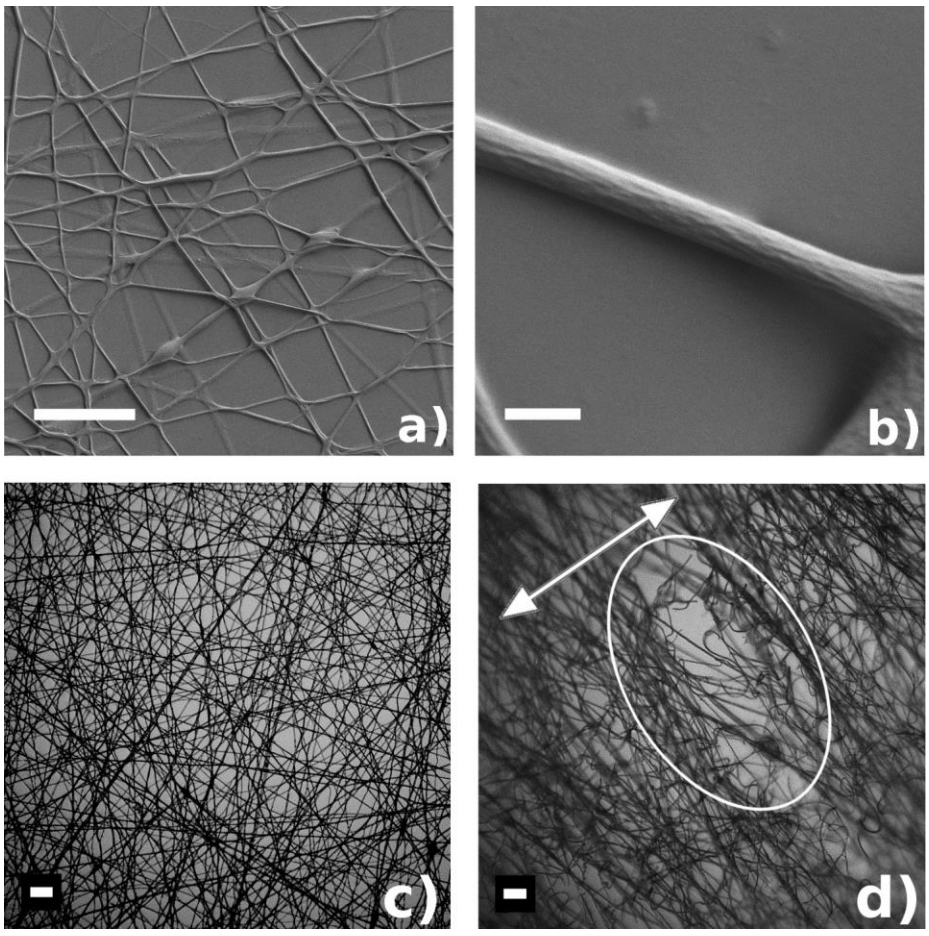

Figure 4.2: PEDOT:Tos fibers on PDMS obtained after 3 min of electrospinning at 20 kV and 15 cm nozzle-collector distance, 30 min of VPP and rinsing in ethanol. a) SEM micrograph of a network of fibers. The fibers appear to be fused together at the intersections, which suggests an easier conduction of the current at the junctions. A few fibers show beaded structures. The

“flatness” of the fibers is due to the removal of the PVP core following rinsing with ethanol (the scale bar is 20 µm). b) Close-up of one PEDOT:Tos fiber (scale bar is 1 µm) with a diameter of about 600 nm. c and d) optical microscopy of a network of fibers c) before and d) after a 100% stretch. The white arrow shows the stretching direction, and the oval highlights a small tear in the network, as well as a few broken fibers (the scale bars in c) and d) are 20 µm).

Our PEDOT:Tos fibers on PDMS show excellent properties as stretchable conductors. Most of the fibers follow the stretching of the PDMS substrate without breaking. By comparing intact fibers (Figure 2c) with stretched ones (Figure 2d), it is possible to notice small tears in the fibers’ mat perpendicular to the stretching direction. We hypothesize that the distortion of the fibers and the appearance of these small localized tears absorb the strains during stretching without the appearance of bigger cracks that would rupture the whole mat apart.

The electrical properties of the fiber mats under stretching were studied using a home-made computer-controlled tensile tester. Eutectic Gallium-Indium (EGaIn, Sigma-Aldrich) was used to form two liquid electrodes to ensure a good connection between the PEDOT:Tos fibers and copper wires used (see inset in Figure 3a) to make the connection to an Agilent B2902A source measure unit. A constant voltage of 200 mV was applied during the measurement.

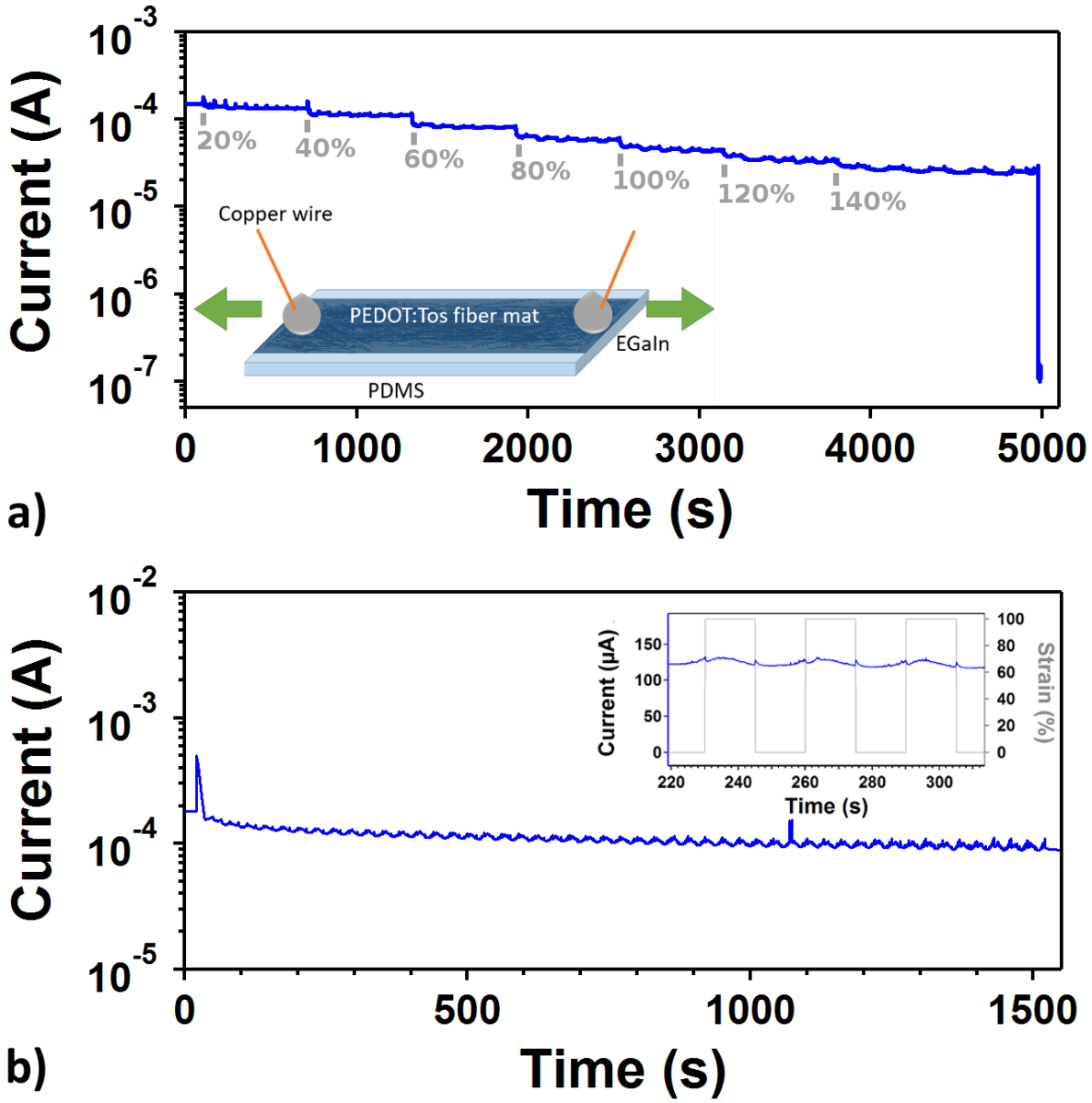

Figure 4.3: a) Current vs time plots for PEDOT:Tos fibers on PDMS. A logarithmic scale is used for the current. The sample was stretched in cycles, from 20% to 140% strain percentages at 0.1 cm/s. Five consecutive cycles of stretching and release were performed at each of the different strains percentage between 20% and 140%. The PDMS substrate broke at 160% strain. The samples were kept in each state (stretched or released) for a resting time of 1min. Inset: scheme of the setup used for this measurement. EGaIn was used for the connection between the fiber mat and the copper wires. The arrows show the stretching direction of the sample. b) Current vs time plots for a similar sample stretched at 100% strain percentage for 50 cycles, with a stretching speed of 0.1 cm/s. One stretching cycle consisted of stretching at 100% strain during 15 s followed by release to the initial

length during 15 s. The 50 cycles were performed without pause. Inset: Close-up of the behavior of the current during three cycles, with indication of the time during which the strains were applied and released. The samples were 1.5 cm long and 1 cm wide. The fibers were obtained after 3 min of electrospinning at 20 kV and 15 cm nozzle-collector distance, 30 min of VPP, and rinsing with ethanol. The measurements were made at 200 mV.

The ability of the PEDOT:Tos fibers to conduct the current under stretching was tested by monitoring the temporal evolution of the current during consecutive stretching cycles at strain percentages ranging from 20% to 140% with respect to the initial sample length. The applied strain percentage is defined as $[(L' - L)/L] \times 100\%$ where L and L' denote, respectively, the relaxed and stretched lengths of the PDMS substrate (e.g. a strain percentage of 20% means a 3-cm film is elongated by 20% of its initial length, reaching 3.6 cm). Figure 3a shows the current vs time evolution for five cycles with resting times at different stretches. The film was first stretched at 20%, kept in this state for one minute, and released to its initial length for 1 min. This process was repeated for five times. The same procedure was applied for strain percentages of 40%, 60%, 80%, 100%, 120%, 140%. The PDMS substrate broke at a 160% strain percentage. Surprisingly, the fibers could be stretched up to a 140% strain percentage while still retaining 1/6 of the initial current. Figure 3a shows that the current decreased (and the resistance increased) by a certain amount (about 10% of the initial current) during the first applied strain percentage. After losing around 10% of the initial current during each initial stretch, the current appears to remain stable during successive stretching and releasing, up to 140%. At a 140% strain percentage, the measured current is about 1/6 of its initial value. Figure 3b shows the current vs time evolution for a sample stretched to 100% strain for 50 cycles without resting time. For each cycle, a first 100% strain was performed, then the film was released immediately to 0% strain. Each full cycle lasted a total of 30s (15s stretching, 15s releasing), and this process was performed 50 times. The current remains stable for 50 cycles, which confirms the high stretchability of our PEDOT:Tos fibers on PDMS .

During any stretching or releasing event, the current inside the fibers show a small spike (inset of Figure 3b). This is probably due to dynamic rearrangements of the conductive pathways inside the non-woven fabric, as suggested by the relative regularity of the patterns in these spikes. These rearrangements are transitory; lower currents are thus obtained once the fibers are in a steady-state

compared to the transitory state. These differences are, however, small and the current after the first few stretches remains almost constant, with variations of around 2% of the initial current between the stretched and the released states.

During these measurements, high stretchability of 140% has been obtained with relatively low loss in current. When stretched at 140%, the film retained 20% of its initial current. Remarkably, the complete loss of conductivity in these fibers is systematically due to the breaking of the PDMS substrate, which in turns leads to the breaking of the fiber layers, rather than breaking of the fibers themselves. It is expected that our fibers could be stretched much more than 140% if deposited on a more stretchable substrate rather than on PDMS. However, it is important to note that a stretchability of 140% is an excellent value for biomedical and wearable applications. By comparison, simple films made by spin-coating a layer of the same solution and using vapor phase polymerization cannot be stretched more than 10% of their initial length without fracturing, independently from the strength of the PDMS. Methods such as pre-stretching and buckling or adding plasticizer to the PEDOT films can be used to improve these results to up to 30% [7], but a higher stretchability can sometimes be required.

In conclusion, using a combination of electrospinning and vapor phase polymerization, we obtained stretchable conducting PEDOT:Tos fibers on PDMS with an average diameter of about 700 nm. These fibers were stretched while a 200 mV bias was applied. After initial current loss at each new stretching percentage, the current appeared to be stable, and the films could be brought back to their initial length, while keeping a relatively high conductivity, up to applied strains as high as 140%. The current stability when stretching the films makes these fibers an interesting candidate for biomedical applications requiring conformable and stretchable electronics.

4.5 Acknowledgements

The authors are grateful to D. Pilon for technical support. This work was supported by the grants Discovery (NSERC), Engage 493111 2015 (NSERC), Établissement de Nouveau Chercheur (FRQNT), PSR-SIIRI 956 (Québec MESI) and John Evans Research Fund (CFI) awarded to F.C. S.Z. is grateful to NSERC for financial support through a Vanier Canada Graduate Scholarship. F.B.G. is grateful to GRSTB for financial support through a scholarship. We have also benefited

from the support of CMC Microsystems through the program MNT financial assistance and FRQNT and its Regroupement stratégique program through a grant awarded to RQMP.

4.6 References

[1] Kim, S. H., Hong, K., Xie, W., Lee, K. H., Zhang, S., Lodge, T. P., & Frisbie, C. D. (2013). Electrolyte- Gated Transistors for Organic and Printed Electronics. *Advanced Materials*, *25*(13), 1822-1846.
[2] Abidian, M. R., & Martin, D. C. (2008). Experimental and theoretical characterization of implantable neural microelectrodes modified with conducting polymer nanotubes. *Biomaterials*, *29*(9), 1273-1283.
[3] Rivnay, J., Owens, R. M., & Malliaras, G. G. (2013). The rise of organic bioelectronics. *Chemistry of Materials*, *26*(1), 679-685.
[4] Zeng, W., Shu, L., Li, Q., Chen, S., Wang, F., & Tao, X. M. (2014). Fiber- based wearable electronics: a review of materials, fabrication, devices, and applications. *Advanced Materials*, *26*(31), 5310-5336.
[5] Lipomi, D. J., & Bao, Z. (2011). Stretchable, elastic materials and devices for solar energy conversion. *Energy & Environmental Science*, *4*(9), 3314-3328.
[6] Lacour, S. P., Wagner, S., Huang, Z., & Suo, Z. (2003). Stretchable gold conductors on elastomeric substrates. *Applied physics letters*, *82*(15), 2404-2406.
[7] Zhang, S., Hubis, E., Tomasello, G., Soliveri, G., Kumar, P., & Cicoira, F. (2017). Patterning of Stretchable Organic Electrochemical Transistors. *Chemistry of Materials*.
[8] Seyedin, M. Z., Razal, J. M., Innis, P. C., & Wallace, G. G. (2014). Strain- Responsive Polyurethane/PEDOT: PSS Elastomeric Composite Fibers with High Electrical Conductivity. *Advanced Functional Materials*, *24*(20), 2957-2966.
[9] Ondarçuhu, T., & Joachim, C. (1998). Drawing a single nanofibre over hundreds of microns. *EPL (Europhysics Letters)*, *42*(2), 215.
[10] Martin, C. R. (1996). Membrane-based synthesis of nanomaterials. *Chemistry of Materials*, *8*(8), 1739-1746.
[11] Ma, P. X., & Zhang, R. (1999). Synthetic nano-scale fibrous extracellular matrix. *Journal of Biomedical Materials Research*, *46*(1), 60–72.
[12] Pomfret, S. J., Adams, P. N., Comfort, N. P., & Monkman, A. P. (2000). Electrical and mechanical properties of polyaniline fibres produced by a one-step wet spinning process. *Polymer*, *41*(6), 2265-2269.
[13] Okuzaki, H., Harashina, Y., & Yan, H. (2009). Highly conductive PEDOT/PSS microfibers fabricated by wet-spinning and dip-treatment in ethylene glycol. *European Polymer Journal*, *45*(1), 256-261.
[14] Rutledge, G. C., & Fridrikh, S. V. (2007). Formation of fibers by electrospinning. *Advanced drug delivery reviews*, *59*(14), 1384-1391.
[15] Gupta, B., Revagade, N., & Hilborn, J. (2007). Poly (lactic acid) fiber: an overview. *Progress in polymer science*, *32*(4), 455-482.
[16] Sill, T. J., & von Recum, H. A. (2008). Electrospinning: applications in drug delivery and tissue engineering. *Biomaterials*, *29*(13), 1989-2006.

[17] Shenoy, S. L., Bates, W. D., Frisch, H. L., & Wnek, G. E. (2005). Role of chain entanglements on fiber formation during electrospinning of polymer solutions: good solvent, non-specific polymer–polymer interaction limit. *Polymer*, *46*(10), 3372-3384.
[18] Laforgue, A., & Robitaille, L. (2010). Production of conductive PEDOT nanofibers by the combination of electrospinning and vapor-phase polymerization. *Macromolecules*, *43*(9), 4194-4200.
[19] Winther-Jensen, B., Breiby, D. W., & West, K. (2005). Base inhibited oxidative polymerization of 3, 4-ethylenedioxythiophene with iron (III) tosylate. *Synthetic metals*, *152*(1-3), 1-4.

CHAPTER 5 COMPLEMENTARY RESULTS

This chapter contains unpublished complementary results obtained in the course of this project.

5.1 Patterning of the fibers

Several tests were done to achieve the patterning of the fibers, to be used in a device fabrication (e.g. for sensors). Patterning of conducting polymers can be achieved by parylene-C patterning [228] or orthogonal photolithography [229]. However, these methods need to be adapted to stretchable substrates. Our group recently developed a method designed to pattern organic materials on PDMS, by patterning parylene-C and using it as a mask that can be easily transferred directly on stretchable substrates and removed once the organic layer has been deposited [230]. We used this method to successfully pattern fibers on PDMS, as shown on Figure 5.1. These patterns however need to remain relatively large (hundreds of micrometers) to prevent the delamination of the fiber mats when the parylene-C mask is removed.

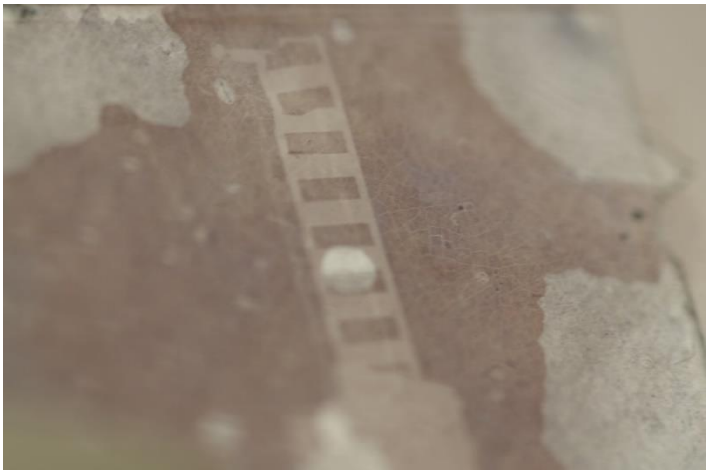

Figure 5.1: Patterned PEDOT:Tos nanofibers on PDMS obtained using parylene transfer pattern. The patterns shown are 800 µm wide and 2 mm long. The top patterns appear to be slightly deformed, due to small wrinkles on the PDMS or on the parylene during the patterning. Bubbles under the PDMS are also visible on the top left and right corners, as well as in the bottom right and on the pattern.

5.2 Complementary electrical measurements

Different procedures were tested to obtain the fibers. These other procedures also yielded interesting results when the samples were stretched. These results will be presented in this section, along with the main differences from the procedure presented in the Chapter 3.

5.2.1 Unrinsed fibers

The fibers were made in the same way as the one presented in the Chapter 3, with the difference that these fibers were not rinsed with ethanol at the end of the process. This means that the PVP core of the fibers, the imidazole, the iron tosylate and the non-polymerized EDOT are still present on these fiber mats. The current was measured during stretching right after the vapor phase polymerization took place, with a voltage of 200 mV. These results are shown on Figure 5.2. This figure indicates that despite the presence of PVP inside the fibers, the mats are still conductive.

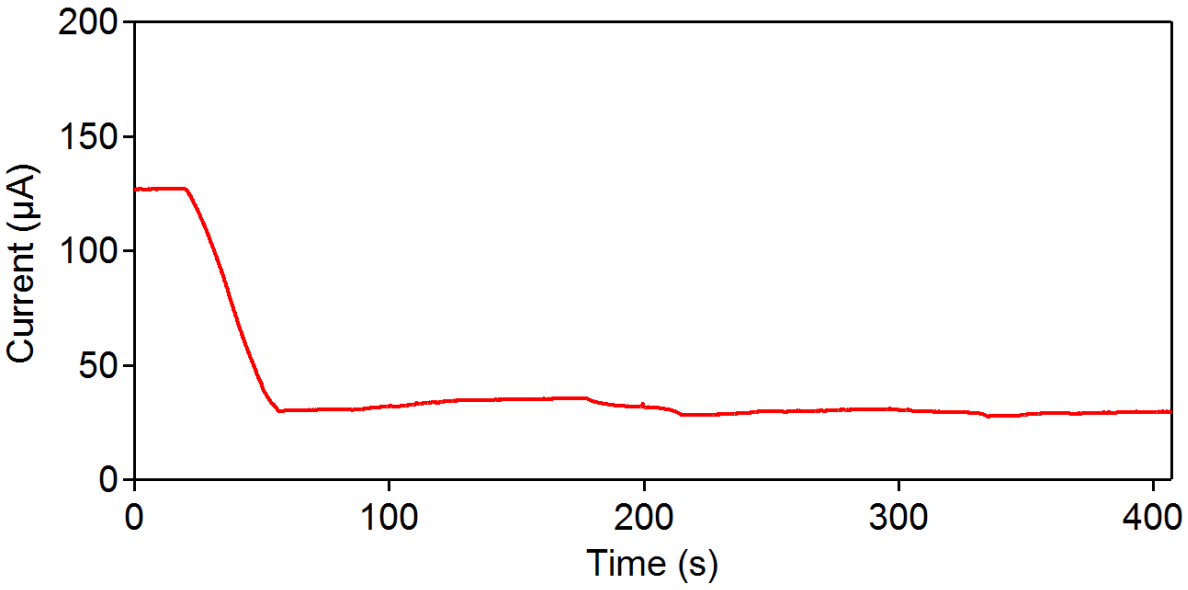

Figure 5.2: Current vs time for fibers obtained after 3min of electrospinning and VPP on PDMS, without ethanol bath, with a voltage of 200mV applied. The initial 120% stretching leads to a drop in the current. After this first drop, the sample was brought back to its initial position, but no recovery of the current was observed.

5.2.2 PEDOT:Tos fibers with a strain-sensing behavior

After the PDMS substrate was prepared following the procedure shown in Chapter 3, it was treated with UV-ozone for 20min. This procedure can improve the adherence of PEDOT films on PDMS and was used as a tentative method to limit the delamination of the fiber mats from the PDMS. This treatment was directly followed by the electrospinning of the oxidant fibers, and the procedure followed was otherwise exactly the one described in Chapter 3. The fiber mats on the UV-ozone treated PDMS were then stretched while the current was being measured, at 200 mV. These results are presented on Figure 5.3, and show a behavior closer to the one of strain-sensors: the current between the stretched and the released state varies significantly and can be used to determine that a strain is applied on the films.

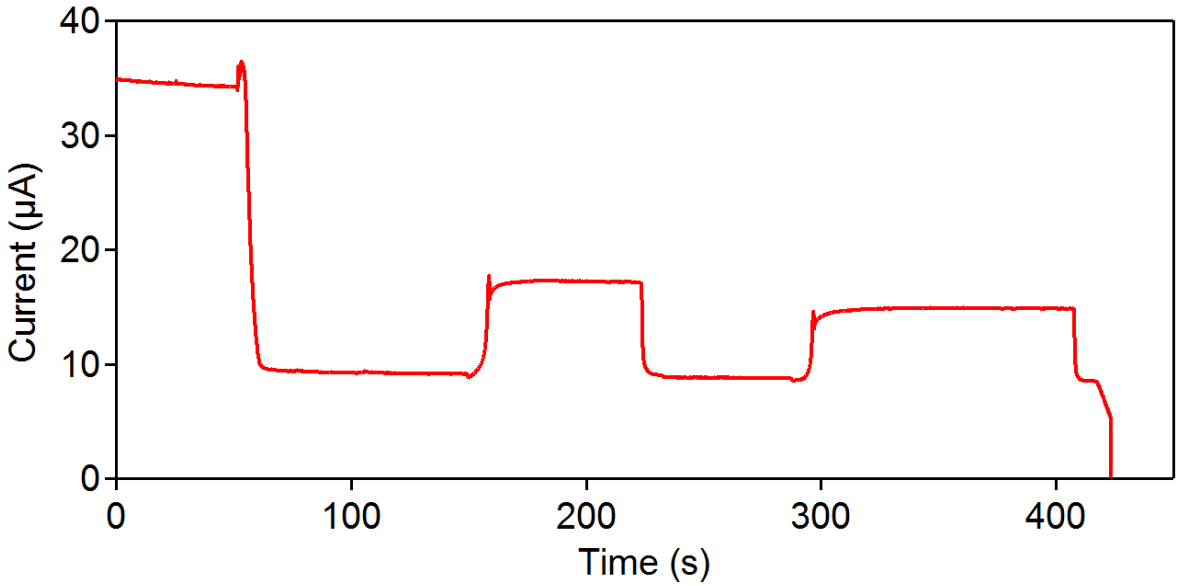

Figure 5.3: Current vs time for fibers obtained after 3min of electrospinning and VPP on PDMS, with a voltage of 200mV applied, when the PDMS underwent a UV-ozone treatment before the electrospinning, stretched at 50% 2 times, followed by a third stretch at 100%. The PDMS film broke during this third stretch.

5.3 Cell cultures

During this project, we had the opportunity to work with the group of Professor Peter Grütter from McGill university in Montréal. They recently developed a protocol to culture embryonic hippocampal neuronal cells of Sprague Dawely rats in the form of organized regions by using microfluidic devices. One of the points of this collaboration was to verify the behaviour of the neurons on various organic conductors, in particular on stretchable organic conductors. As such, they tried using PDMS coated with PEDOT:Tos nanofibers prepared in our lab to see if the cells could grow on these samples. At present, we are optimizing the sample preparation procedure to allow successful cell culture. Preliminary results showed that the neuron cells that were cultured on these samples did not survive. These results are likely due to the way the PDMS was prepared. The presence of monomers (both from PDMS and PEDOT) that were not completely removed before the nanofibers were tested probably killed the neurons, since these monomers are toxic for these cells. To avoid these problems, we have been working on a protocol modification that would allow us to produce PDMS while still removing as much monomer as possible.

CHAPTER 6 GENERAL DISCUSSION

The goal of this project was to obtain stretchable conducting fibers to be used in biomedical applications. To achieve such a result, a two-step process involving electrospinning and vapor phase polymerization was used to produce nanofibers directly on a stretchable PDMS substrate. In this chapter, the results presented in the article in Chapter 4 and the complementary results presented in Chapter 5 will be discussed more thoroughly.

6.1 Main results

Conductive nanofibers were successfully produced on a PDMS substrate, using a combination of electrospinning and vapor phase polymerization. These fibers, once rinsed, could be stretched at 140% of their initial length and still be conductive, with a current of $1/6^{th}$ of the initial one. This section will discuss these results at more length.

6.1.1 Appearance of the fiber mats before/after stretching

Non-woven fiber mats were produced. The random position and orientation of the nanofibers allowed for an easier stretching, by allowing the whole structure to mechanically adapt to the movements of the PDMS, while keeping contact nodes at the points where the fibers crossed. These contact nodes were improved by the vapor phase polymerization, which allowed for the creation of a homogeneous structure at the connection between fibers. Indeed, polymerization happened in an indiscriminate fashion on the contact points, and resulted in a good coverage of both fibers of the contact at the same time, thus later improving the electrical contact between fibers at the nodes. These structures at the contacts between two fibers can be seen on Figure 4.2a), where the contacts appear as a homogeneous structure.

The appearance of small holes inside the structure during stretching, as seen on figure Figure 4.2d) is due to the local mechanical forces on the fibers as they are rearranged to follow the movement on the PDMS. Fibers perpendicular to the stretching direction have more freedom to move following the stretching, while the fibers parallel to the stretching direction seem to break to

accommodate the movements of the whole structure. However, this cannot be confirmed without a comparison with aligned fibers, which will be the object of future studies.

6.1.2 Current measurement while stretching

The produced non-woven mats were stretched while the current was measured, with an applied voltage of 200 mV. The tests performed showed that, after a first stretch was performed at any given percentage of the initial length, the current would then remain stable when the film was stretched and released with the maximum strain percentage. Stretching more would lead to a further rise in resistance and thus a further loss in current. The current would then in turn stabilize at this new slightly lower value. This behavior is clearly shown on Figure 4.3a), which highlights the existence of this behavior of "maximum strain memory". It has also been shown that even after 50 cycles of stretching at 100% and releasing, the fiber mats kept a similar behavior, as shown on Figure 4.3b), with small spikes due to dynamical rearrangements of the conductive pathways. These dynamical rearrangements are probably due to physical movements inside the fiber mats, during which the nanofibers are slightly reoriented to accommodate the movements of the PDMS substrate. During this process, the nanofibers tend to regroup more at the beginning of any stretching, thus creating more connections and more conductive pathways for the current. The idea that the nanofibers have a certain freedom to rearrange is in accordance with the microscope observations of the fiber mats during stretching.

Complementary results regarding the fibers conductivity while stretching were also obtained. Rinsing the fibers appears to be a crucial step, not only because it allows to remove the unreacted chemicals, but also because removing the PVP core from inside the fibers leads to a different electrical and mechanical behavior (Figure 4.3 and Figure 5.2). On Figure 5.2, the absence of the spikes otherwise shown on every other graph "current vs time" could be due to the presence of the PVP core. Its stretchability and its lack of conductivity probably led to fibers where the PEDOT:Tos coating does no longer form a conductive pathway due to the elongation of the PVP fibers it was resting on. This leads to highly stable and stretchable devices that can also exploit the intrinsic stretchability of the PVP nanofibers to strengthen the whole structure. Unfortunately, this comes at the cost of removing the unwanted chemicals from the surface of the fibers mats, which is a major drawback for biomedical applications. Moreover, the presence of a PVP core within the

fibers also means that the PVP can still be affected by the ambient humidity and dissolve, which could cause long-term stability problem. Therefore, removing as much of it as possible is a crucial step for the long-term stability of these films. It is also expected that keeping the PVP would have a negative impact on the fibers conductivity due to its dielectric nature, but additional studies are needed to further address this issue.

During this project, it was also demonstrated that strain sensing behaviors could easily be achieved by these fiber mats, as shown on Figure 5.3. However, these strain sensors are based on the use of UV-ozone treatment to render the PDMS surface more brittle [60], as mentioned in the literature review in Chapter 2. This leads to the formation of small cracks on the PDMS surface during stretching, a behavior that has been largely used for stretchable films. Thus, this strain-sensing behavior is not inherent to the PEDOT:Tos nanofibers themselves and was not studied more thoroughly in the frame of this project. Instead, the focus was made on studying the behavior of the fibers on PDMS without the appearance of the small ruptures observed in other films after UV-ozone treatment.

6.2 Future challenges

6.2.1 Preparation of the solution

The solution used to produce the fibers by electrospinning contained PVP as a carrier polymer, iron tosylate as the oxidant, and imidazole as the base inhibitor for the polymerization. The choice of imidazole is unusual, and pyridine is more used in the literature to limit the acidity in the medium during the polymerization. Due to the possibility for the human skin to absorb traces of pyridine remaining on top of the film, to the irritations and burns that can be caused by this compound, and to the well-known risks for the human health of inhaling large quantities of pyridine [2231], we decided to use a chemical that cannot be absorbed directly through the skin as the base inhibitor, such as imidazole. However, this choice also has drawbacks: even though imidazole cannot be absorbed by the body through the epidermis, it still is irritant for the human skin and can cause burns [232]. It also presents the disadvantage of forming crystals with the iron that can alter the morphology of the film [213], as mentioned in the literature review in Chapter 2. The impact of these crystals needs to be clarified.

6.2.2 Relative humidity during electrospinning

Once the mixture was prepared and thoroughly mixed to ensure that the PVP and the imidazole were properly dissolved, it was used for electrospinning. Although most of the parameters of this process are well-known, the success of the procedure also depends on the humidity conditions inside the laboratory. This step was always performed at a relative humidity as low as possible, usually between 15% and 18%. Lowering the humidity in the electrospinning hood was done by heating up the air inside. However, it was sometimes difficult to lower the relative humidity under 20%. The effect of water on the fibers is a weakness of the process that would require a better control over the humidity for more accurate studies. In this project, vapor phase polymerization was done right after electrospinning to mitigate the effects of humidity on the freshly electrospun samples.

Using another polymer for electrospinning could constitute an improvement on the current recipe. PVP was chosen due to the ease with which it can be electrospun. Indeed, PVP possesses a high molecular weight and can easily be dissolved into alcohols. It is thus an easy polymer to electrospin, as shown by the literature review that highlights the facts that the electrospinning of PVP has been reported multiple times. Other easily-electrospun polymers such as PEO could have been chosen for this project. However, PVP has a very good solubility in butanol, the solvent in which the iron tosylate is soluble, and this is the reason why it was chosen for this project. Finding a better carrier polymer for the electrospinning that would be less affected by humidity without requiring days of mixing to prepare the solution is expected to significantly improve the results, by reducing the effects of the relative humidity on the fiber mats and thus increasing their long-term stability. Moreover, this would prevent the partial dissolution of the polymer fibers between the electrospinning and the vapor phase polymerization, which is a parameter that cannot be well controlled in the current process.

6.2.3 Limitations of using PDMS as the support for the fibers

The PVP fibers were directly electrospun on top of a PDMS substrate. Due to the nature of the substrate used during this project, the charges on the freshly electrospun fibers could not easily be

dissipated into a conductive material. This could be a problem for thicker films, that might be difficult to produce due to a charge accumulation on the surface of the fiber mats.

The fiber mats made on PDMS during this project could be stretched to 140% without rupturing, and still conducted current when stretched at more than 2 times their original length, as shown on Figure 4.3. This is sufficient for most applications, but it could still be interesting to study the possibility of stretching these fiber mats even more. To do so, a few tests were performed on more stretchable substrates such as Ecoflex® and the stretchable tape 3M™ VHB™, to see how much the fibers could be stretched. However, as this was not the focus of this project, only preliminary results were obtained. In particular, Ecoflex® is more difficult to process than PDMS and cannot be spin-coated, so it had to be drop-casted. This resulted in a substrate with a rough surface that did not favor the formation of the fiber mats. As for the stretchable tape 3M™ VHB™, it possesses two sticky faces, which resulted in difficulties when trying to peel off and manipulate the final fiber mats. The fiber mats obtained appeared to have been locally strained too much, resulting in huge losses in conductivity. More work on these substrates could be done in a future project to get a better understanding of how much stretching these fiber mats can undergo before losing their conductivity. However, for biomedical applications, the question of the breathability of these two less-studied substrates also needs to be addressed.

It is however important to note that the presence of a stretchable substrate was always necessary to induce the changes necessary to stretch the non-woven structure of the fibers. The fiber mats do not show a good stretchability when they are not supported by a stretchable substrate, and free-standing mats rupture easily if a pulling force is applied to them. This seems to indicate that the fiber mats require a mechanical support to prevent the local tears that form during stretching from rupturing the whole film from part to part.

6.2.4 Improving the stretchability

We found that the fiber mats could be stretched while still remaining conductive. However, several methods could be explored to improve the stretchability. An option would be to combine electrospinning with other methods used to improve films stretchability, such as buckling [25-26]. This could lead to even better results regarding the conductivity when the fiber mats are stretched.

Finally, another option would be to use the instabilities of electrospinning itself to produce more loosely arranged fibers. As explained during the literature review, increasing the distance between the spinneret and the collector leads to an increased level of instability. By sufficiently increasing the distance between the spinneret and the collector, it becomes possible to witness a second and even a third bending instability, which means that the fibers would tend to form coils. This could lead to serpentine–like shapes, as reported in the literature review and thus improve the stretchability of the fibers mats on PDMS or on more stretchable substrates as suggested in the previous section.

6.2.5 Testing the removal of the PVP core

During this project, we considered that part of the PVP in the core was removed by rinsing with ethanol. This claim is backed by several evidences in our results. The first indication that part of the PVP is indeed removed during the rinsing is shown in Figure 4.2a) and b). In these SEM pictures the fibers appear flat (Figure 4.2a)). This flat shape could be due to the collapsing of the fibers on themselves after the removal of the core. Figure 4.2b) shows another fiber, that did not collapse. However, this one presents a structure similar to the one of the fibers after shrinkage that were previously reported [219].

Comparing Figure 4.3 and Figure 5.2 also serves as a supplementary proof that PVP was at least partially removed during rinsing. Indeed, these two figures seem to indicate that the removal of the PVP core modifies the mechanical and electrical properties of the fiber mats. Such changes in the properties of the mats were expected, due to the difference between the mechanical and electrical properties of PVP compared to those of PEDOT:Tos.

These different observations were used as an indication that PVP had been partially removed, but it would be interesting in a following project to study to what extent the PVP has been removed. This could be done by various technique. Fourier Transform Infrared Spectroscopy (FTIR) would possibly give information on the structure of the fibers after rinsing by comparison between the peaks observed on an unrinsed sample and a rinsed sample.

CHAPTER 7 CONCLUSION AND RECOMMENDATIONS

In this work, we presented a two-step method to obtain conductive non-woven nanofiber mats on a stretchable substrate. This process uses both electrospinning, a widely studied technique to produce fibers from polymers, and vapor phase polymerization, a method that allows for the in-situ polymerization of conducting polymers (among others) on the surface of pre-existing structures. This two-step process presents the advantage of being usable for the production of nanofibers made of a conductive polymer, here PEDOT:Tos, by using electrospinning. Although the low molecular weight and the rigid backbone due to the conjugation of PEDOT render its direct electrospinning difficult, electrospinning a carrier polymer like PVP from a solution also containing an oxidant easily yields fibers, which can then be used as a template for the in-situ polymerization of the PEDOT. We showed that this method could easily yield conductive PEDOT:Tos nanofibers on stretchable substrates such as PDMS. This is the first time that nanofibers made of a conductive polymer have been obtained on PDMS using a method based on electrospinning.

We also demonstrated that these fibers made on PDMS could easily be patterned, using a previously reported method using parylene-C as a reusable mask for stretchable substrates. This is however limited to quite ~~big~~ large patterns, with dimensions of the scale of ~~one millimeter~~hundreds of micrometers. For smaller patterns, the whole mat of fibers ~~would~~ could delaminate during parylene peel off. We then studied both the morphology of these fibers and their electrical properties under stress by repeatedly stretching and releasing the films. The individual fibers had an average diameter of almost 700 nm at the end of the process. Some of them appeared to have collapsed due to the removal of their PVP core during the ethanol rinsing following the vapor phase polymerization. A few beads appeared on the mats, whose effects were not studied. When the mats were stretched, the stress led some fibers to rupture, leading to the formation of small tears inside the non-woven mats. These however did not lead to complete rupture of the mats. During the whole stretching process, the fiber mats stayed conductive, although their resistance increased slightly. The presence of small spikes during the process is believed to be due to dynamic rearrangements of the conductive pathways due to the movements of the fibers, that tend to regroup at the beginning of the stretching, thus increasing the number of possible electrical contacts. In particular, we demonstrated that the PEDOT:Tos films could be stretched to 140% and still retain around $1/6^{th}$ of their initial current. This behavior could be exploited in many biomedical applications, since it

allows to develop highly stretchable organic electronics displaying an electrical conductivity upon strain application.

Strain-sensing behaviors were observed with fibers made on UV-ozone treated PDMS. The treated PDMS surface tends to become more brittle and thus ruptures more easily, leading to the formation of micro-cracks. This behaviour could be studied more thoroughly for the information it could provide on the mechanisms leading to the mechanical and electrical behaviors that have been observed during the course of this project, and in particular the way the PDMS surface affects the fiber mats. Another interesting point to study would be the maximum stress that can be undergone by these fibers, using other stretchable substrates such as Ecoflex® and 3M™ VHB™ tape. Although this work demonstrated the ability of these PEDOT:Tos fibers to undergo strains as high as 140% while still being conductive, it is expected that higher strains could also be applied on the fiber mats without reaching their rupture point. However, at higher strains, it could also become necessary to improve the conductivity of the fiber mats. To do so, several strategies could be investigated. The first one would be to use buckling of the fiber mats or similar methods to easily slightly improve their stretchability by limiting the stress undergone by individual fibers at the lower strains, and thus keeping a similar conductivity for these lower strains. Another idea to improve the stretchability at lower strains and reduce the stress undergone by the fibers would be to make use of the secondary bending instability that appears in electrospinning when the distance between the spinneret and the collector is increased. This is expected to lead to non-woven fiber mats that would not be perfectly straight but would tend to bend or coil on themselves. Due to this new shape, it is expected that higher strains could be applied before a clear drop in conductivity can be witnessed.

As a follow-up project, it could also be interesting to try to functionalize these fibers to see if a sensing behavior can be obtained, and in particular if sensing can be achieved independently of the state (stretched or released) of the mats. Sensing devices based on fibers are the most obvious candidates for a new study following this work. It is expected that they would yield far better results than conducting thin films in this domain. What is more, we also showed that a relatively simple method could be used to pattern these fiber mats for such functions. These patterns however need to remain quite large to prevent the delamination of the fibers, and other methods such as photolithography using a fluorinated photoresist (such as the OSCoR photoresist from Orthogonal, Inc.) could also be investigated to pattern the films with smaller dimensions. Finally, the

preliminary work we performed with the neuron cell cultures can also be continued by improving the current procedure we use to first ensure the cells survival and to test their ability to grow according to mechanical forces or electrical signals.

BIBLIOGRAPHY

[1] Weston, A. D., & Hood, L. (2004). Systems biology, proteomics, and the future of health care: toward predictive, preventative, and personalized medicine. *Journal of proteome research*, *3*(2), 179-196.
[2] Swan, M. (2009). Emerging patient-driven health care models: an examination of health social networks, consumer personalized medicine and quantified self-tracking. *International journal of environmental research and public health*, *6*(2), 492-525.
[3] Axisa, F., Schmitt, P. M., Gehin, C., Delhomme, G., McAdams, E., & Dittmar, A. (2005). Flexible technologies and smart clothing for citizen medicine, home healthcare, and disease prevention. *IEEE transactions on information technology in biomedicine*, *9*(3), 325-336.
[4] Lymberis, A., & Olsson, S. (2003). Intelligent biomedical clothing for personal health and disease management: state of the art and future vision. *Telemedicine Journal and e-health*, *9*(4), 379-386.
[5] Bonato, P. (2003). Wearable sensors/systems and their impact on biomedical engineering. *IEEE Engineering in Medicine and Biology Magazine*, *22*(3), 18-20.
[6] Arumugam, V., Naresh, M. D., & Sanjeevi, R. (1994). Effect of strain rate on the fracture behaviour of skin. *Journal of Biosciences*, *19*(3), 307-313.
[7] Edwards, C., & Marks, R. (1995). Evaluation of biomechanical properties of human skin. *Clinics in dermatology*, *13*(4), 375-380.
[8] Chiang, C. K., Fincher Jr, C. R., Park, Y. W., Heeger, A. J., Shirakawa, H., Louis, E. J., ... & MacDiarmid, A. G. (1977). Electrical conductivity in doped polyacetylene. *Physical Review Letters*, *39*(17), 1098.
[9] Nobel Media AB. (2014). The Nobel Prize in Chemistry 2000. *Nobelprize.org.* Retrieved December 26, 2016, from http://www.nobelprize.org/nobel_prizes/chemistry/laureates/2000/
[10] Berggren, M., & Richter- Dahlfors, A. (2007). Organic bioelectronics. *Advanced Materials*, *19*(20), 3201-3213.
[11] Rivnay, J., Owens, R. M., & Malliaras, G. G. (2013). The rise of organic bioelectronics. *Chemistry of Materials*, *26*(1), 679-685.
[12] Lima, M. D., Li, N., De Andrade, M. J., Fang, S., Oh, J., Spinks, G. M., ... & Kim, S. J. (2012). Electrically, chemically, and photonically powered torsional and tensile actuation of hybrid carbon nanotube yarn muscles. *Science*, *338*(6109), 928-932.
[13] Benight, S. J., Wang, C., Tok, J. B., & Bao, Z. (2013). Stretchable and self-healing polymers and devices for electronic skin. *Progress in Polymer Science*, *38*(12), 1961-1977.
[14] Chortos, A., & Bao, Z. (2014). Skin-inspired electronic devices. *Materials Today*, *17*(7), 321-331.
[15] Kim, D. H., Lu, N., Ma, R., Kim, Y. S., Kim, R. H., Wang, S., ... & Yu, K. J. (2011). Epidermal electronics. *science*, *333*(6044), 838-843.
[16] Pang, C., Lee, C., & Suh, K. Y. (2013). Recent advances in flexible sensors for wearable and implantable devices. *Journal of Applied Polymer Science*, *130*(3), 1429-1441.
[17] Wagner, S., & Bauer, S. (2012). Materials for stretchable electronics. *Mrs Bulletin*, *37*(03), 207-213.
[18] Yeo, W. H., Kim, Y. S., Lee, J., Ameen, A., Shi, L., Li, M., ... & Huang, Y. (2013). Multifunctional epidermal electronics printed directly onto the skin. *Advanced Materials*, *25*(20), 2773-2778.

[19] Jia, W., Bandodkar, A. J., Valdés-Ramírez, G., Windmiller, J. R., Yang, Z., Ramírez, J., ... & Wang, J. (2013). Electrochemical tattoo biosensors for real-time noninvasive lactate monitoring in human perspiration. *Analytical chemistry*, *85*(14), 6553-6560.
[20] Pang, C., Lee, G. Y., Kim, T. I., Kim, S. M., Kim, H. N., Ahn, S. H., & Suh, K. Y. (2012). A flexible and highly sensitive strain-gauge sensor using reversible interlocking of nanofibres. *Nature materials*, *11*(9), 795-801.
[21] Jeong, J. W., Yeo, W. H., Akhtar, A., Norton, J. J., Kwack, Y. J., Li, S., ... & Cheng, H. (2013). Materials and Optimized Designs for Human- Machine Interfaces Via Epidermal Electronics. *Advanced Materials*, *25*(47), 6839-6846.
[22] Rogers, J. A., Someya, T., & Huang, Y. (2010). Materials and mechanics for stretchable electronics. *Science*, *327*(5973), 1603-1607.
[23] Suo, Z., Ma, E. Y., Gleskova, H., & Wagner, S. (1999). Mechanics of rollable and foldable film-on-foil electronics. *Applied Physics Letters*, *74*(8), 1177-1179.
[24] Sekitani, T., Zschieschang, U., Klauk, H., & Someya, T. (2010). Flexible organic transistors and circuits with extreme bending stability. *Nature materials*, *9*(12), 1015-1022.
[25] Khang, D. Y., Rogers, J. A., & Lee, H. H. (2009). Mechanical buckling: mechanics, metrology, and stretchable electronics. *Advanced Functional Materials*, *19*(10), 1526-1536.
[26] Lipomi, D. J., & Bao, Z. (2011). Stretchable, elastic materials and devices for solar energy conversion. *Energy & Environmental Science*, *4*(9), 3314-3328.
[27] Bowden, N., Brittain, S., Evans, A. G., Hutchinson, J. W., & Whitesides, G. M. (1998). Spontaneous formation of ordered structures in thin films of metals supported on an elastomeric polymer. *Nature*, *393*(6681), 146-149.
[28] Lacour, S. P., Wagner, S., Huang, Z., & Suo, Z. (2003). Stretchable gold conductors on elastomeric substrates. *Applied physics letters*, *82*(15), 2404-2406.
[29] Choi, W. M., Song, J., Khang, D. Y., Jiang, H., Huang, Y. Y., & Rogers, J. A. (2007). Biaxially stretchable "wavy" silicon nanomembranes. *Nano Letters*, *7*(6), 1655-1663.
[30] Khang, D. Y., Jiang, H., Huang, Y., & Rogers, J. A. (2006). A stretchable form of single-crystal silicon for high-performance electronics on rubber substrates. *Science*, *311*(5758), 208-212.
[31] Kim, D. H., Ahn, J. H., Choi, W. M., Kim, H. S., Kim, T. H., Song, J., ... & Rogers, J. A. (2008). Stretchable and foldable silicon integrated circuits. *Science*, *320*(5875), 507-511.
[32] Lacour, S. P., Chan, D., Wagner, S., Li, T., & Suo, Z. (2006). Mechanisms of reversible stretchability of thin metal films on elastomeric substrates. *Applied Physics Letters*, *88*(20), 204103.
[33] Lambricht, N., Pardoen, T., & Yunus, S. (2013). Giant stretchability of thin gold films on rough elastomeric substrates. *Acta materialia*, *61*(2), 540-547.
[34] Lacour, S. P., Jones, J., Suo, Z., & Wagner, S. (2004). Design and performance of thin metal film interconnects for skin-like electronic circuits. *IEEE Electron Device Letters*, *25*(4), 179-181.
[35] Lacour, S. P., Jones, J., Wagner, S., Li, T., & Suo, Z. (2005). Stretchable interconnects for elastic electronic surfaces. *Proceedings of the IEEE*, *93*(8), 1459-1467.
[36] Kim, D. H., Song, J., Choi, W. M., Kim, H. S., Kim, R. H., Liu, Z., ... & Rogers, J. A. (2008). Materials and noncoplanar mesh designs for integrated circuits with linear elastic responses to extreme mechanical deformations. *Proceedings of the National Academy of Sciences*, *105*(48), 18675-18680.
[37] Lee, P., Lee, J., Lee, H., Yeo, J., Hong, S., Nam, K. H., ... & Ko, S. H. (2012). Highly stretchable and highly conductive metal electrode by very long metal nanowire percolation network. *Advanced materials*, *24*(25), 3326-3332.

[38] Moon, G. D., Lim, G. H., Song, J. H., Shin, M., Yu, T., Lim, B., & Jeong, U. (2013). Highly stretchable patterned gold electrodes made of Au nanosheets. *Advanced Materials*, *25*(19), 2707-2712.
[39] Brosteaux, D., Axisa, F., Gonzalez, M., & Vanfleteren, J. (2007). Design and fabrication of elastic interconnections for stretchable electronic circuits. *IEEE Electron Device Letters*, *28*(7), 552-554.
[40] Kim, D. H., Kim, Y. S., Wu, J., Liu, Z., Song, J., Kim, H. S., ... & Rogers, J. A. (2009). Ultrathin silicon circuits with strain- isolation layers and mesh layouts for high- performance electronics on fabric, vinyl, leather, and paper. *Advanced Materials*, *21*(36), 3703-3707.
[41] Xu, S., Zhang, Y., Cho, J., Lee, J., Huang, X., Jia, L., ... & Cheng, H. (2013). Stretchable batteries with self-similar serpentine interconnects and integrated wireless recharging systems. *Nature communications*, *4*, 1543.
[42] Amjadi, M., Pichitpajongkit, A., Lee, S., Ryu, S., & Park, I. (2014). Highly stretchable and sensitive strain sensor based on silver nanowire–elastomer nanocomposite. *ACS nano*, *8*(5), 5154-5163.
[43] Lee, P., Ham, J., Lee, J., Hong, S., Han, S., Suh, Y. D., ... & Ko, S. H. (2014). Highly stretchable or transparent conductor fabrication by a hierarchical multiscale hybrid nanocomposite. *Advanced Functional Materials*, *24*(36), 5671-5678.
[44] Hu, L., Pasta, M., Mantia, F. L., Cui, L., Jeong, S., Deshazer, H. D., ... & Cui, Y. (2010). Stretchable, porous, and conductive energy textiles. *Nano letters*, *10*(2), 708-714.
[45] Yu, C., Masarapu, C., Rong, J., Wei, B., & Jiang, H. (2009). Stretchable Supercapacitors Based on Buckled Single- Walled Carbon- Nanotube Macrofilms. *Advanced Materials*, *21*(47), 4793-4797
[46] Sekitani, T., Noguchi, Y., Hata, K., Fukushima, T., Aida, T., & Someya, T. (2008). A rubberlike stretchable active matrix using elastic conductors. *Science*, *321*(5895), 1468-1472.
[47] Sekitani, T., Nakajima, H., Maeda, H., Fukushima, T., Aida, T., Hata, K., & Someya, T. (2009). Stretchable active-matrix organic light-emitting diode display using printable elastic conductors. *Nature materials*, *8*(6), 494-499.
[48] Hu, L., Yuan, W., Brochu, P., Gruner, G., & Pei, Q. (2009). Highly stretchable, conductive, and transparent nanotube thin films. *Applied Physics Letters*, *94*(16), 161108.
[49] Chun, K. Y., Oh, Y., Rho, J., Ahn, J. H., Kim, Y. J., Choi, H. R., & Baik, S. (2010). Highly conductive, printable and stretchable composite films of carbon nanotubes and silver. *Nature nanotechnology*, *5*(12), 853-857.
[50] Kaltenbrunner, M., Kettlgruber, G., Siket, C., Schwödiauer, R., & Bauer, S. (2010). Arrays of ultracompliant electrochemical dry gel cells for stretchable electronics. *Advanced materials*, *22*(18), 2065-2067.
[51] Liang, J., Li, L., Tong, K., Ren, Z., Hu, W., Niu, X., ... & Pei, Q. (2014). Silver nanowire percolation network soldered with graphene oxide at room temperature and its application for fully stretchable polymer light-emitting diodes. *Acs Nano*, *8*(2), 1590-1600.
[52] Muth, J. T., Vogt, D. M., Truby, R. L., Mengüç, Y., Kolesky, D. B., Wood, R. J., & Lewis, J. A. (2014). Embedded 3D printing of strain sensors within highly stretchable elastomers. *Advanced Materials*, *26*(36), 6307-6312.
[53] Chae, S. H., Yu, W. J., Bae, J. J., Duong, D. L., Perello, D., Jeong, H. Y., ... & Duan, X. (2013). Transferred wrinkled Al2O3 for highly stretchable and transparent graphene–carbon nanotube transistors. *Nature materials*, *12*(5), 403-409.

[54] Lee, J., Wu, J., Shi, M., Yoon, J., Park, S. I., Li, M., ... & Rogers, J. A. (2011). Stretchable GaAs photovoltaics with designs that enable high areal coverage. *Advanced Materials*, *23*(8), 986-991.
[55] Someya, T., Kato, Y., Sekitani, T., Iba, S., Noguchi, Y., Murase, Y., ... & Sakurai, T. (2005). Conformable, flexible, large-area networks of pressure and thermal sensors with organic transistor active matrixes. *Proceedings of the National Academy of Sciences of the United States of America*, *102*(35), 12321-12325.
[56] Takahashi, T., Takei, K., Gillies, A. G., Fearing, R. S., & Javey, A. (2011). Carbon nanotube active-matrix backplanes for conformal electronics and sensors. *Nano letters*, *11*(12), 5408-5413.
[57] Hu, W., Niu, X., Li, L., Yun, S., Yu, Z., & Pei, Q. (2012). Intrinsically stretchable transparent electrodes based on silver-nanowire–crosslinked-polyacrylate composites. *Nanotechnology*, *23*(34), 344002.
[58] Araki, T., Nogi, M., Suganuma, K., Kogure, M., & Kirihara, O. (2011). Printable and stretchable conductive wirings comprising silver flakes and elastomers. *IEEE Electron Device Letters*, *32*(10), 1424-1426.
[59] Vosgueritchian, M., Lipomi, D. J., & Bao, Z. (2012). Highly conductive and transparent PEDOT: PSS films with a fluorosurfactant for stretchable and flexible transparent electrodes. *Advanced functional materials*, *22*(2), 421-428.
[60] Lipomi, D. J., Lee, J. A., Vosgueritchian, M., Tee, B. C. K., Bolander, J. A., & Bao, Z. (2012). Electronic properties of transparent conductive films of PEDOT: PSS on stretchable substrates. *Chemistry of Materials*, *24*(2), 373-382.
[61] Lipomi, D. J., Tee, B. C. K., Vosgueritchian, M., & Bao, Z. (2011). Stretchable organic solar cells. *Advanced Materials*, *23*(15), 1771-1775.
[62] Kwon, S. J., Kim, T. Y., Lee, B. S., Lee, T. H., Kim, J. E., & Suh, K. S. (2010). Elastomeric conducting polymer nano-composites derived from ionic liquid polymer stabilized-poly (3, 4-ethylenedioxythiophene). *Synthetic Metals*, *160*(9), 1092-1096.
[63] Choong, C. L., Shim, M. B., Lee, B. S., Jeon, S., Ko, D. S., Kang, T. H., ... & Jeong, Y. J. (2014). Highly stretchable resistive pressure sensors using a conductive elastomeric composite on a micropyramid array. *Advanced Materials*, *26*(21), 3451-3458.
[64] Kim, J. T., Pyo, J., Rho, J., Ahn, J. H., Je, J. H., & Margaritondo, G. (2012). Three-dimensional writing of highly stretchable organic nanowires. *ACS Macro Letters*, *1*(3), 375-379.
[65] Wang, C., Zheng, W., Yue, Z., Too, C. O., & Wallace, G. G. (2011). Buckled, stretchable polypyrrole electrodes for battery applications. *Advanced Materials*, *23*(31), 3580-3584.
[66] Stoyanov, H., Kollosche, M., Risse, S., Waché, R., & Kofod, G. (2013). Soft conductive elastomer materials for stretchable electronics and voltage controlled artificial muscles. *Advanced Materials*, *25*(4), 578-583.
[67] Yu, Z., Niu, X., Liu, Z., & Pei, Q. (2011). Intrinsically Stretchable Polymer Light- Emitting Devices Using Carbon Nanotube- Polymer Composite Electrodes. *Advanced materials*, *23*(34), 3989-3994.
[68] Zhu, S., So, J. H., Mays, R., Desai, S., Barnes, W. R., Pourdeyhimi, B., & Dickey, M. D. (2013). Ultrastretchable fibers with metallic conductivity using a liquid metal alloy core. *Advanced Functional Materials*, *23*(18), 2308-2314.
[69] Zeng, W., Shu, L., Li, Q., Chen, S., Wang, F., & Tao, X. M. (2014). Fiber- based wearable electronics: a review of materials, fabrication, devices, and applications. *Advanced Materials*, *26*(31), 5310-5336.

[70] Yun, Y. J., Hong, W. G., Kim, W. J., Jun, Y., & Kim, B. H. (2013). A novel method for applying reduced graphene oxide directly to electronic textiles from yarns to fabrics. *Advanced Materials*, *25*(40), 5701-5705.
[71] Gould, P. (2003). Textiles gain intelligence. *Materials today*, *6*(10), 38-43.
[72] Seyedin, M. Z., Razal, J. M., Innis, P. C., & Wallace, G. G. (2014). Strain- Responsive Polyurethane/PEDOT: PSS Elastomeric Composite Fibers with High Electrical Conductivity. Advanced Functional Materials, 24(20), 2957-2966.
[73] Ma, R., Lee, J., Choi, D., Moon, H., & Baik, S. (2014). Knitted fabrics made from highly conductive stretchable fibers. *Nano letters*, *14*(4), 1944-1951.
[74] Lima, M. D., Fang, S., Lepró, X., Lewis, C., Ovalle-Robles, R., Carretero-González, J., ... & Haines, C. S. (2011). Biscrolling nanotube sheets and functional guests into yarns. *Science*, *331*(6013), 51-55.
[75] Li, D., & Xia, Y. (2004). Electrospinning of nanofibers: reinventing the wheel?. *Advanced materials*, *16*(14), 1151-1170.
[76] Tarabella, G., Villani, M., Calestani, D., Mosca, R., Iannotta, S., Zappettini, A., & Coppedè, N. (2012). A single cotton fiber organic electrochemical transistor for liquid electrolyte saline sensing. *Journal of Materials Chemistry*, *22*(45), 23830-23834.
[77] Choi, S., & Jiang, Z. (2006). A novel wearable sensor device with conductive fabric and PVDF film for monitoring cardiorespiratory signals. *Sensors and Actuators A: Physical*, *128*(2), 317-326.
[78] Pacelli, M., Loriga, G., Taccini, N., & Paradiso, R. (2006, September). Sensing fabrics for monitoring physiological and biomechanical variables: E-textile solutions. In *Medical Devices and Biosensors, 2006. 3rd IEEE/EMBS International Summer School on* (pp. 1-4). IEEE.
[79] Shim, B. S., Chen, W., Doty, C., Xu, C., & Kotov, N. A. (2008). Smart electronic yarns and wearable fabrics for human biomonitoring made by carbon nanotube coating with polyelectrolytes. *Nano letters*, *8*(12), 4151-4157.
[80] Pantelopoulos, A., & Bourbakis, N. G. (2010). A survey on wearable sensor-based systems for health monitoring and prognosis. *IEEE Transactions on Systems, Man, and Cybernetics, Part C (Applications and Reviews)*, *40*(1), 1-12.
[81] Lim, L. T., Auras, R., & Rubino, M. (2008). Processing technologies for poly (lactic acid). *Progress in polymer science*, *33*(8), 820-852.
[82] Ondarçuhu, T., & Joachim, C. (1998). Drawing a single nanofibre over hundreds of microns. *EPL (Europhysics Letters)*, *42*(2), 215.
[83] Xing, X., Wang, Y., & Li, B. (2008). Nanofiber drawing and nanodevice assembly in poly (trimethylene terephthalate). *Optics express*, *16*(14), 10815-10822.
[84] Ohta, T. (1983). Review on processing ultra high tenacity fibers from flexible polymer. *Polymer Engineering & Science*, *23*(13), 697-703.
[85] Haggenmueller, R., Gommans, H. H., Rinzler, A. G., Fischer, J. E., & Winey, K. I. (2000). Aligned single-wall carbon nanotubes in composites by melt processing methods. *Chemical physics letters*, *330*(3), 219-225.
[86] Miaudet, P., Badaire, S., Maugey, M., Derre, A., Pichot, V., Launois, P., ... & Zakri, C. (2005). Hot-drawing of single and multiwall carbon nanotube fibers for high toughness and alignment. *Nano letters*, *5*(11), 2212-2215.
[87] Pomfret, S. J., Adams, P. N., Comfort, N. P., & Monkman, A. P. (2000). Electrical and mechanical properties of polyaniline fibres produced by a one-step wet spinning process. *Polymer*, *41*(6), 2265-2269.

[88] Foroughi, J., Spinks, G. M., Wallace, G. G., & Whitten, P. G. (2008). Production of polypyrrole fibres by wet spinning. *Synthetic Metals*, *158*(3), 104-107.
[89] Okuzaki, H., & Ishihara, M. (2003). Spinning and characterization of conducting microfibers. *Macromolecular rapid communications*, *24*(3), 261-264.
[90] Okuzaki, H., Harashina, Y., & Yan, H. (2009). Highly conductive PEDOT/PSS microfibers fabricated by wet-spinning and dip-treatment in ethylene glycol. *European Polymer Journal*, *45*(1), 256-261.
[91] Cong, H. P., Ren, X. C., Wang, P., & Yu, S. H. (2012). Wet-spinning assembly of continuous, neat, and macroscopic graphene fibers. *Scientific reports*, *2*.
[92] Xu, Z., & Gao, C. (2014). Graphene in macroscopic order: liquid crystals and wet-spun fibers. *Accounts of chemical research*, *47*(4), 1267-1276.
[93] Gupta, B., Revagade, N., & Hilborn, J. (2007). Poly (lactic acid) fiber: an overview. *Progress in polymer science*, *32*(4), 455-482.
[94] Iwamoto, S., Isogai, A., & Iwata, T. (2011). Structure and mechanical properties of wet-spun fibers made from natural cellulose nanofibers. *Biomacromolecules*, *12*(3), 831-836.
[95] Xia, Y., Yang, P., Sun, Y., Wu, Y., Mayers, B., Gates, B., ... & Yan, H. (2003). One-dimensional nanostructures: synthesis, characterization, and applications. *Advanced materials*, *15*(5), 353-389.
[96] Che, G., Lakshmi, B. B., Martin, C. R., Fisher, E. R., & Ruoff, R. S. (1998). Chemical vapor deposition based synthesis of carbon nanotubes and nanofibers using a template method. *Chemistry of Materials*, *10*(1), 260-267.
[97] Tao, S. L., & Desai, T. A. (2007). Aligned Arrays of Biodegradable Poly (ϵ-caprolactone) Nanowires and Nanofibers by Template Synthesis. *Nano letters*, *7*(6), 1463-1468.
[98] Bishop, D. J., Licini, J. C., & Dolan, G. J. (1985). Lithium quench- condensed microstructures and the Aharonov–Bohm effect. *Applied physics letters*, *46*(10), 1000-1002.
[99] Jorritsma, J., Gijs, M. A. M., Kerkhof, J. M., & Stienen, J. G. H. (1996). General technique for fabricating large arrays of nanowires. *Nanotechnology*, *7*(3), 263.
[100] Müller, T., Heinig, K. H., & Schmidt, B. (2001). Formation of Ge nanowires in oxidized silicon V-grooves by ion beam synthesis. *Nuclear Instruments and Methods in Physics Research Section B: Beam Interactions with Materials and Atoms*, *175*, 468-473.
[101] Zhang, X. Y., Zhang, L. D., Meng, G. W., Li, G. H., Jin-Phillipp, N. Y., & Phillipp, F. (2001). Synthesis of ordered single crystal silicon nanowire arrays. *Advanced Materials*, *13*(16), 1238.
[102] Cao, H. Q., Xu, Y., Hong, J. M., Liu, H. B., Yin, G., Li, B. L., ... & Xu, Z. (2001). Sol–gel template synthesis of an array of single crystal CdS nanowires on a porous alumina template. *Advanced Materials*, *13*(18), 1393-1394.
[103] Burford, R. P., & Tongtam, T. (1991). Conducting polymers with controlled fibrillar morphology. *Journal of materials science*, *26*(12), 3264-3270.
[104] Dong, H., Prasad, S., Nyame, V., & Jones, W. E. (2004). Sub-micrometer conducting polyaniline tubes prepared from polymer fiber templates. *Chemistry of materials*, *16*(3), 371-373.
[105] Bognitzki, M., Hou, H., Ishaque, M., Frese, T., Hellwig, M., Schwarte, C., ... & Greiner, A. (2000). Polymer, metal, and hybrid nano-and mesotubes by coating degradable polymer template fibers (TUFT process). *Advanced Materials*, *12*(9), 637-640.
[106] Huang, Z. M., Zhang, Y. Z., Kotaki, M., & Ramakrishna, S. (2003). A review on polymer nanofibers by electrospinning and their applications in nanocomposites. *Composites science and technology*, *63*(15), 2223-2253.

[107] Ma, P. X., & Zhang, R. (1999). Synthetic nano-scale fibrous extracellular matrix. *Journal of biomedical materials research*, *46*(1), 60-72.
[108] Zhang, R., & Ma, P. X. (1999). Poly (α-hydroxyl acids)/hydroxyapatite porous composites for bone-tissue engineering. I. Preparation and morphology.
[109] Zhang, R., & Ma, P. X. (1999). Porous poly (L-lactic acid)/apatite composites created by biomimetic process.
[110] Nam, Y. S., & Park, T. G. (1999). Porous biodegradable polymeric scaffolds prepared by thermally induced phase separation. *Journal of biomedical materials research*, *47*(1), 8-17.
[111] Wei, G., & Ma, P. X. (2004). Structure and properties of nano-hydroxyapatite/polymer composite scaffolds for bone tissue engineering. *Biomaterials*, *25*(19), 4749-4757.
[112] Whitesides, G. M., & Grzybowski, B. (2002). Self-assembly at all scales. *Science*, *295*(5564), 2418-2421.
[113] Liu, G., Qiao, L., & Guo, A. (1996). Diblock copolymer nanofibers. *Macromolecules*, *29*(16), 5508-5510.
[114] Liu, G., Ding, J., Qiao, L., Guo, A., Dymov, B. P., Gleeson, J. T., ... & Saijo, K. (1999). Polystyrene- block- poly (2- cinnamoylethyl methacrylate) Nanofibers—Preparation, Characterization, and Liquid Crystalline Properties. *Chemistry–A European Journal*, *5*(9), 2740-2749.
[115] Hartgerink, J. D., Beniash, E., & Stupp, S. I. (2001). Self-assembly and mineralization of peptide-amphiphile nanofibers. *Science*, *294*(5547), 1684-1688.
[116] Doshi, J., & Reneker, D. H. (1993, October). Electrospinning process and applications of electrospun fibers. In *Industry Applications Society Annual Meeting, 1993., Conference Record of the 1993 IEEE* (pp. 1698-1703). IEEE.
[117] Kim, F. S., Ren, G., & Jenekhe, S. A. (2010). One-dimensional nanostructures of π-conjugated molecular systems: assembly, properties, and applications from photovoltaics, sensors, and nanophotonics to nanoelectronics. *Chemistry of Materials*, *23*(3), 682-732.
[118] Tucker, N., Stanger, J. J., Staiger, M. P., Razzaq, H., & Hofman, K. (2012). The History of the Science and Technology of Electrospinning from 1600 to 1995. *Journal of Engineered Fabrics & Fibers (JEFF)*, *7*(3).
[119] Cooley, J. F. (1900). *GB Patent No. 06385*. United Kindgom
[120] Cooley, J. F. (1902). *U.S. Patent No. 692,631*. Washington, DC: U.S. Patent and Trademark Office.
[121] Morton, W. J. (1902). *U.S. Patent No. 705,691*. Washington, DC: U.S. Patent and Trademark Office.
[122] Hagiwara, K. (1927). *Brevet canadien no CA 271440*. Gatineau, QC: Office de la propriété intellectuelle du Canada.
[123] Formhals, A. (1934). *U.S. Patent No. 1,975,504*. Washington, DC: U.S. Patent and Trademark Office.
[124] Formhals, A. (1931). Brevet français no FR 707.191. Paris: Ministère du Commerce et de l'Industrie, Direction de la Propriété Intellectuelle.
[125] Formhals, A. (1939). *U.S. Patent No. 2,160,962*. Washington, DC: U.S. Patent and Trademark Office.
[126] Formhals, A. (1940). *U.S. Patent No. 2,187,306*. Washington, DC: U.S. Patent and Trademark Office.
[127] Formhals, A. (1943). *U.S. Patent No. 2,323,025*. Washington, DC: U.S. Patent and Trademark Office.

[128] Formhals, A. (1944). *U.S. Patent No. 2,349,950*. Washington, DC: U.S. Patent and Trademark Office.
[129] Lushnikov, A. (1997). Igor'Vasilievich Petryanov-Sokolov (1907–1996). *Journal of Aerosol Science*, *28*(4), 545-546.
[130] Whitehouse, C. M., Dreyer, R. N., Yamashita, M., & Fenn, J. B. (1989). Electrospray ionization for mass-spectrometry of large biomolecules. *Science*, *246*(4926), 64-71.
[131] Wu, Y., Yu, B., Jackson, A., Zha, W., Lee, L. J., & Wyslouzil, B. E. (2009). Coaxial electrohydrodynamic spraying: a novel one-step technique to prepare oligodeoxynucleotide encapsulated lipoplex nanoparticles. *Molecular pharmaceutics*, *6*(5), 1371-1379.
[132] Zeleny, J. (1914). The electrical discharge from liquid points, and a hydrostatic method of measuring the electric intensity at their surfaces. *Physical Review*, *3*(2), 69.
[133] Zeleny, J. (1917). Instability of electrified liquid surfaces. *Physical review*, *10*(1), 1.
[134] Vonnegut, B., & Neubauer, R. L. (1952). Production of monodisperse liquid particles by electrical atomization. *Journal of Colloid Science*, *7*(6), 616-622.
[135] Drozin, V. G. (1955). The electrical dispersion of liquids as aerosols. *Journal of colloid science*, *10*(2), 158-164.
[136] Simons, H. L. (1966). *U.S. Patent No. 3,280,229*. Washington, DC: U.S. Patent and Trademark Office.
[137] Taylor, G. (1969, December). Electrically driven jets. In *Proceedings of the Royal Society of London A: Mathematical, Physical and Engineering Sciences* (Vol. 313, No. 1515, pp. 453-475). The Royal Society.
[138] Baumgarten, P. K. (1971). Electrostatic spinning of acrylic microfibers. *Journal of colloid and interface science*, *36*(1), 71-79.
[139] Rutledge, G. C., & Fridrikh, S. V. (2007). Formation of fibers by electrospinning. *Advanced Drug Delivery Reviews*, *59*(14), 1384-1391.
[140] Kim, K., & Turnbull, R. J. (1976). Generation of charged drops of insulating liquids by electrostatic spraying. *Journal of Applied Physics*, *47*(5), 1964-1969.
[141] Reneker, D. H., & Yarin, A. L. (2008). Electrospinning jets and polymer nanofibers. Polymer, 49(10), 2387-2425.
[142] Shin, Y. M., Hohman, M. M., Brenner, M. P., & Rutledge, G. C. (2001). Electrospinning: A whipping fluid jet generates submicron polymer fibers. *Applied physics letters*, *78*(8), 1149-1151.
[143] Reneker, D. H., Yarin, A. L., Fong, H., & Koombhongse, S. (2000). Bending instability of electrically charged liquid jets of polymer solutions in electrospinning. *Journal of Applied physics*, *87*(9), 4531-4547.
[144] Fong, H., Chun, I., & Reneker, D. H. (1999). Beaded nanofibers formed during electrospinning. *Polymer*, *40*(16), 4585-4592.
[145] Sill, T. J., & von Recum, H. A. (2008). Electrospinning: applications in drug delivery and tissue engineering. *Biomaterials*, *29*(13), 1989-2006.
[146] Sun, B., Long, Y. Z., Zhang, H. D., Li, M. M., Duvail, J. L., Jiang, X. Y., & Yin, H. L. (2014). Advances in three-dimensional nanofibrous macrostructures via electrospinning. *Progress in Polymer Science*, *39*(5), 862-890.
[147] Zong, X., Kim, K., Fang, D., Ran, S., Hsiao, B. S., & Chu, B. (2002). Structure and process relationship of electrospun bioabsorbable nanofiber membranes. *Polymer*, *43*(16), 4403-4412.
[148] Katti, D. S., Robinson, K. W., Ko, F. K., & Laurencin, C. T. (2004). Bioresorbable nanofiber- based systems for wound healing and drug delivery: Optimization of fabrication

parameters. *Journal of Biomedical Materials Research Part B: Applied Biomaterials*, *70*(2), 286-296.
[149] Tripatanasuwan, S., Zhong, Z., & Reneker, D. H. (2007). Effect of evaporation and solidification of the charged jet in electrospinning of poly (ethylene oxide) aqueous solution. *Polymer*, *48*(19), 5742-5746.
[150] Greiner, A., & Wendorff, J. H. (2008). Functional self-assembled nanofibers by electrospinning. In *Self-Assembled Nanomaterials I* (pp. 107-171). Springer Berlin Heidelberg.
[151] Dalton, P. D., Klee, D., & Möller, M. (2005). Electrospinning with dual collection rings. *Polymer*, *46*(3), 611-614.
[152] Gibson, P., Schreuder-Gibson, H., & Rivin, D. (2001). Transport properties of porous membranes based on electrospun nanofibers. *Colloids and Surfaces A: Physicochemical and Engineering Aspects*, *187*, 469-481.
[153] Tsai, P. P., Schreuder-Gibson, H., & Gibson, P. (2002). Different electrostatic methods for making electret filters. *Journal of Electrostatics*, *54*(3), 333-341.
[154] Ding, B., Wang, M., Yu, J., & Sun, G. (2009). Gas sensors based on electrospun nanofibers. *Sensors*, *9*(3), 1609-1624.
[155] Kenawy, E. R., Bowlin, G. L., Mansfield, K., Layman, J., Simpson, D. G., Sanders, E. H., & Wnek, G. E. (2002). Release of tetracycline hydrochloride from electrospun poly (ethylene-co-vinylacetate), poly (lactic acid), and a blend. *Journal of controlled release*, *81*(1), 57-64.
[156] Buchko, C. J., Chen, L. C., Shen, Y., & Martin, D. C. (1999). Processing and microstructural characterization of porous biocompatible protein polymer thin films. *Polymer*, *40*(26), 7397-7407.
[157] Jin, H. J., Fridrikh, S. V., Rutledge, G. C., & Kaplan, D. L. (2002). Electrospinning Bombyx mori silk with poly (ethylene oxide). *Biomacromolecules*, *3*(6), 1233-1239.
[158] Lee, C. H., Shin, H. J., Cho, I. H., Kang, Y. M., Kim, I. A., Park, K. D., & Shin, J. W. (2005). Nanofiber alignment and direction of mechanical strain affect the ECM production of human ACL fibroblast. *Biomaterials*, *26*(11), 1261-1270.
[159] Greiner, A., & Wendorff, J. H. (2007). Electrospinning: a fascinating method for the preparation of ultrathin fibers. *Angewandte Chemie International Edition*, *46*(30), 5670-5703.
[160] Jalili, R., Morshed, M., & Ravandi, S. A. H. (2006). Fundamental parameters affecting electrospinning of PAN nanofibers as uniaxially aligned fibers. *Journal of applied polymer science*, *101*(6), 4350-4357.
[161] Li, D., Wang, Y., & Xia, Y. (2003). Electrospinning of polymeric and ceramic nanofibers as uniaxially aligned arrays. *Nano letters*, *3*(8), 1167-1171.
[162] Li, D., Wang, Y., & Xia, Y. (2004). Electrospinning nanofibers as uniaxially aligned arrays and layer- by- layer stacked films. *Advanced Materials*, *16*(4), 361-366.
[163] Richard-Lacroix, M., & Pellerin, C. (2013). Molecular orientation in electrospun fibers: from mats to single fibers. *Macromolecules*, *46*(24), 9473-9493.
[164] Theron, A., Zussman, E., & Yarin, A. L. (2001). Electrostatic field-assisted alignment of electrospun nanofibres. *Nanotechnology*, *12*(3), 384.
[165] Bornat, A. (1987). *U.S. Patent No. 4,689,186*. Washington, DC: U.S. Patent and Trademark Office.
[166] Berry, J. P. (1991). *U.S. Patent No. 5,024,789*. Washington, DC: U.S. Patent and Trademark Office.
[167] Deitzel, J. M., Kleinmeyer, J. D., Hirvonen, J. K., & Tan, N. B. (2001). Controlled deposition of electrospun poly (ethylene oxide) fibers. *Polymer*, *42*(19), 8163-8170.

[168] Liu, H., & Hsieh, Y. L. (2002). Ultrafine fibrous cellulose membranes from electrospinning of cellulose acetate. *Journal of Polymer Science Part B: Polymer Physics*, *40*(18), 2119-2129.
[169] Zhang, D., & Chang, J. (2008). Electrospinning of three-dimensional nanofibrous tubes with controllable architectures. *Nano letters*, *8*(10), 3283-3287.
[170] Sundararaghavan, H. G., Metter, R. B., & Burdick, J. A. (2010). Electrospun fibrous scaffolds with multiscale and photopatterned porosity. *Macromolecular bioscience*, *10*(3), 265-270.
[171] Brown, T. D., Dalton, P. D., & Hutmacher, D. W. (2011). Direct writing by way of melt electrospinning. *Advanced Materials*, *23*(47), 5651-5657.
[172] Park, S. M., & Kim, D. S. (2015). Electrolyte- Assisted Electrospinning for a Self-Assembled, Free- Standing Nanofiber Membrane on a Curved Surface. *Advanced Materials*, *27*(10), 1682-1687.
[173] Granato, F., Bianco, A., Bertarelli, C., & Zerbi, G. (2009). Composite polyamide 6/polypyrrole conductive nanofibers. *Macromolecular rapid communications*, *30*(6), 453-458.
[174] Luo, C. J., Nangrejo, M., & Edirisinghe, M. (2010). A novel method of selecting solvents for polymer electrospinning. *Polymer*, *51*(7), 1654-1662.
[175] Shenoy, S. L., Bates, W. D., Frisch, H. L., & Wnek, G. E. (2005). Role of chain entanglements on fiber formation during electrospinning of polymer solutions: good solvent, non-specific polymer–polymer interaction limit. *Polymer*, *46*(10), 3372-3384.
[176] Di Benedetto, F., Camposeo, A., Pagliara, S., Mele, E., Persano, L., Stabile, R., ... & Pisignano, D. (2008). Patterning of light-emitting conjugated polymer nanofibres. *Nature nanotechnology*, *3*(10), 614-619.
[177] Tu, D., Pagliara, S., Camposeo, A., Persano, L., Cingolani, R., & Pisignano, D. (2010). Single light-emitting polymer nanofiber field-effect transistors. *Nanoscale*, *2*(10), 2217-2222.
[178] González, R., & Pinto, N. J. (2005). Electrospun poly (3-hexylthiophene-2, 5-diyl) fiber field effect transistor. *Synthetic Metals*, *151*(3), 275-278.
[179] Kang, T. S., Lee, S. W., Joo, J., & Lee, J. Y. (2005). Electrically conducting polypyrrole fibers spun by electrospinning. *Synthetic Metals*, *153*(1), 61-64.
[180] Chronakis, I. S., Grapenson, S., & Jakob, A. (2006). Conductive polypyrrole nanofibers via electrospinning: electrical and morphological properties. *Polymer*, *47*(5), 1597-1603.
[181] Cardenas, J. R., De França, M. G. O., De Vasconcelos, E. A., De Azevedo, W. M., & da Silva Jr, E. F. (2007). Growth of sub-micron fibres of pure polyaniline using the electrospinning technique. *Journal of Physics D: Applied Physics*, *40*(4), 1068.
[182] Zhang, W., Huang, Z., Yan, E., Wang, C., Xin, Y., Zhao, Q., & Tong, Y. (2007). Preparation of poly (phenylene vinylene) nanofibers by electrospinning. *Materials Science and Engineering: A*, *443*(1), 292-295.
[183] Norris, I. D., Shaker, M. M., Ko, F. K., & MacDiarmid, A. G. (2000). Electrostatic fabrication of ultrafine conducting fibers: polyaniline/polyethylene oxide blends. *Synthetic metals*, *114*(2), 109-114.
[184] Pinto, N. J., Johnson Jr, A. T., MacDiarmid, A. G., Mueller, C. H., Theofylaktos, N., Robinson, D. C., & Miranda, F. A. (2003). Electrospun polyaniline/polyethylene oxide nanofiber field-effect transistor. *Applied physics letters*, *83*(20), 4244-4246.
[185] Pinto, N. J., Ramos, I., Rojas, R., Wang, P. C., & Johnson, A. T. (2008). Electric response of isolated electrospun polyaniline nanofibers to vapors of aliphatic alcohols. *Sensors and Actuators B: Chemical*, *129*(2), 621-627.
[186] Aussawasathien, D., Dong, J. H., & Dai, L. (2005). Electrospun polymer nanofiber sensors. *Synthetic Metals*, *154*(1), 37-40.

[187] Moayeri, A., & Ajji, A. (2015). Fabrication of polyaniline/poly (ethylene oxide)/non-covalently functionalized graphene nanofibers via electrospinning. *Synthetic Metals*, *200*, 7-15.
[188] Laforgue, A., & Robitaille, L. (2008). Fabrication of poly-3-hexylthiophene/polyethylene oxide nanofibers using electrospinning. *Synthetic metals*, *158*(14), 577-584.
[189] Lee, S., Moon, G. D., & Jeong, U. (2009). Continuous production of uniform poly (3-hexylthiophene)(P3HT) nanofibers by electrospinning and their electrical properties. *Journal of Materials Chemistry*, *19*(6), 743-748.
[190] Chen, J. Y., Kuo, C. C., Lai, C. S., Chen, W. C., & Chen, H. L. (2011). Manipulation on the morphology and electrical properties of aligned electrospun nanofibers of poly (3-hexylthiophene) for field-effect transistor applications. *Macromolecules*, *44*(8), 2883-2892.
[191] Sundarrajan, S., Murugan, R., Nair, A. S., & Ramakrishna, S. (2010). Fabrication of P3HT/PCBM solar cloth by electrospinning technique. *Materials Letters*, *64*(21), 2369-2372.
[192] Bianco, A., Bertarelli, C., Frisk, S., Rabolt, J. F., Gallazzi, M. C., & Zerbi, G. (2007). Electrospun polyalkylthiophene/polyethyleneoxide fibers: Optical characterization. *Synthetic metals*, *157*(6), 276-281.
[193] Zhang, W., Yan, E., Huang, Z., Wang, C., Xin, Y., Zhao, Q., & Tong, Y. (2007). Preparation and study of PPV/PVA nanofibers via electrospinning PPV precursor alcohol solution. *European polymer journal*, *43*(3), 802-807.
[194] Li, D., Babel, A., Jenekhe, S. A., & Xia, Y. (2004). Nanofibers of conjugated polymers prepared by electrospinning with a two- capillary spinneret. *Advanced Materials*, *16*(22), 2062-2066.
[195] Vohra, V., Giovanella, U., Tubino, R., Murata, H., & Botta, C. (2011). Electroluminescence from conjugated polymer electrospun nanofibers in solution processable organic light-emitting diodes. *ACS nano*, *5*(7), 5572-5578.
[196] El-Aufy, A. (2004). *Nanofibers and nanocomposites poly(3,4 -ethylene dioxythiophene)/poly(styrene sulfonate) by electrospinning* (Order No. 3119331). Available from ProQuest Dissertations & Theses Global. (305175575). Retrieved from https://search.proquest.com/docview/305175575?accountid=40695
[197] Martínez, O., Bravo, A. G., & Pinto, N. J. (2009). Fabrication of Poly (vinylidene fluoride− trifluoroethylene)/Poly (3, 4-ethylenedioxythiophene)− polystyrene sulfonate composite nanofibers via electrospinning. *Macromolecules*, *42*(20), 7924-7929.
[198] Pinto, N. J., Rivera, D., Melendez, A., Ramos, I., Lim, J. H., & Johnson, A. C. (2011). Electrical response of electrospun PEDOT-PSSA nanofibers to organic and inorganic gases. *Sensors and Actuators B: Chemical*, *156*(2), 849-853.
[199] Huang, T. M., Batra, S., Hu, J., Miyoshi, T., & Cakmak, M. (2013). Chemical cross-linking of conducting poly (3, 4-ethylenedioxythiophene): poly (styrenesulfonate)(PEDOT: PSS) using poly (ethylene oxide)(PEO). *Polymer*, *54*(23), 6455-6462.
[200] Pisesweerayos, P., Dangtip, S., Supaphol, P., & Srikhirin, T. (2014). Electrically Conductive Ultrafine Fibers of PVA-PEDOT/PSS and PVA-AgNPs by Means of Electrospinning. In *Advanced Materials Research* (Vol. 1033, pp. 1024-1035). Trans Tech Publications.
[201] Liu, N., Fang, G., Wan, J., Zhou, H., Long, H., & Zhao, X. (2011). Electrospun PEDOT: PSS–PVA nanofiber based ultrahigh-strain sensors with controllable electrical conductivity. *Journal of Materials Chemistry*, *21*(47), 18962-18966.
[202] Kiristi, M., Oksuz, A. U., Oksuz, L., & Ulusoy, S. (2013). Electrospun chitosan/PEDOT nanofibers. *Materials Science and Engineering: C*, *33*(7), 3845-3850.

[203] Zhao, W., Yalcin, B., & Cakmak, M. (2015). Dynamic assembly of electrically conductive PEDOT: PSS nanofibers in electrospinning process studied by high speed video. *Synthetic Metals*, *203*, 107-116.
[204] Zhao, W., Nugay, I. I., Yalcin, B., & Cakmak, M. (2016). Flexible, stretchable, transparent and electrically conductive polymer films via a hybrid electrospinning and solution casting process: In-plane anisotropic conductivity for electro-optical applications. *Displays*.
[205] Winther-Jensen, B., & West, K. (2004). Vapor-phase polymerization of 3, 4-ethylenedioxythiophene: A route to highly conducting polymer surface layers. *Macromolecules*, *37*(12), 4538-4543.
[206] Im, S. G., & Gleason, K. K. (2007). Systematic control of the electrical conductivity of poly (3, 4-ethylenedioxythiophene) via oxidative chemical vapor deposition. *Macromolecules*, *40*(18), 6552-6556.
[207] Bhattacharyya, D., Howden, R. M., Borrelli, D. C., & Gleason, K. K. (2012). Vapor phase oxidative synthesis of conjugated polymers and applications. *Journal of Polymer Science Part B: Polymer Physics*, *50*(19), 1329-1351.
[208] Ojio, T., & Miyata, S. (1986). Transparent and conducting polypyrrole composite films prepared by vapor-phase polymerization. *Nippon Kagaku Kaishi*, (3), 348-355.
[209] Mohammadi, A., Hasan, M. A., Liedberg, B., Lundström, I., & Salaneck, W. R. (1986). Chemical vapour deposition (CVD) of conducting polymers: Polypyrrole. *Synthetic metals*, *14*(3), 189-197.
[210] Kim, J., Kim, E., Won, Y., Lee, H., & Suh, K. (2003). The preparation and characteristics of conductive poly (3, 4-ethylenedioxythiophene) thin film by vapor-phase polymerization. *Synthetic metals*, *139*(2), 485-489.
[211] Winther-Jensen, B., Forsyth, M., West, K., Andreasen, J. W., Wallace, G., & MacFarlane, D. R. (2007). High current density and drift velocity in templated conducting polymers. *Organic electronics*, *8*(6), 796-800.
[212] Levermore, P. A., Chen, L., Wang, X., Das, R., & Bradley, D. D. (2007). Fabrication of Highly Conductive Poly (3, 4- ethylenedioxythiophene) Films by Vapor Phase Polymerization and Their Application in Efficient Organic Light- Emitting Diodes. *Advanced Materials*, *19*(17), 2379-2385.
[213] Winther-Jensen, B., Breiby, D. W., & West, K. (2005). Base inhibited oxidative polymerization of 3, 4-ethylenedioxythiophene with iron (III) tosylate. *Synthetic metals*, *152*(1), 1-4.
[214] Winther-Jensen, B., Forsyth, M., West, K., Andreasen, J. W., Bayley, P., Pas, S., & MacFarlane, D. R. (2008). Order–disorder transitions in poly (3, 4-ethylenedioxythiophene). *Polymer*, *49*(2), 481-487.
[215] Admassie, S., Zhang, F., Manoj, A. G., Svensson, M., Andersson, M. R., & Inganäs, O. (2006). A polymer photodiode using vapour-phase polymerized PEDOT as an anode. *Solar Energy Materials and Solar Cells*, *90*(2), 133-141.
[216] Kim, M., Lee, Y. S., Kim, Y. C., Choi, M. S., & Lee, J. Y. (2011). Flexible organic light-emitting diode with a conductive polymer electrode. *Synthetic Metals*, *161*(21), 2318-2322.
[217] Jang, K. S., Kim, D. O., Lee, J. H., Hong, S. C., Lee, T. W., Lee, Y., & Nam, J. D. (2010). Synchronous vapor-phase polymerization of poly (3, 4-ethylenedioxythiophene) and poly (3-hexylthiophene) copolymer systems for tunable optoelectronic properties. *Organic Electronics*, *11*(10), 1668-1675.

[218] Nguyen, H. D., Ko, J. M., Kim, H. J., Kim, S. K., Cho, S. H., Nam, J. D., & Lee, J. Y. (2008). Electrochemical properties of poly (3, 4-ethylenedioxythiophene) nanofiber non-woven web formed by electrospinning. *Journal of nanoscience and nanotechnology*, *8*(9), 4718-4721.
[219] Laforgue, A., & Robitaille, L. (2010). Production of conductive PEDOT nanofibers by the combination of electrospinning and vapor-phase polymerization. *Macromolecules*, *43*(9), 4194-4200.
[220] Laforgue, A. (2010). Electrically controlled colour-changing textiles using the resistive heating properties of PEDOT nanofibers. *Journal of Materials Chemistry*, *20*(38), 8233-8235.
[221] Laforgue, A. (2011). All-textile flexible supercapacitors using electrospun poly (3, 4-ethylenedioxythiophene) nanofibers. *Journal of Power Sources*, *196*(1), 559-564.
[222] Elschner, A., Kirchmeyer, S., Lovenich, W., Merker, U., & Reuter, K. (2010). *PEDOT: principles and applications of an intrinsically conductive polymer*. CRC Press.
[223] Larsen, S. T., Vreeland, R. F., Heien, M. L., & Taboryski, R. (2012). Characterization of poly (3, 4-ethylenedioxythiophene): tosylate conductive polymer microelectrodes for transmitter detection. *Analyst*, *137*(8), 1831-1836.
[224] Kwon, O. S., Park, S. J., Lee, J. S., Park, E., Kim, T., Park, H. W., ... & Jang, J. (2012). Multidimensional conducting polymer nanotubes for ultrasensitive chemical nerve agent sensing. *Nano letters*, *12*(6), 2797-2802.
[225] Bashir, T., Fast, L., Skrifvars, M., & Persson, N. K. (2012). Electrical resistance measurement methods and electrical characterization of poly (3, 4- ethylenedioxythiophene)-coated conductive fibers. *Journal of Applied Polymer Science*, *124*(4), 2954-2961.
[226] Feng, Z. Q., Wu, J., Cho, W., Leach, M. K., Franz, E. W., Naim, Y. I., ... & Martin, D. C. (2013). Highly aligned poly (3, 4-ethylene dioxythiophene)(PEDOT) nano-and microscale fibers and tubes. *Polymer*, *54*(2), 702-708.
[227] Park, H., Lee, S. J., Kim, S., Ryu, H. W., Lee, S. H., Choi, H. H., ... & Kim, J. H. (2013). Conducting polymer nanofiber mats via combination of electrospinning and oxidative polymerization. *Polymer*, *54*(16), 4155-4160.
[228] DeFranco, J. A., Schmidt, B. S., Lipson, M., & Malliaras, G. G. (2006). Photolithographic patterning of organic electronic materials. *Organic Electronics*, *7*(1), 22-28.
[229] Taylor, P. G., Lee, J. K., Zakhidov, A. A., Chatzichristidi, M., Fong, H. H., DeFranco, J. A., ... & Ober, C. K. (2009). Orthogonal patterning of PEDOT: PSS for organic electronics using hydrofluoroether solvents. *Advanced Materials*, *21*(22), 2314-2317.
[230] Zhang, S., Hubis, E., Tomasello, G., Soliveri, G., Kumar, P., & Cicoira, F. (2017). Patterning of Stretchable Organic Electrochemical Transistors. *Chemistry of Materials*.
[231] The National Institute for Occupational Safety and Health (NIOSH). (July 22, 2015). International Chemical Safety Cards (ICSC) – Pyridine. From https://www.cdc.gov/niosh/ipcsneng/neng0323.html
[232] The National Institute for Occupational Safety and Health (NIOSH). (July 22, 2015). International Chemical Safety Cards (ICSC) – Imidazole. From https://www.cdc.gov/niosh/ipcsneng/neng1721.html